Aged Muscle Stem Cell Sensitivity to Matrix Stiffening Disrupts Differentiation Kinetics through Dysregulation of SIRT3

by

Hikaru Mamiya

Bachelor of Science, University of California, Berkeley, 2011

Submitted to the Graduate Faculty of the

Swanson School of Engineering in partial fulfillment

of the requirements for the degree of

Doctor of Philosophy

University of Pittsburgh

2022

UNIVERSITY OF PITTSBURGH

SWANSON SCHOOL OF ENGINEERING

This dissertation was presented

by

Hikaru Mamiya

It was defended on

April 12, 2021

and approved by

Aaron Barchowsky, PhD, Professor, Department of Environmental and Occupational Health

David A. Vorp, PhD, Professor, Department of Bioengineering

Anne M. Robertson, PhD, Professor, Department of Mechanical Engineering & Materials Science

Thomas A. Rando, PhD, Professor, Department of Neurology and Neurological Sciences, Stanford University

Dissertation Director: Fabrisia Ambrosio, PhD, MPT, Associate Professor, Department of Physical Medicine & Rehabilitation, Department of Bioengineering

Aged Muscle Stem Cell Sensitivity to Matrix Stiffening Disrupts Differentiation Kinetics through Dysregulation of SIRT3

Hikaru Mamiya, PhD

University of Pittsburgh, 2022

Aging is typically associated with decreased functional mobility, which can be caused by declines in skeletal muscle regenerative capacity and functional recovery after injury. For efficient muscle regeneration, resident muscle stem cells (MuSCs) are essential. However, over time, MuSCs display a progressively diminished myogenic lineage specification. While aged MuSCs display cell-autonomous deficits that drive impaired regeneration, a young microenvironment restores a youthful cellular phenotype. Although most studies to date have focused on the effects of circulating factors on age-related MuSC dysfunction, little is known about the impact of biophysical niche alterations on MuSC behavior over time. In this dissertation work, we evaluated whether aged MuSC dysfunction is mediated by increased muscle stiffness. Further, given the role of mitochondria in dictating stem cell fate, we investigated whether mitochondria-associated gene expression is perturbed in response to a stiff microenvironment.

First, the impact of substrate stiffness on MuSC characteristics was assessed at the level of nuclear morphology, single-cell transcripts, and protein expression. *In vitro* data revealed that aged MuSC nuclear morphology recapitulates that of young MuSCs when cells were exposed to a substrate engineered to mimic the stiffness of young muscle. As nuclear morphological changes influence gene expression and, thus, stem cell fate, we next examined whether changes in nuclear morphology were associated with improved myogenicity. Single cell RNA-seq and imaging flow cytometry revealed that exposure to a soft substrate increased aged MuSC activation as evidenced

by Pax7 and MyoD1 expression at both mRNA and protein levels, respectively, suggesting rejuvenation of aged MuSCs. Notably, young MuSCs were resistant to stiffness alterations, and a stiff substrate did not significantly affect lineage progression. Further investigation implicated SIRT3, a master regulator of mitochondria, as a novel mechano-sensitive factor regulating MuSC fate. Finally, we tested whether reduction of aged muscle stiffness enhances regenerative capacity *in vivo*. We found that modulation of aged muscle elasticity led to enhanced myofiber cross-sectional area and force recovery. Consistent with *in vitro* findings, SIRT3 expression at the injury site was also enhanced with reduced stiffness in aged muscle. Our findings highlight a previously unrecognized role of SIRT3 in MuSC activation and muscle regeneration in response to microenvironmental stiffness.

Table of Contents

List of Tables

List of Figures

Preface

The microenvironment, or niche, is a critical component that dictates stem cell fate. The significance of the microenvironment at the cellular level is the central theme of this dissertation, yet the importance of the microenvironment is no different at the organism level as well. Every trainee is like a stem cell. He/she has the potential to be successful in his/her academic journey. However, it would be impossible to survive a doctoral program and become fruitful without solid support and guidance. The journey to the completion of this doctoral degree has been extraordinarily intense and rough; it was considerably more challenging than I had possibly imagined before entering the Ph.D. program. It was only possible to complete this dissertation with enormous support. I have been fortunate to receive such terrific assistance to grow to be the best version of myself possible — the one I had never imagined to become several years ago.

First, I am incredibly grateful to my advisor Dr. Fabrisia Ambrosio. I cannot thank her enough for welcoming me to the lab. In addition to science, she taught me great attributes, communication skills, and creative mindsets that will be valued in any future career. She has never stopped inspiring me. I also have been fortunate to have our lab manager, Sunita, and Dr. Amrita. They welcomed and taught me a lot from day one and made me feel at home in the lab in no time. Sunita has always put tremendous effort into doing background work to make sure every lab members' projects move forward as smoothly as possible. Thank you. I would also like to thank Amrita, the other longest teammate of mine, who has always been willing to help me. Her positive attitude and big smile have always been cheerful. I would like to show appreciation to our "mouse mafia," Abish and Zach, for organizing our mice so well and helping me with *in vivo* experiments. I cannot emphasize enough how much time I have saved thanks to your help. Sruthi, another

graduate student who joined our lab after me, has been a great support as well. It was truly inspirational to see her grow rapidly as a scientist. Thank you also for making my project a much more exciting story. Hirotaka and Kai, our extremely hard-working post-doctoral fellows, have always been willing to help me despite their busy schedules, and we soon became night work friends. Thank you for making night work more enjoyable. Lena, my undergraduate student trainee, and Amanda, our lab technician, dedicated a tremendous amount of time to help my project move forward. I cannot thank you enough, as my project would have taken another five years without your help.

I would like to thank my committee members — Dr. Aaron Barchowsky, Dr. Thomas A. Rando, Dr. David A. Vorp, and Dr. Anne M. Robertson — for their tremendous support and guidance. Their valuable feedback directed my dissertation work to become a better story. Thank you, Dr. Philip LeDuc, Dr. Antonio D'Amore, and his current and former lab members, Gabriele, Sam, and Drake, for helping me with the collaborative work. Without your help, this work would not have been possible. I also cannot thank enough Dr. Sanjeev Shroff for not only making the Pitt Bioengineering graduate program splendid but also introducing me to the opportunity to join the Ambrosio lab.

I am deeply grateful for many friends I have made before and during the graduate program at the University of Pittsburgh. Thank you, Kosuke and Momo, who have been my best friends and continued to be highly supportive despite us being nearly 7,000 miles away and not being able to see one another often. Thank you, Daisuke and Naoki. You two have been like my family in Pittsburgh. I will never forget all your support, inspiration, and the fun moments you gave me. You made me feel at home in Pittsburgh. I would also like to show my appreciation to Hye Won, Steve, Deja, and Mike for the extraordinary support you have provided me at the critical times of my life in the United States.

Finally, I would like to thank my family, who has given me so much love and support. My father, Shigemitsu, my mother, Machiko, and grandmother, Hisako, have always made strenuous endeavors to support me so that I can focus on whatever I need to do to pursue my journey. Thank you, my warmhearted and cheerful sisters, Mai and Aya. I genuinely appreciate how nicely you have been treating me. You are my oasis. Thank you, my cat, Luna, who unfortunately passed away last February. You were lovely and friendly. You were always by my side, helping me unwind all the stress I experienced from time to time during the almost entire 15 years of my US life. Last but not least, I would also like to thank all my cousins, who are close like siblings. The annual gathering of cousins and extended family has been genuinely revitalizing for me. My family and extended families have always been the most significant sources of my energy. Because of you, I have been able to drive myself to work extra hard at difficult times during my academic journey. I cannot thank you all enough.

1.0 Introduction

1.1 Aging and Its Implication in Current Society

The Epic of Gilgamesh, an ancient Mesopotamian odyssey that is the earliest surviving work of literature, was among the first to describe the idea of immortality and revitalization. After the battle of the Cedar Forest where Gilgamesh and his friend, Enkidu, slay the Guardian, the gods decided that Enkidu must pay the price with his own blood. Grief over Enkidu's death led Gilgamesh to realize that he, too, will eventually die. It is this realization that motivated Gilgamesh to undertake a long and dangerous journey across the Land of Night and the Waters of Death in search of eternal life.

Since the 20th century B.C., the concept of rejuvenation, reincarnation, and eternal life has been expressed in numerous arts and literature created across the world. Throughout history, tales of immortality have been common, and stories illustrating these topics are still favored by many people today. This universal theme depicts mankind's strong desire to live longer and younger. Unfortunately, these two aspirations do not always coincide.

Human life expectancy fluctuated between 30 and 40 years without any increasing trend before the mid-19th century (Max Roser, Esteban Ortiz-Ospina, & Hannah Ritchie, 2013). However, thanks to improved public health and medical advancements in the past decades, life expectancy has been increasing globally at an unprecedented rate (United Nations, 2017). Now, the average life expectancy is over 70 years globally and exceeds 80 years in some countries such as Japan (Max Roser et al., 2013). Furthermore, the number of people 60 years and older exceeded 900 million globally in 2015. This number is expected to reach 2 billion by 2050 (WHO, 2018).

Although most people view the idea of an ever-expanding lifespan appealing, aging typically leads to a higher risk of morbidity and injuries, which often compromises quality of life (Cuevas-Trisan, 2017; Hansen & Kennedy, 2016). Age-associated diseases, such as cardiovascular diseases, cancer, Alzheimer's disease, and other dementias accounted for approximately 50% of all the causes of deaths in the United States in 2017 (Finegold, Asaria, & Francis, 2013; Franceschi et al., 2018; Heron, 2019). Moreover, increased life expectancy is inextricably intertwined with an expanding economic burden (R. Lee & Mason, 2017). Now, more than ever, a better understanding of biological mechanisms underlying organismal aging is needed if we are to achieve the goal of enhanced healthspan of our population.

1.2 Overview of the Current Understanding of Aging

Aging research was arguably formalized in the early 20th century when the terms 'Gerontology' and 'Geriatrics' were coined by Ilya Ilyich Mechnikov in 1903 and by Ignatz Leo Nascher in 1909, respectively (Clarfield, 1990; Krishnan, 2020; Morley, 2004). However, aging research remained limited until the National Institute on Aging (NIA) was founded in 1974, after which time the number of publications relating to aging nearly tripled ("History | National Institute on Aging," n.d.; "PubMed," n.d.). Since this time, the field of aging research has been rapidly expanding. Today, approximately 40,000 aging papers are published each year, over 100 times more than in 1974 ("PubMed," n.d.). This massive upsurge has propelled the advancement of the relatively new field of aging research over the last few decades.

What is aging, and what have we learned in the last few decades? One might consider that aging is dictated simply by the passage of time from birth, defined as chronological age, during

which time organismal function progressively declines. However, aging is clearly non-linear, and extensive heterogeneity exists in the aging process among individuals. Whereas some individuals look and function in a manner that is older than their actual age, others are seemingly younger and robust. The inequity of the aging trajectory suggests that aging is not merely a passage of time but a reflection of changes in biological processes caused by a combination of internal and external factors. This physiological age estimate is termed 'biological age.' Whereas chronological age tracks time's arrow, biological age is gauged by physiological and biological functions (Jazwinski & Kim, 2019). With this concept and our current scientific knowledge, aging can be defined as follows: "*The random change in the structure and function of molecules, cells, and organisms that is caused by the passage of time and by one's interaction with the environment. Aging increases the probability of death*." (McDonald, 2013). The recent profound growth of aging research has enhanced our understanding of this "random change." Currently, generally accepted mechanisms of aging include genetic instability, telomere attrition, epigenetic alteration, and loss of proteostasis, which lead to deregulated nutrient sensing, intercellular communication, mitochondrial dysfunction, cellular senescence, and stem cell exhaustion (López-Otín, Blasco, Partridge, Serrano, & Kroemer, 2013; M. B. Schultz & Sinclair, 2016). Consequently, these so-called "hallmarks of aging" drive tissue and organ dysfunction, loss of homeostasis, as well as attenuated tissue regeneration. The culmination of these declines causes progressively compromised organismal health.

1.3 Aging, Muscle, and Muscle Stem Cells

The importance of skeletal muscle health on organismal functioning may not be as obvious as in other tissues and organs, such as the brain and cardiovascular tissues. Nevertheless, the relevance of healthy muscle function to overall well-being cannot be overlooked. A myriad of studies have demonstrated a positive association between skeletal muscle function and healthspan (Lavasani et al., 2012; McLeod, Breen, Hamilton, & Philp, 2016; Metter, Talbot, Schrager, & Conwit, 2002) and an inverse relationship between muscle function and all-cause mortality (W. J. Lee et al., 2017; Roshanravan et al., 2017). For instance, one study that measured the grip strength of men over a 25-year period revealed that an accelerated rate of strength decline is associated with higher mortality (Metter et al., 2002). Another study reported that individuals over the age of 60 classified in the highest tertile of muscular strength had approximately 50% reduction in mortality rates from all causes, as compared to those in the lower third of the strength (Ruiz et al., 2008). The mechanisms of the beneficial effect of healthy skeletal muscle function on organismal health are not entirely understood. However, skeletal muscle has been suggested to play a key role in the maintenance of functions of other organs, including the brain, heart, and liver (W. Chen, Wang, You, & Shan, 2020; Delezie & Handschin, 2018; Pedersen & Febbraio, 2005), which could account for the positive correlation between muscle function and overall health.

Given the importance of skeletal muscle health for the maintenance of an individual's health, sustaining muscle function is evidently critical for a longer healthspan. Common contributors to age-related declines in muscle function include increased fat infiltration, decreased myofiber number, and alpha-motor neurons (McLeod et al., 2016). Moreover, just as is seen in so many tissues throughout the body, aging also impairs the regenerative capacity of skeletal muscle.

Stem cells play a critical role in tissue maintenance and regeneration, and stem cell exhaustion leads to an aged phenotype in many tissues and organs, including the epidermis, thymus, and cardiovascular tissues (Castilho, Squarize, Chodosh, Williams, & Gutkind, 2009; H. Liu et al., 2007; Minamino & Komuro, 2008; Ruzankina et al., 2007). Likewise, in skeletal muscle, healthy resident muscle stem cells (MuSCs) are essential for muscle regeneration (Shefer, Van de Mark, Richardson, & Yablonka-Reuveni, 2006; Shi & Garry, 2006). Typically, young, healthy muscle has a great capacity to restore its original architecture and restore its function after injury (Conboy, Conboy, Smythe, & Rando, 2003). However, the muscle's ability to regenerate efficiently curtails over time (Conboy et al., 2003). It has been suggested that this decreased regenerative capacity is primarily attributed to impaired MuSC function in aged muscle (Cosgrove et al., 2014; Sousa-Victor et al., 2014).

MuSCs are located beneath the muscle fiber basal lamina (MAURO, 1961). The MuSC population declines after birth, accounting for less than 6 % of the total nuclear content by 30 days of age in mice (E. Schultz, 1974). This number decreases to 2-3% in adulthood (Roth et al., 2000). This rare population of MuSCs expresses Pax7, a critical transcription factor for renewal and maintenance of MuSCs (Oustanina, Hause, & Braun, 2004; Seale et al., 2000). Upon injury, young, healthy quiescent MuSCs become activated and proliferate, co-expressing Pax7 and MyoD, a master regulator of myogenesis (Abdel Khalek et al., 2014; Hinits et al., 2011; Rudnicki et al., 1993). Following activation, Pax7 expression decreases, and cells fuse to form multinucleated functional myofibers (Le Grand & Rudnicki, 2007). Over time, however, MuSCs display diminished ability to activate, proliferate, and terminally differentiate toward a myogenic lineage, leading to impaired muscle regeneration and weakness (Brack et al., 2007; Conboy et al., 2003, 2005; Kimmel, Hwang, Scaramozza, Marshall, & Brack, 2020; Schäfer et al., 2006; E. Schultz &

Lipton, 1982). Several factors consistent with the hallmarks of aging have been implicated as culprits in stem cell aging, including cellular senescence, epigenetic alterations, and nutrient sensing (López-Otín et al., 2013; M. B. Schultz & Sinclair, 2016). Mitochondrial dysfunction, which is inextricably intertwined with the aforementioned hallmarks, is a hallmark of aging in itself (García-Prat et al., 2016; Kasper et al., 2009; López-Otín et al., 2013; H Zhang et al., 2016).

1.3.1 Mitochondrial Function and Its Significance in Aging

Historically, mitochondria have been considered the "powerhouse of the cell" due to their role in producing most of the energy that cells require in the form of adenosine triphosphate (ATP) by oxidative phosphorylation (OXPHOS) (Siekevitz, 1957). OXPHOS takes place at the electron transport chain on the inner mitochondrial membrane. Efficient ATP production through OXPHOS is essential for living organisms as ATP is involved not only in muscle contraction but also in other processes such as nucleic acid and protein synthesis, one of the most fundamental molecules for cellular function. However, a growing body of literature has demonstrated that the significance of mitochondria extends far beyond its role as the "powerhouse." For example, mitochondria play essential roles in a multitude of cellular functions, including intracellular signaling, cell cycle, and apoptosis (Green and John C. Reed, 1998; McBride, Neuspiel, & Wasiak, 2006), all of which are critical cellular functions important in dictating stem cell fate. Certainly, an escalating number of studies suggest that mitochondria function impacts stem cell identity and fate decisions (Ansó et al., 2017; Cheikhi et al., 2019; Jin et al., 2018; Khacho et al., 2016). MuSCs undergo a dynamic metabolic shift from OXPHOS in quiescence to upregulation of glycolysis during activation and proliferation, then back to OXPHOS at the terminal differentiation (Bhattacharya & Scimè, 2020; Ryall et al., 2015). This metabolic shift is suggested to be tightly connected with

MuSC fate decision (Bhattacharya & Scimè, 2020). Although our understanding of these mechanisms is limited, several aspects of mitochondria, including mitochondrial DNA integrity, mitophagy, and dynamics, have been shown to control stem cell responses (Jin et al., 2018; Khacho et al., 2016; Norddahl et al., 2011), further highlighting the crucial role of mitochondria function in dictating stem cell fate.

Throughout the body, increasing age is associated with compromised mitochondrial function (Sahu et al., 2018; Weber & Reichert, 2010). During OXPHOS, mitochondrial reactive oxygen species (ROS) are produced. ROS are part of crucial signaling pathways for cell fate decisions, such as cell proliferation, differentiation, and apoptosis (Burdon, 1995; Herbert, Bono, & Savi, 1996; J. Li et al., 2006). Indeed, ROS is associated with the activation and differentiation of MuSCs (Kozakowska, Pietraszek-Gremplewicz, Jozkowicz, & Dulak, 2015). Whereas ROS is detoxified at a moderate level by antioxidant enzymes in young, healthy cells (Veal, Day, & Morgan, 2007), cellular ROS accumulates with age, and excessive ROS leads to MuSC senescence (García-Prat & Muñoz-Cánoves, 2017). The increased ROS, along with the failure of detoxification by antioxidant enzymes, causes damage to nucleic acids, enzymes, and other biomolecules (Melov et al., 1999; Weber & Reichert, 2010), thereby leading to dysfunctional cellular systems that are commonly associated with tissue aging (Stadtman, 2002). In addition, recent studies demonstrated that mitochondrial ultrastructure is compromised with aging (Crane, Devries, Safdar, Hamadeh, & Tarnopolsky, 2010; El'darov, Vays, Vangeli, Kolosova, & Bakeeva, 2015; Sahu et al., 2018). Structural features that dictate mitochondrial ultrastructure, such as the mitochondria matrix and the folds of the inner mitochondrial membrane, or cristae, undergo reversible ultrastructural changes according to their functional state (Hackenbrock, 1966). Compromised cristae integrity is a driver of apoptotic pathways (Scorrano et al., 2002).

Furthermore, cristae morphology dictates the efficiency of mitochondrial respiration and cellular growth (Cogliati et al., 2013). Restoration of disrupted mitochondrial ultrastructure by the mitochondrially-targeted peptide, SS-31, demonstrated reduced mitochondria DNA damage, increased mitochondrial function, and differentiation capacity of muscle progenitor cells, leading to better regeneration of muscle (Sahu et al., 2018). These findings suggest that age-associated impairment of mitochondria crista integrity leads to abnormal stem cell fate and, thus, functional tissue decline.

Mitochondrial shape and dynamics are other essential determinants of organelle function that are compromised with aging (Y. J. Liu, McIntyre, Janssens, & Houtkooper, 2020; Weir et al., 2017; Y. Zhang et al., 2019). Mitochondria undergo constant fusion and fission to form a dynamic network structure, changing shape within minutes (Duarte et al., 2012). The mitochondrial network structure dynamics not only influences ATP production (Benard et al., 2007), but it is also important for other processes, such as mixing of mitochondrial DNA and removal of dysfunctional mitochondria to maintain mitochondrial quality (Meyer, Leuthner, & Luz, 2017). Indeed, disordered mitochondrial dynamics can cause pathologies such as cancer, cardiovascular disease, and neurodegenerative diseases (Archer, 2013).

To achieve highly dynamic mitochondrial structure alteration process, mitochondrial trafficking relies on cytoskeletal scaffolding, such as actin and microtubule networks (Bartolák-Suki, Imsirovic, Nishibori, Krishnan, & Suki, 2017; Morris & Hollenbeck, 1995). The actin network is essential for short-distance mitochondrial movements and immobilization of mitochondria (Boldogh & Pon, 2006). For long-distance transport, microtubules are essential (Melkov & Abdu, 2018; Vale, 2003), and inhibition of microtubule assembly completely arrests mitochondrial motility (Ligon & Steward, 2000). Actin fiber and microtubule networks are

regulated by extracellular mechanical cues (Nemir & West, 2010). For instance, extracellular biophysical properties, such as extracellular matrix (ECM) concentration and stiffness, causes changes in actin stress fiber and microtubule network formation (Kim, Sun, Lu, Zhang, & Wang, 2014; Mooney, Langer, & Ingber, 1995; Tojkander, Gateva, & Lappalainen, 2012). This mechanosensitive nature of the cytoskeletal network suggests that age-related alterations in muscle composition and mechanical properties could impact cytoskeletal network organization. This then further impairs mitochondria trafficking and, thus, undermines mitochondrial function as a whole.

1.4 Reversibility of Aging and the Importance of Stem Cell Niche

Whereas aged MuSCs exhibit deficits in mitochondrial function and myogenicity, as described above, studies of MuSC aging mechanisms showed the existence of "youthful" circulatory and other microenvironmental biomolecular factors that seem to be capable of improving aged MuSC function by reversing muscle aging at least in part (Brack et al., 2007; Brack & Muñoz-Cánoves, 2016; Conboy et al., 2003, 2005; Gopinath & Rando, 2008; Sahu et al., 2018; Sinha et al., 2014; Yousef et al., 2014). For instance, Conboy et al. demonstrated the restored function of aged MuSCs with the heterochronic parabioses model, where the circulatory system of young and aged animals are shared (Conboy et al., 2005). Using this model, investigators demonstrated that regeneration of tibialis anterior muscle from aged mice was enhanced to the level similar to young muscle (Conboy et al., 2005). The enhanced regenerative capacity was consistent with improved proliferation and activation of aged MuSCs when exposed to young blood *in vitro* (Conboy et al., 2005). These findings have since inspired numerous studies into the identification of circulatory biomolecules capable of transposing a youthful phenotype to aged stem cells.

In addition to the potential rejuvenating effects of circulatory factors on stem cell function, Engler et al. have similarly shown that biophysical factors may dictate cellular fate and function (Engler et al., 2004; Engler, Sen, Sweeney, & Discher, 2006). Specifically, matrices engineered to mimic the stiffness of brain, muscle, or collagenous bone promoted mesenchymal stem cells differentiation toward neurogenic, myogenic, or osteogenic lineages, respectively (Engler et al., 2006). Considering skeletal muscle is a tissue continuously exposed to mechanical stimuli, it is natural to speculate that myogenic cells and MuSCs are similarly highly mechanosensitive. Indeed, myogenic cells cultured on a substrate engineered to mimic the stiffness typical of normal muscle

(~12 kPa) robustly differentiated toward a myogenic lineage and formed myotubes with numerous myosin striations, whereas as a softer or stiffer microenvironment disrupted myogenic lineage specification and striation formation (Engler et al., 2004). Similar to myocytes, MuSCs are also mechanosensitive. Urciuolo et al. demonstrated a decreased number of quiescent MuSCs, increased number of activated MuSCs, and increased differentiating cells when MuSCs were cultured on 7 kPa, as compared to 12 kPa with media for maintenance of quiescent state (Urciuolo et al., 2013). Findings from another group also exhibited that MuSC quiescence positively correlated with substrate elasticity over the tested range (2, 6, 12, and 25 k Pa) (Quarta et al., 2016). Interestingly, these MuSC fate alterations caused by mechanical stimuli further dictate MuSC function, even after the cells are transferred to a new condition. For example, Gilbert et al. examined the engraftment of young MuSCs cultured on hydrogel with the stiffness of 12 kPa or 42 kPa and found a decline of MuSC engraftment potential when cells were cultured on 42 kPa substrate prior to transplantation into host muscle (Gilbert et al., 2010). Strikingly, a substrate engineered to mimic young, healthy muscle improved aged MuSC engraftment and subsequent regeneration after transplantation (Cosgrove et al., 2014). These previous reports indicate that tissue compliance is a vital element in the regulation of MuSC regenerative capacity and that pathological- and age-associated alterations of tissue stiffness may lead to abnormal MuSC function and concomitant impairment of muscle regeneration.

1.5 Age-Associated Alterations of Skeletal Muscle Biomechanical Properties and Their Impact on MuSC Fate

It is generally accepted that aged muscle has elevated rigidity when compared to young muscle. Recently, using biaxial muscle testing, Stearns-Reider and colleagues demonstrated that aged muscle displayed increased stiffness along the direction of ECM (i.e., perpendicular to the myofibers), but no change along the axis of myofibers when compared to young muscle (Stearns-Reider et al., 2017). These findings suggest that modulation of ECM abundance, composition, and structural properties, such as orientation, cross-linking, and tortuosity, may dictate muscle stiffness. Indeed, aged muscle displayed decreased tortuosity of collagen (Stearns-Reider et al., 2017), a primary structural ECM protein in muscle (Gillies & Lieber, 2011). Collagen cross-linking, which is mediated mainly by lysyl oxidase (LOX) and LOX-like enzymes (Bonnans, Chou, & Werb, 2014; Mitsuo Yamauchi, Terajima, & Shiiba, 2019), was also shown to increase in muscle with age (Gosselin, Adams, Cotter, McCormick, & Thomas, 1998). Several studies have also reported atypical ECM deposition and increased stiffness of aged muscle (Freitas-Rodríguez, Folgueras, & López-Otín, 2017; Gao, Kostrominova, Faulkner, & Wineman, 2008; Lacraz et al., 2015; Mann et al., 2011; Rosant, Nagel, & Pérot, 2007).

A negative impact of these age-related ECM changes was also reported *ex-vivo* in a study in which the authors demonstrated the myogenic-to-fibrogenic conversion of MuSCs seeded onto decellularized aged ECM (Stearns-Reider et al., 2017). These findings suggest that the age-associated alteration of ECM stiffness may contribute to the increased fibrogenic differentiation of MuSC during muscle regeneration. These findings further illustrate the vital role of microenvironment stiffness on MuSC fate within the physiologically relevant range. Nonetheless, little is known about the mechanisms by which age-associated muscle stiffening disturbs MuSC

fate. Thus, understanding the mechanisms of age-related muscle functional decline due to muscle stiffness alteration will be crucial for the development of the treatment to maintain healthy muscle in the elderly population.

1.6 Hypotheses and Specific Aims

Despite the widespread recognition of elevated muscle stiffness with age, to our knowledge, the magnitude of change has not been generally agreed upon due to a lack of a standardized method and outcome measure, making comparisons across the studies extremely challenging. Moreover, a few studies reported controversial results, with some studies demonstrating little change in muscle stiffness among different age groups and others showing decreased stiffness of aged muscle (Dresner et al., 2001; Eby et al., 2015). Therefore, the difference between young and aged muscle elasticity is not evident. In these studies, measurements of young and aged muscle stiffnesses from our laboratory were reported. Furthermore, there is much to be investigated into the impact of the muscle microenvironmental stiffness shift within the physiologically relevant range on MuSC function and the potential mechanisms by which aberrant stiffness drives the aged MuSC phenotype. Given the mitochondrial dysfunction associated with age and the potential role of mitochondria in dictating MuSC function as reviewed in Chapter 1.3.1, the link between age-associated modifications of micromechanical environment and decreased mitochondrial function is worth further exploration as a possible mechanism of age-related MuSC functional decline. These thesis studies tested the primary hypothesis that *biomechanical signals emanating from the aged skeletal muscle ECM have a detrimental effect on MuSC mitochondrial function, ultimately driving a MuSC fibrogenic conversion*.

To assess this hypothesis, first, the effect of age-related muscle stiffness alteration on MuSC fate was examined. Next, the mechanisms by which a stiff microenvironment drives MuSC dysfunction were investigated with the focus on mitochondrial function. Finally, an *in vivo* model was used to evaluate whether modulation of aged muscle biomechanical microenvironment improves muscle regeneration. Two specific aims tested our primary hypothesis:

Specific Aim 1: To investigate whether aberrant MuSC fate in response to a stiff microenvironment is mediated by mitochondrial dysfunction

Specific Aim 2: To evaluate whether modulation of aged muscle biomechanical microenvironment improves muscle regeneration

2.0 Aged Muscle Stem Cell Sensitivity to Matrix Stiffening Disrupts Differentiation Kinetics Through Dysregulation of SIRT3

Data presented in this chapter have been prepared for journal submission.

Contributing Authors:

Hikaru Mamiya, Amrita Sahu, Sruthi Sivakumar, Hirotaka Iijima, Zach Clemens, Lena Richards, Amanda Miller, Sunita N. Shinde, Gabriele Nasello, Anne M. Robertson, David A. Vorp, Aaron Barchowsky, Antonio D'Amore, Thomas A. Rando, Fabrisia Ambrosio

2.1 Summary

Aging is typically associated with declines in skeletal muscle regenerative capacity and functional recovery after injury. For efficient muscle regeneration, resident muscle stem cells (MuSCs) are essential. However, over time, MuSCs display a progressively diminished myogenic lineage specification. Here, we utilized single-cell level analysis at mRNA and protein levels to investigate the influence of age-related biophysical alterations on MuSC fate. Single cell RNA-seq and imaging flow cytometry revealed that aged MuSC activation was enhanced by exposure to a soft substrate. Moreover, given mitochondrial activity has been shown to play a role in dictating stem cell fate, we investigated whether mitochondria-associated gene expression is perturbed in response to a stiff microenvironment. Our data suggest that the age-dependent decrease in levels of MuSC SIRT3, a key mitochondria-associated protein that regulates several critical mitochondrial functions, is restored to youthful levels when cells are exposed to a soft

microenvironment. Further, we show that SIRT3 expression facilitates MuSC activation *in vitro* and muscle regeneration and function *in vivo*. Our findings highlight a previously unrecognized mechano-dependent role of SIRT3 in MuSC activation and muscle regeneration.

2.2 Introduction

Skeletal muscle regenerative capacity and functional recovery after an injury decline with advancing age, leading to decreased mobility, increased morbidity, and, ultimately, reduced quality of life of older individuals. The age-associated decrease in muscle regenerative capacity is, in part, caused by functional impairment of resident muscle stem cells (MuSCs), which display an impaired activation, proliferation, and myogenic lineage specification over time (Brack et al., 2007; Conboy et al., 2003, 2005; E. Schultz & Lipton, 1982). MuSC lineage progression is highly dependent on meticulous regulation of mitochondrial metabolites and OXPHOS dynamics, a regulation that is impaired with age (Bhattacharya & Scimè, 2020; Hongbo Zhang, Menzies, & Auwerx, 2018). Yet, factors instigating energetic declines over time are poorly understood. Whereas aged MuSCs clearly display cell-autonomous deficits that contribute to impaired regeneration (Cosgrove et al., 2014; Sousa-Victor et al., 2014), a growing number of studies suggest that aberrant biophysical properties of the extracellular matrix (ECM) may represent critical drivers of MuSC functional decline (Cosgrove et al., 2014; Gilbert et al., 2010; Quarta et al., 2016; Stearns-Reider et al., 2017).

Tissue mechanical properties direct stem cell fate, and a series of elegant *in vitro* studies have demonstrated the exquisite mechanosensitivity of stem cells (Dupont et al., 2011; Engler et al., 2006; Gilbert et al., 2010). For instance, mesenchymal stem cells spontaneously differentiated

toward a myogenic lineage when seeded on a soft substrate engineered to mimic the compliance of young, healthy muscle (elastic modulus (E): 8 – 17 kPa). On the other hand, osteogenic differentiation was observed when cells were seeded on a stiffer substrate (E: 25 – 40 kPa) (Engler et al., 2006). As biophysical characteristics of the ECM are altered with aging (Gosselin et al., 1998; Stearns-Reider et al., 2017; ZIMMERMAN, MCCORMICK, VADLAMUDI, & THOMAS, 1993), these *in vitro* findings underscore the potential impact of age-associated abnormal ECM remodeling on MuSC function *in vivo*.

Aged muscle is typically characterized by abnormal ECM deposition and increased tissue stiffness (Freitas-Rodríguez et al., 2017; Gao et al., 2008; Lacraz et al., 2015; Mann et al., 2011; Rosant et al., 2007). In addition, with increasing age, collagen cross-linking accumulates, contributing to an overall increased muscle stiffness (Gosselin et al., 1998). Further contributing to altered biophysical ECM properties with increasing age, recent studies from our laboratory have revealed decreased collagen tortuosity and a concomitant increased muscle rigidity along the axis of collagen fibrils in aged muscle (Stearns-Reider et al., 2017). These age-related ECM alterations have direct effects on MuSC lineage specification. MuSCs seeded onto decellularized ECM from aged muscle displayed an increased fibrogenic conversion when compared to cells cultured on decellularized ECM derived from young muscle (Stearns-Reider et al., 2017). However, the downstream mechanosensitive mediators between ECM biophysical factors and stem cell fate determination are poorly understood.

In these studies, we tested the hypothesis that a "stiff" microenvironment, which is a characteristic of aged muscle, drives MuSC mitochondrial dysfunction, thereby impairing MuSC myogenicity and functional skeletal muscle regeneration. *In vitro*, the impact of substrate stiffness on MuSC characteristics was assessed at the level of nuclear morphology, single-cell transcripts,

and protein expression. We found that young MuSCs were resistant to alterations in substrate stiffness, maintaining a consistent lineage progression, regardless of biophysical cues. Aged MuSCs, on the other hand, were highly sensitive to extrinsic mechanical stimuli. Specifically, single-cell analysis indicated that aged MuSCs exposed to a stiff substrate delayed myogenic lineage progression. Further investigation implicated SIRT3, a master regulator of mitochondria, as a novel mechano-sensitive factor that is downregulated when aged MuSCs are cultured on a stiff substrate. This finding suggests that SIRT3 levels may act as a factor that mediates external mechanical cues to mitochondrial function, thus, regulating MuSC fate. *In vivo*, we found that decreasing the stiffness of aged muscle by inhibiting collagen cross-linking increased SIRT3 expression and improved functional muscle regeneration in aged animals. Together, these results implicate SIRT3 expression as a novel age-dependent mechanosensitive mediator of muscle regeneration.

2.3 Results

2.3.1 Aged Skeletal Muscle Is Approximately 3.5 Times Stiffer Than Young Counterparts, a Change That Drives Aberrant MuSC Lineage Specification

Several studies have previously reported increased muscle stiffness over time (Gosselin et al., 1998; Lacraz et al., 2015; Rosant et al., 2007; Stearns-Reider et al., 2017). However, the reported stiffness of aged muscle has not been consistent in the literature (Alfuraih, Tan, O'Connor, Emery, & Wakefield, 2019; Eby et al., 2015; Gajdosik, Vander Linden, & Williams, 1999). This discrepancy may be due to the lack of standardized experimental methods for soft tissue stiffness measurements. For example, bulk scale measurements such as ultrasound, magnetic resonance elastography (MRE), and uniaxial mechanical testing do not necessarily capture the microscale stiffness sensed by the cells (D'Amore et al., 2014), resulting in a potential disconnect between whole muscle biophysical properties and cell responses. Moreover, uniaxial mechanical testing is limited because it does not allow for assessment of out-of-axis properties of biological tissue, nor does it allow for the detection of potential changes in tissue mechanics dictated by alterations in the 2D micro-architecture. To overcome these limitations, we investigated microscale muscle stiffness in young (4-6 months) and aged (22-24 months) skeletal muscle. An in-plane maximum Green's strain energy map was derived using the biaxial mechanical characterization of young and aged muscles, as previously described (D'Amore et al., 2014). From this data, we performed a finite element simulation of fiber network mechanical behavior (**Figure 1A**). This method is capable of predicting microscale stiffness from macroscale measurements of biaxial mechanical testing. Data revealed that the peak of the Green's strain deformation histogram, E_f, was significantly lower in the aged muscle when compared to the young

counterparts (**Figure 1B, C**). Equi-stress biaxial data were then utilized to derive the constants of Yeoh's constitutive equation used in the finite element fiber network model (D'Amore et al., 2014). Experimentally-derived fiber mesh model predictions (Carleton, D'Amore, Feaver, Rodin, & Sacks, 2015; D'Amore et al., 2014) revealed that aged muscle is approximately 3.5-fold stiffer than young muscle. This calculation is based on the material properties [C_{10}, C_{20}; Yeoh model] that have been determined by fitting the experimental biaxial data with the model biaxial response prediction. More details on the formulation utilized to model the ECM mechanics are provided in previously published work (D'Amore et al., 2018). Consistent with our findings, other studies reported a range of 8 - 17 kPa for the young muscle stiffness (Engler et al., 2004; Gilbert et al., 2010; Lacraz et al., 2015). From these findings, we estimated aged muscle stiffness to be in the range of 28 to 60 kPa.

Changes in biophysical properties of the stem cell microenvironment alter cell responses via mechanotransductive signaling cascades, and extrinsic mechanical strains sensed by cells induce downstream nuclear deformation, resulting in chromosomal reorganization and gene expression alterations (Pajerowski, Dahl, Zhong, Sammak, & Discher, 2007; Spagnol & Dahl, 2014). To quantify age-related alterations in MuSC nuclear morphology, we used a cell image analysis software, CellProfiler™, to obtain 53 morphological features of young and aged MuSC nuclei cultured on a 2D substrate (**Figure 1D**). Unsupervised Principal Component Analysis (PCA) followed by supervised Linear Discriminant Analysis (LDA) revealed that young and aged MuSCs display significantly distinct nuclear morphologies, as evidenced by segregated clustering features (**Figure 1E; Appendix Figure 1A, B**). PC1 features effectively classified cells according to age. Key PC1 factors were then determined based on loading matrix ranking. Among the key PC1 factors allowing for age-associated discrimination, we found that nuclear area was significantly decreased in aged cells when compared to young counterparts (**Figure 1E)**.

We cannot, however, discount the possibility that differences observed between groups may be an artifact of an adherent cell culture system. To address this potential confounding factor, we performed imaging flow cytometry analysis of young and aged MuSCs and evaluated whether age-dependent nuclear morphological features are retained and detected in suspension (**Figure 1F**). As was observed in the adherent culture model, dimension reduction by PCA and subsequent LDA revealed that suspended young and aged MuSC nuclei clustered separately (**Figure 1G; Appendix Figure 1C**). Interestingly, however, the nuclear area of suspended aged MuSCs was significantly larger as compared to young MuSCs (**Figure 1G**). When we compared nuclear area within tissue cross-sections of young versus aged muscle, we found that aged nuclei were significantly larger relative to young counterparts (**Figure 1H, I**). These findings are consistent

with previous reports demonstrating an increased nuclear area in basal keratinocytes and mitral cells with aging *in vivo* (Hinds & McNelly, 1977; Liao et al., 2013) and suggest that evaluation of cell morphological characteristics in suspension may provide a more physiologically-relevant estimate of relative group differences according to age.

In order to probe whether increased aged muscle stiffness may contribute to the observed alterations in MuSC nuclear size, we fabricated silicone-based organic polymer, polydimethylsiloxane (PDMS) substrates to mimic the stiffness of young (elastic modulus (E): 12 kPa)) or aged muscle (E: 29 kPa), according to a previous report (Iberite, Salerno, Canale, Rosa, & Ricotti, 2019). After one week of culture on the soft or stiff substrate, the nuclear morphology of young and aged MuSCs was characterized in suspension (**Figure 1J**). Imaging flow cytometry-based analysis of nuclear features followed by PCA and LDA revealed that stiff substrates significantly altered nuclear morphological features in aged, but not young, MuSCs (**Figure 1K, L**), suggesting that aged MuSCs may be more sensitive to changes in biophysical characteristics emanating from the microenvironment when compared to young counterparts. Specifically, we found that aged cells exposed to a stiff environment displayed a significantly increased nuclear area when compared to aged cells seeded on a soft substrate (**Figure 1M**). Young MuSCs, however, displayed a relative resistance to changes in nuclear area according to substrate stiffness (**Figure 1M**).

2.3.2 Aged MuSCs Cultured on a Soft Substrate Display a More Youthful Lineage Progression

The above findings are consistent with previous studies demonstrating altered nuclear morphology, structure, and integrity in aged cells (Pathak, Soujanya, & Mishra, 2021; Webster,

Witkin, & Cohen-Fix, 2009), alterations that are likely influenced by microenvironmental stiffness changes over time. However, whether and how aging affects cellular sensitivity to extrinsic biophysical stimuli and its impact on stem cell fate determination is unknown. To comprehensively define the trajectory of MuSC fate according to age and in response to varying substrate stiffness, we performed single cell RNA-seq (scRNA-seq) on young and aged MuSCs cultured on soft or stiff PDMS substrates for one week (**Appendix Figure 2A - C**). We chose scRNA-seq because it allows for evaluation of sub-population heterogeneity and, specifically, MuSC lineage progression across experimental groups.

First, MuSC lineage progression was described according to the presence of well-established myogenic differentiation markers, Pax7, Myf5, Myod1, Myogenin, and Desmin (**Figure 2A**). After dimensionality reduction of scRNA-seq data from young and aged MuSCs exposed to soft or stiff PDMS substrates, each cell was plotted according to the five myogenic differentiation markers (**Figure 2B**). Of note, there was a negligible number of quiescent cells (*Pax7*+, *Myod1*-) in our populations, likely owing to the fact that cells were cultured for one week. Based on the myogenic markers and unsupervised clustering, we then performed pseudotime analysis in order to define four stages of differentiation: early activation, late activation, early differentiation, and late differentiation at the seven-day culture time point (**Figure 2C**). In aged MuSCs exposed to stiff substrates, *Pax7* was lowest at the early and late activation stages. In contrast, *Pax7* expression of young MuSCs cultured on a stiff substrate was relatively high (**Figure 2D**). Along with a blunted *Pax7* expression in aged cells, a stiff substrate increased expression of *Myod1* at early and late activation (**Figure 2E**). These observations are consistent with findings showing lower *Pax7* and higher *Myod1* mRNA levels in aged MuSCs when compared to young MuSCs (Chakkalakal, Jones, Basson, & Brack, 2012), suggesting that aged MuSCs display mRNA

levels of *Pax7* and *Myod1* that are closer to the mRNA profile of young MuSCs when cultured on a soft substrate. We then confirmed PAX7 and MYOD1 expression at the protein level across the experimental groups using imaging flow cytometry. Freshly isolated aged MuSCs exhibited an increased number of quiescent (PAX7+/MYOD-) and fewer activated (PAX7+/MYOD+) cells when compared to young MuSCs (**Figure 2F, G**). Of note, approximately 87% of MuSCs are found to express MyoD within nine hours post-euthanasia (Zammit et al., 2002), in line with our observation of ~70% of activated cells in the young cell populations of our samples. These findings support previous reports suggesting aberrant activation of aged MuSCs (Kimmel et al., 2020; L. Liu et al., 2018). Accordingly, a stiff substrate resulted in impaired activation of aged MuSCs, as evidenced by a decrease in the percentage of PAX7+/MYOD+ cells when compared to aged cells cultured on a soft substrate (**Figure 2H, I**). Activation/differentiation of young MuSCs, on the other hand, was unchanged regardless of whether cells were seeded on a soft or stiff substrate (**Figure 2H, I**), findings that were consistent with the lack of changes in nuclear morphology when young MuSCs were seeded onto a soft or stiff substrate (**Figure 1M**). Taken together, these findings suggest that aging may sensitize MuSC to mechanical signals emanating from the microenvironment and that this sensitivity contributes to perturbations in MuSC differentiation kinetics.

2.3.3 The Age-Dependent Response to Substrate Stiffness Converges on the MYC-SIRT3 Axis

MuSC progression from quiescence to proliferation and differentiation is a metabolically dependent process that requires meticulous regulation of mitochondrial structure and function (Bhattacharya & Scimè, 2020; Dell'Orso et al., 2019; Rocheteau, Gayraud-Morel, Siegl-

Cachedenier, Blasco, & Tajbakhsh, 2012). Studies have shown that mitochondrial dysfunction — a well-known hallmark of aging (López-Otín et al., 2013)— directly influences MuSC activation and differentiation (Bhattacharya & Scimè, 2020; Hori, Hiramuki, Nishimura, Sato, & Sehara-Fujisawa, 2019; Majmundar et al., 2015; Ryall et al., 2015; Tang & Rando, 2014; X. Yang, Yang, Wang, & Kuang, 2017). With this in mind, we probed for changes in mitochondrial gene expression in quiescent versus activated MuSCs and compared mitochondrial gene expression profiles of MuSCs isolated from uninjured and injured muscles. For this, we accessed scRNA-seq data of young and aged MuSCs isolated from uninjured muscle that is available from the Tabula Muris consortium (**Appendix Figure 3A - C**). In addition, we performed scRNA-seq analysis obtained from young and aged MuSCs isolated from tibialis anterior (TA) muscles one day after injury (**Appendix Figure 4**). Strikingly, whereas young MuSCs displayed a robust response of mitochondria-associated gene expression in response to injury, this response was markedly blunted in aged MuSCs (**Figure 3A**). Given that mitochondrial function is intimately intertwined with cytoskeletal features that are responsive to extrinsic biophysical stimuli (Bartolák-Suki et al., 2017; Morris & Hollenbeck, 1995; Nemir & West, 2010), we posited that increasing matrix stiffness disrupts cellular energetics with aging, in turn altering MuSC fate.

To test this hypothesis and better understand the resistance of young cells to substrate stiffness and the relative sensitivity of aged cells, we revisited the scRNA-seq data from young and aged MuSC samples cultured on soft or stiff substrates and compared mitochondria-associated genes across the four groups. Unexpectedly, the bulk of mitochondria-associated genes showed no age-dependent response to substrate stiffness. However, four genes — *Nme2*, *Bloc1s1*, *Gstp1*, and *Gstp2* —displayed a robust, yet inverse, response to substrate stiffness according to age. Specifically, whereas the expression of these four genes was increased in aged MuSCs in response

to a stiff substrate, their expression was proportionately decreased in young MuSCs (**Figure 3B**). In other words, decreased expression of these four genes was increased by approximately 1- to 2-fold in aged MuSCs when cultured on a stiff microenvironment, but the opposite response was observed in young MuSCs when cultured under the same conditions. This finding suggests that these four genes may contribute to the age-dependent mitochondrial response of cells to varying substrate stiffness.

To probe for a common signaling cascade of these four genes, we performed transcription factor enrichment analysis using the ChEA3 software. Of a total of 1,632 transcription factors regulating these genes, *Myc* was the only gene that was both common to all four genes and also displayed an age-dependent response to substrate stiffness. Specifically, evaluation of *Myc* expression dynamics according to age and in response to substrate stiffness revealed that *Myc* expression gradually decreased as young MuSCs progressed into differentiation stages, but that aged MuSCs displayed increasing *Myc* expression with lineage progression (**Figure 3C**). *Myc* is of interest for its critical role in stem cell fate regulation previously reported in hematopoietic and epidermal stem cells (Gandarillas & Watt, 1997; Wilson et al., 2004). Importantly, *Myc* has been shown *in vitro* to inhibit myoblast differentiation (Luo et al., 2019).

Next, we explored the *Myc*-driven molecular network regulation in young versus aged MuSCs by generating a protein-protein network using the string database with BLOC1S1, NME2, GSTP1, GSTP2, and MYC as input variables. The five proteins did not directly interact (**Appendix Figure 5A**), suggesting the presence of an intermediate factor(s). When we probed for co-factors of MYC that may regulate BLOC1S1, NME2, GSTP1, and GSTP2, SIRT3 and SOD2 emerged as candidates of interest (S.-T. Li et al., 2020; Z. Liu et al., 2015; Yao et al., 2014), and the addition of SIRT3 and SOD2 in the protein-protein network improved the network connectivity, as

evidenced by the increased average node degree from 0.8 to 1.71 (**Figure 3D**). NME2 upregulates MYC, which in turn, leads to degradation of the deacetylase, SIRT3, via activation of SKP2-mediated ubiquitination and subsequent proteasomal function (S.-T. Li et al., 2020; Yao et al., 2014). SIRT3 is important for activation of the antioxidant, SOD2, to reduce ROS-mediated mitochondrial damage, a function shared by GSTP proteins (Meng et al., 2019; Yin et al., 2018). The BLOC-1 complex also has a potential role in counteracting the action of SIRT3 (Scott, Webster, Li, & Sack, 2012). Taken together, our findings suggest that the age-dependent mechanosensitivity of aged MuSC fate may be mediated by SIRT3 (**Figure 3E**).

2.3.4 SIRT3 Protein Levels, Critical for Functional Muscle Regeneration, Are Decreased in MuSCs Seeded on a Stiff Substrate

Though it is well-established that age-related declines in SIRT3 are a driver of mitochondrial dysfunction over time (Joseph et al., 2012; Kincaid & Bossy-Wetzel, 2013; Zeng et al., 2014), no studies to date have identified a role for SIRT3 in MuSC lineage progression. Moreover, no studies have investigated whether declines in SIRT3 contribute to a compromised regenerative response of aged skeletal muscle. To examine whether SIRT3 expression is decreased with aging, MuSCs were freshly isolated from young and aged TAs one day after injury. Imaging flow cytometry revealed significantly reduced SIRT3 levels in aged MuSCs compared to young counterparts (**Figure 4A**). To further confirm the potential impact of SIRT3 expression on MuSC fate, we isolated MuSCs from young $SIRT3^{-/-}$ mice and age-matched wild-type counterparts one day after an injury and evaluated PAX7 and MYOD expression across the groups. Consistent with aged MuSCs (**Figure 2F, G**), $SIRT3^{-/-}$ MuSCs displayed a higher PAX7+/MYOD- quiescent MuSC population and a lower PAX7+/MYOD+ activated population (**Figure 4B, C**). This altered MuSC lineage progression in $Sirt3^{-/-}$ mice was concomitant with reduced muscle weight and a blunted functional recovery after an injury (**Figure 4D, E; Appendix Table 1**).

The aforementioned findings suggest that SIRT3 levels may be differentially regulated according to age and mechanical signals emanating from the microenvironment. To test this hypothesis, we evaluated the potential mechanosensitivity of SIRT3 by quantifying SIRT3 protein levels in young and aged MuSCs cultured on soft or stiff substrates. Both young and aged MuSCs displayed reduced SIRT3 expression when cultured on the stiffer substrates, though the magnitude of change in SIRT3 levels in young MuSCs was blunted when compared to aged counterparts (**Figure 4F G**). Of note, we did not observe any change in SIRT3 transcripts across the

experimental groups **(Appendix Figure 5B)**. This finding suggests that the protein-level differences observed with aging and in response to a stiff substrate are likely to be a function of post-translational regulation, which would be consistent with the role of MYC for SIRT3 protein degradation**.** Consistent with a loss of SIRT3 with aging and a stiff microenvironment, we observed a concomitant increase in genes that may be suggestive of mitochondrial stress, including *Pink1*, *Lonp1*, *Map1lc3b*, and *Fis1* (**Figure 4H**).

We then used a loss-of-function paradigm to probe the direct effect of mechanotransductive signaling on SIRT3 expression in MuSCs. Dose testing was performed to identify the optimal dose for administration of Latrunculin A (Lat A) **(Appendix Figure 6A, B)**, which impairs mechanotransductive responses through inhibition of actin polymerization (Panciera, Azzolin, Cordenonsi, & Piccolo, 2017)**.** When aged MuSCs seeded on a stiff substrate were treated with Lat A, SIRT3 expression was increased to levels comparable to aged MuSCs seeded onto a soft substrate (**Figure 4I, J**). Young MuSCs, however, were relatively resistant to modulation of SIRT3 via mechanotransductive signaling (**Figure 4I, K**). These results suggest that mechanical signals from the microenvironment regulate MuSC SIRT3 protein levels in an age-dependent manner.

2.3.5 Inhibition of Collagen Cross-Linking in Aged Muscle Increases SIRT3 Protein Levels and Improves Skeletal Muscle Regeneration

To test the physiological relevance of the above *in vitro* findings, we tested whether modulation of ECM stiffness in aged mice could enhance skeletal muscle regeneration *in vivo*. There is abundant evidence demonstrating that aging drives an increase in collagen cross-linking in several tissues, including skeletal muscle (Thomas, McCormick, Zimmerman, Vadlamudi, & Gosselin, 1992; M Yamauchi, Woodley, & Mechanic, 1988; ZIMMERMAN et al., 1993),

suggesting that an age-related increase in tissue stiffness may be attributed to the alterations in ECM cross-linking density and network architecture. The primary enzyme that induces collagen cross-linking is lysyl oxidase (LOX) (Mitsuo Yamauchi & Sricholpech, 2012). Therefore, we manipulated the skeletal muscle cross-linking in aged mice by injecting a LOX inhibitor, β-aminopropionitrile (BAPN), subcutaneously every day for six weeks. After four weeks of injections, a cardiotoxin injury was induced to TAs bilaterally (**Figure 5A**). We chose BAPN since it has been reported to reduce collagen cross-linking and stiffness in lung, aorta, bone, and skeletal muscle (Brüel, Ortoft, & Oxlund, 1998; Mammoto, Jiang, Jiang, & Mammoto, 2013; McNerny, Gong, Morris, & Kohn, 2015; Spengler, Baylink, & Rosenquist, 1977; Willems, Miller, & Stauber, 2001). There were no significant changes in body weight six weeks of daily BAPN injections at two different dosages (Low: 80 µg/µL and High: 290 µg/µL). In addition, a limited tissue set (muscle, aorta, heart, liver, and kidney) submitted to Jackson Labs for histopathological assessment revealed no evidence of pathology (n=3/dose; **Appendix Figure 7A**). We also confirmed that mature collagen cross-linking in BAPN-treated aged animals was significantly decreased when compared to age-matched control counterparts (**Appendix Figure 7B**).

We first revisited the CellProfiler image analysis along with PCA and LDA to examine the effect of BAPN treatment on nuclear shape of regenerating muscle *in vivo*. While control and BAPN groups did not segregate when analyzed by PCA, LDA indicated significantly different morphological characteristics between the control and BAPN groups in aged MuSCs (**Figure 5B**). Further examination into nuclear morphologies revealed that BAPN treatment groups of aged muscles displayed significantly reduced MuSC nuclear area, thereby trending towards a more youthful MuSC nuclear phenotype (**Figure 1G, I; Figure 5C**).

We next evaluated whether decreased mature cross-linked collagen with BAPN treatment enhances SIRT3 levels at an injury site and improves muscle regenerative capacity. Consistent with our *in vitro* findings, the data demonstrated that SIRT3 expression was enhanced at the injury site when aged mice were treated with BAPN (**Figure 5D**). Accordingly, we found that the myofiber cross-sectional area of regenerating fibers at 14 dpi in BAPN-treated aged mice was significantly increased compared to the control counterparts (**Figure 5E, F**). Interestingly, there was a significant correlation between nuclear area and myofiber cross-sectional area when considering aged control and BAPN groups (**Figure 5G**). However, this correlation was lost when young control sample was included in the analysis, as evidenced by linear regression analysis (aged groups: R^2=0.20, p=0.04; all groups: R^2=0.13, p=0.06). These findings are consistent with the aforementioned relative sensitivity of aged nuclei morphology to microenvironmental cues when compared to young counterparts (**Figure 5G**). We then examined whether the youthful myofiber and nuclear morphology characteristics observed in BAPN treated aged animals resulted in enhanced muscle function. Indeed, *in situ* contractile testing of aged TA muscles revealed that muscle function was enhanced to the level commensurate with young muscle after BAPN treatment (**Figure 5H**). The half relaxation time of aged muscle, an indication of muscle composition and quality, was also reduced to the level comparable to young muscle with BAPN treatment (**Figure 5I**). Of note, there was no appreciable difference in muscle function between uninjured groups after exposure to saline or BAPN (**Appendix Figure 7C**). These data suggest that muscle stiffness is important for MuSC function and regenerative cascades but may be less important in the context of muscle homeostasis. Taken together, these data suggest that SIRT3 may mediate signals from extrinsic microenvironment to mitochondrial function, ultimately dictating MuSC fate, and hence, muscle regeneration.

2.4 Discussion

In this study, we tested the hypothesis that aberrant lineage specification of aged MuSCs is mediated by ECM-induced alterations of mitochondrial function. To test this hypothesis, we first implemented a combination of *in vitro* studies to evaluate the direct impact of substrate stiffness on subpopulation heterogeneity at the level of nuclear morphology, single-cell transcripts, and protein expression. We found that exposure of aged MuSCs onto a soft substrate restored a nuclear area comparable to that of young MuSC counterparts. Given that nuclear size dictates cellular gene expression and responses (Webster et al., 2009), we posited that the observed changes in nuclear morphology disrupt aged MuSC fate. Indeed, pseudotime analysis using single cell RNA-seq demonstrated a decreased activation of aged MuSCs when compared to young counterparts, an effect that was exacerbated by a stiff microenvironment. These findings were confirmed at the protein level, as determined by the expression of PAX7 and MYOD, two canonical markers of stem cell quiescence and activation, respectively. Importantly, we observed that, whereas young MuSCs were relatively resistant to changes in extrinsic matrix properties, aged MuSCs were sensitized to biophysical cues emanating from the microenvironment. Further investigation into the potential mechanisms by which aged MuSC fate is dictated on various microenvironment stiffness suggested that SIRT3 may be a critical mechano-sensitive factor that regulates other key mitochondria-associated gene alterations. The data revealed a previously unrecognized role for SIRT3 in MuSC activation and muscle regeneration. Finally, we tested the physiological relevance of the *in vitro* findings by evaluating whether reduction of aged muscle stiffness leads to enhanced muscle regeneration in aged mice. Indeed, we found that modulation of biophysical ECM characteristics enhanced myofiber cross-sectional area and force-producing capacity, effects that were concomitant with increased SIRT3 protein levels at the site of muscle

injury. As to the future potential clinical application of these findings, in order to enhance MuSC transplantation efficacy, we envision that it one day may be possible to pre-condition and expand aged MuSCs on a soft substrate *in vitro*, sort out "aged" MuSCs non-invasively based on nuclear morphology, and transfer only rejuvenated MuSCs to a host muscle tissue. In addition, our findings suggest that modulation of muscle stiffness, especially in an elderly population, maybe an essential intervention to improve muscle regeneration after an injury or during rehabilitation.

Stem cell fate is influenced by stiffness of the surrounding niche (Dupont et al., 2011; Engler et al., 2006; Gilbert et al., 2010). While age-associated alterations of muscle stiffness have been well-documented (Lacraz et al., 2015; Rosant et al., 2007), the link between the increased muscle stiffness and its direct impact on MuSC function is largely unknown. One of the potential links is stiffness-induced nuclear deformation, as the nuclear shape directly impacts gene expression and stem cell fate (Dahl, Booth-Gauthier, & Ladoux, 2010). Therefore, we first posited that age-associated increase in muscle stiffness alters MuSC nuclear morphologies. We found that while young MuSCs displayed resistance to nuclear size alterations regardless of substrate stiffness, aged MuSC were highly sensitive to biophysical substrate characteristics, with a stiff microenvironment further exacerbating an aged phenotype. Importantly, although aged MuSCs displayed a decreased nuclear area relative to young MuSCs when cultured on a 2D substrate, an increased nuclear size with aging and in response to a stiff substrate was observed when cells were evaluated under suspension, in which cytoskeletal influences are minimized. These seemingly paradoxical findings may be a reflection of a higher stiffness of aged MuSC nuclei that makes them more resistant to spreading when in contact with a 2D substrate as compared to young counterparts, though the effect of aging on nuclear stiffness is still debated (Heys, Cram, & Truscott, 2004; Phillip, Aifuwa, Walston, & Wirtz, 2015). Notably, disruption in nuclear lamin

levels is associated with accelerated aging syndromes and lamin-related disorders that lead to muscle diseases (Ghosh & Zhou, 2014). These factors may be worth further investigation to unveil potential mechanisms of age-dependent mechanosensitivity of MuSCs as lamin A deficiency is also associated with impaired mechanotransduction (Lammerding et al., 2005). Further studies connecting MuSC fate alterations and nuclear morphological changes due to mechanosensitive lamin expression may be an interesting direction for future research.

While it has been previously demonstrated that increased matrix stiffness impairs terminal stem cell differentiation, including MuSC myogenicity, studies to date have only evaluated terminal endpoints (Engler et al., 2006; Gilbert et al., 2010). To better understand lineage progression dynamics during which matrix stiffness disrupts MuSC fate, we performed pseudotime trajectory analysis using scRNA-seq. Based on these findings, we found that decreased myogenicity of aged MuSCs cultured on a stiff microenvironment may be attributed to a relative decrease in *Pax7* during early activation and a concomitant increased expression of *Myod1*. This pattern is consistent with a previous report showing that aged MuSCs exhibit lower *Pax7* and higher *Myod1* mRNA levels when compared to young MuSCs (Chakkalakal et al., 2012). In addition, our data confirmed previous studies showing that in young, healthy cells, *Pax7* gene expression does not decline linearly through lineage specification, as indicated by pseudotime analysis (Kimmel et al., 2020). Instead, the expression level is non-monotonic, increasing in late activation and early differentiation stages, then decreasing again with late differentiation. While Kimmel et al. found significant differences in activation, but only moderate changes in transcriptional states between young and aged MuSCs at 18 hours after MuSC isolation, we extended the cell culture time to include the late differentiation stage. We found that expression of myogenic markers, *Pax7* and *Myod1*, were altered in age- and stiffness-dependent manner.

Furthermore, our scRNA-seq data at early and late activation stages indicated that physiologically-relevant increases in stiffness differentially influence myogenic marker levels in young and aged MuSCs. These differences in myogenic marker levels were not found previously in single cell level with pseudotime analysis when MuSCs were cultured on a supraphysiological plastic cell culture dishes. Taken together, these findings suggest that careful temporal regulation of *Pax7* and *Myod1* is fundamental throughout myogenic lineage progression and that this temporal regulation is disrupted both with aging and in response to a stiff matrix.

Lineage progression of MuSCs requires meticulous regulation of mitochondrial function, which declines over time (Bhattacharya & Scimè, 2020; Dell'Orso et al., 2019; Rocheteau et al., 2012; Sahu et al., 2018). On the other hand, restoration of mitochondrial function enhances muscle progenitor cell activation, as evidenced by MYOD expression, and increases functional recovery after injury in aged mice (Sahu et al., 2018). The data presented here reveal that age-dependent mitochondrial dysfunction may be a result of increased skeletal muscle stiffness over time. We identified four mechanosensitive mitochondrial genes — NME2, BLOC1S1, GSTP1, and GSTP2 —that were differentially responsive according to age. At the intersection of these four genes, we identified the MYC-SIRT3-SOD2 axis. NME2 upregulates MYC, which promotes SKP2-mediated SIRT3 degradation and decreases oxidative phosphorylation (S.-T. Li et al., 2020; Mendelsohn & Larrick, 2014; Yao et al., 2014). While we did not probe for MYC nor SKP2 protein expression in this study, aged MuSCs cultured on a stiff substrate exhibited a down-regulation of SIRT3 that may be the result of the MYC-SKP2-mediated SIRT3 degradation. The activity of SIRT3 can also be diminished by mitochondrial protein lysine acetylation by the BLOC-1 protein complex, which includes BLOC1S1 (Scott et al., 2012). SIRT3 regulation of expression and activation is critical for ROS production, which is tied to stem cell function (Brown et al., 2013). Here, we demonstrated age- and stiffness-dependent regulation of SIRT3 levels, which in turn dictate MuSC differentiation kinetics for the first time to the best of our knowledge.

MuSCs go through a metabolic shift and change from OXPHOS to glycolysis and upregulate ROS as they activate and differentiate (Bhattacharya & Scimè, 2020; Latil et al., 2012; Ryall et al., 2015). ROS levels are regulated by SOD2, which is activated by SIRT3 (Qiu, Brown, Hirschey, Verdin, & Chen, 2010; Tao et al., 2010). Also, SIRT3 regulates OXPHOS by regulating the activity of acetyl-CoA synthetase 2 (Ahn et al., 2008). Therefore, age- and stiffness-dependent

regulation of SIRT3 may be disrupting MuSC differentiation kinetics through ROS and OXPHOS modulation. Further mechanisms by which SIRT3 modulation influences MuSC activation kinetics may be an interesting future research topic.

Taken together, the data implicate matrix stiffness as a regulator of SIRT3 levels and, potentially, activity. This reduced activity of SIRT3 leads to inactivation of SOD2, which results in increased mitochondrial ROS, ultimately causing mitochondrial damage and MuSC fate alterations (Meng et al., 2019; Yin et al., 2018). SIRT3 has been widely known to be a master regulator of mitochondrial functions, including but not limited to mitochondrial dynamics, suppression of ROS, and metabolic pathways within mitochondria, all of which influence MuSC fate (Ansari et al., 2017; Lombard, Tishkoff, & Bao, 2011; Meng et al., 2019; Samant et al., 2014). However, a direct role for SIRT3 in age-related declines in MuSC function and skeletal muscle regeneration has not been previously demonstrated. Here, we showed that SIRT3 levels are blunted in aged MuSCs upon activation after injury, as compared to young counterparts. Furthermore, data obtained with MuSCs from $SIRT3^{-/-}$ mice suggest that suppression of SIRT3 leads to increased quiescence and decreased MuSC activation, resulting in impaired muscle regeneration. Therefore, our data suggest that SIRT3 is an age-dependent mechanosensitive factor that may play a critical role in MuSC lineage progression. SIRT3 may also play an essential role in later stages of MuSC fate, as evidenced by abrogated myogenic differentiation of C2C12 myoblast cell line with SIRT3 inhibition (Abdel Khalek et al., 2014). Future studies to further elucidate SIRT3 dynamics through myogenic lineage progression and the mechanism by which SIRT3 levels become sensitive to mechanical cues over time are warranted.

2.5 Methods

2.5.1 Animals

C57BL/6 young (3-5 months old) and aged (22-24 months old) mice were received from the Jackson Laboratory or NIA rodent colony. 129-Sirt3<tm1.1Fwa>/J (Sirt3 KO) mice were received from the Jackson Laboratory. All animal studies were approved by the Institutional Animal Care and Use Committee of the University of Pittsburgh. The animals were assessed before the studies, and any animals with obvious signs of health problems were excluded from the studies. All animals were then randomly assigned to intervention groups and ear-tagged. All investigators performing endpoint analyses were blinded to each experimental group whenever possible. Animals showing apparent signs of health problems prior to the endpoint analyses were excluded prior to the start of the studies.

2.5.2 Primary Muscle Stem Cell Isolation and Cell Culture

MuSCs were freshly isolated from young/aged control and saline/BAPN treated mice for each experiment using Fluorescent Activated Cell Sorting (FACS) as CD31-, CD45-, Sca1-, and Integrin α7+. Propidium iodide, 1mg/ml aqueous solution (25535-16-4, Alfa Aesar, Lancashire, UK) was used as a dead cell marker. Cells were sorted based on live-cell and negative population of CD31+ and CD45+ cells. The detailed protocol was described previously (L. Liu, Cheung, Charville, & Rando, 2015; Yi & Rossi, 2011) (**Appendix Figure 8**). The sorted cells were seeded on PDMS substrates at ~ 160 – 200 cells/ mm^2 within 1.5 hours after the sorting.

2.5.3 Multiphoton Imaging and Characterization of ECM Topography

Second-harmonic generation (SHG) imaging was used to evaluate collagen fibril network characteristics in young/aged control and BAPN treated muscle as previously described (C. Zhang et al., 2015). Briefly, TA was harvested from non-injured animals, and the fresh muscles were submerged in CUBIC R1 solution and incubated with continuous rotation at 37 °C for a week, after which the solution was changed to PBS and stored at 4 °C until the samples were imaged. All SHG imaging was performed using an Olympus multi-photon microscope (Model FV1000, ASW software, Tokyo, Japan). 25x water immersion objective lens (420650-9901; numerical aperture [NA] = 0.8, Carl Zeiss AG, Oberkochen, Germany) was used. The excitation wavelength was set at 830 nm. RXD1 350 - 450 was used to take images of collagen fibrils. Laser power and scan speed were set to 4% and 4 µs/pixel, respectively, and z-stack images were taken with 2µm separation. Fiber intersection density, diameter, and orientation index were obtained using ImageJ software.

2.5.4 Biaxial Testing

Biaxial tensile testing of the intact gastrocnemius muscle was conducted as previously described (Stearns-Reider et al., 2017). Briefly, the medial head of gastrocnemius muscle was collected from young/aged control or BAPN treated groups and placed in Ringer's solution for at least one hour before biaxial mechanical testing. Muscle samples were cut into squares (~5 mm x 5 mm) after measuring the sample thickness at five individual points and attached to 50-gram load cells with two loops of suture connected to each side with four hooks. The samples' deformation was measured by real-time tracking of the coordinates of a four-marker array positioned in the

central region of the specimen. Gradient tensor F was calculated from shape functions as described by D'Amore et al. (D'Amore et al., 2014). Equi-stress protocol was executed with the specimens submerged in PBS at room temperature utilizing a tare load of 0.5 grams and a cycle time of 10 seconds each. Samples were preconditioned and tested up to the stress of 32 kPa, which is a critical load determined to be the maximum stress value that both young and aged native gastrocnemius muscle can tolerate without permanent deformation. All data were referenced to the post-preconditioned free-float state (D'Amore et al., 2014, 2016).

2.5.5 Computational Analysis (In-Plane Green's Strain Map)

A structural determinist model was utilized to quantify single fiber Green's strain (E_f) within the gastrocnemius muscle samples that were experimentally evaluated with biaxial tensile tests. The modeling approach was originally developed and is described in (D'Amore et al., 2018). Fiber mesh models were generated for the young and aged tissue samples. First, sample network architectural features were evaluated with SHG imaging. More specifically, experimentally-derived fiber intersection density (ID), diameter (D), and orientation index (OI) (D'Amore, Stella, Wagner, & Sacks, 2010) were the input parameters for the mesh generator (D'Amore et al., 2018, 2010); thus, the newly created topologies represent young and aged collagen matched the distribution of fiber nodes, orientation, and connectivity extracted with digital image processing of collagen SHG images (D'Amore et al., 2014). Based on the biaxial test symmetry, to reduce the cost of the computational analysis, only one-quarter of the system was modeled with square fiber network meshes of 500 μm by 500 μm (D'Amore et al., 2018). Biaxial tensile tests were then simulated in Abaqus 6.14 (Dassault Systèmes, Waltham, MA), as described in (D'Amore et al., 2018). Boundary conditions were set on two edges of the square mesh, where axial displacements

were equal to 0 along the axes of symmetry, while axial loads from the actual biaxial tests were applied on the remaining edges. All fibers were modeled B22 beam elements, and the Yeoh hyperelastic material model under the assumption of incompressibility was also utilized (Yeoh, 1993). For each analysis, results were automatically extracted with a custom Python module (Nasello et al., 2021) to calibrate the Yeoh material parameters by fitting the experimental biaxial data. Model prediction included fiber strain maps [E_f] and deformation as well as strain histogram on the biaxial tensile configurations.

2.5.6 PDMS Fabrication

PDMS substrates with different stiffness were prepared, as described by Iberite et al. (Iberite et al., 2019). Briefly, Sylgard 527 was prepared by mixing 1) equal weights or 2) 1:1.8 weight ratio of Dielectric Gel Part A and Part B and mixed well manually for 12 kPa and 29 kPa substrates, respectively to mimic the stiffness of previously reported young, healthy muscle and aged muscle obtained by our computational estimation described above. The mixtures were degassed using a vacuum desiccator for 30 minutes. Next, PDMS was poured into 60 mm diameter Petri dishes to make ~1.2 mm thick substrate for cell culture. Alternatively, 30 µL of PDMS was poured onto an 18 mm circular coverslip followed by a one-minute spin at 930 rpm using a spin coater (Laurell WS-650SZ-6NPP/A1/AR1) to make ~ 100 µm-thick films for cell culture for immunocytochemistry imaging of cell on PDMS substrates. PDMS substrates were cured at 60 °C for 16 hours for all experiments. PDMS substrates were treated with plasma cleaner (Harrick Plasma, Ithaca, NY) at the medium power setting for 20 seconds and soaked in water until the next step. Water was replaced with 70% ethanol and sterilized for 30 minutes under UV light in a cell culture hood. PDMS substrates were rinsed with sterile water three times and coated with 50

µg/mL of fibronectin (F4759, Sigma-Aldrich, St. Louis, MO) diluted in water for one hour at room temperature. Fibronectin solution was then removed, and the substrates were rinsed with water twice, followed by a PBS rinse before cell seeding. PDMS substrates were never left dry after plasma treatment.

2.5.7 Immunostaining and Image Acquisition

For the nuclear morphology analysis, freshly isolated young or aged MuSCs by FACS were cultured on soft or stiff PDMS substrates for a week before nuclear staining and imaging of the cells on the PDMS substrates to avoid potential alterations in cell morphology by transfer of the cells. For the staining of other experiments for morphological analysis of adherent cells, MuSCs were fixed and stained with DAPI two days after seeding, which is just enough time to allow MuSC adhesion to the substrate. Following antibodies were used for the other immunostaining studies: Mouse anti-PAX7 antibody at 5 µg/mL (DSHB, Iowa, U.S.A.), Rabbit anti-MyoD antibody at 1:500 (sc-760, Santa Cruz, Texas, U.S.A.), Mouse anti-c-Myc antibody at 1:250 (NB600-302, Novus Biologicals, Oxfordshire, UK), and Rabbit anti-SIRT3 antibody at 1:500 (ab 86671, Abcam, Cambridge, UK).

2.5.8 Quantification of Nuclear Morphology for Adherent Cell Culture

For the quantification of nuclear morphology in adherent cell culture, DAPI images were obtained at 40x magnification using an A1 confocal microscope (Nikon, Tokyo, Japan). Afterward, image processing and morphome feature extraction were performed using CellProfiler software (v4.0, The Broad Institute). Fifty-three shape features of nuclei were determined using the “identify primary objects” followed by the “measure object size shape” and “export to spread sheet” module.

Principal Component Analysis (PCA; unsupervised) and PCA-linear discriminant analysis (PCA-LDA; supervised) were performed to facilitate the identification of segregation of the nuclear morphological features identified by CellProfiler software (Carpenter et al., 2006). In PCA-LDA analysis, the small number of PCs, corresponding to the sample size in each group, were included to prevent overfitting (L.-F. Chen, Liao, Ko, Lin, & Yu, 2000). To determine variables of nuclear shape contributing to PCs, loading matrix, a correlation between the original variable and PCs, were extracted.

2.5.9 Immunofluorescence Probing for Myogenic and Mitochondrial Function Markers in Cells Using Imaging Flow Cytometry

Isolated MuSCs were plated on soft/stiff substrates and cultured for seven days. Following this, the cells were trypsinized with 0.25% trypsin for one minute at 37°C and collected in 1.5 mL Eppendorf tubes for subsequent analysis. The pelleted cells were fixed, permeabilized, blocked, and stained with immunofluorescence dye for myogenic markers: Pax7, MyoD; and mitochondrial function markers: Sirt3 with a nuclear marker DAPI, using the same protocol as described in the immunofluorescence staining section.

2.5.9.1 Imaging Flow Cytometry:

Stained cells were imaged at the single-cell resolution using imaging flow cytometry (Flow cytometry core, Department of Immunology, University of Pittsburgh). The imaging flow cytometry was conducted using a 60X objective at a resolution of 0.3 μm^2/pixel. Filtered sheath buffers were used to ensure the absence of debris and non-cellular components. Samples were acquired using INSPIRE® software with the highest sensitivity by acquiring images at the lowest speed. All used lasers for fluorochromes employed were used at the optimal power settings that were based on an unstained cell control. Gating was performed on unstained control cells for acquiring images of single and focused cells (**Appendix Figure 9**).

2.5.9.2 Imaging Flow Cytometry Analysis of Nuclear Morphology

IDEAS software was used to analyze the myogenic composition of the cellular profile and differences in mitochondrial function markers. For analyzing myogenic profile, a nuclear co-

localization step was done to detect the true-positive data in the imaging dataset. In addition, nuclear morphology features used for downstream computational analysis were extracted using IDEAS software per cell. Every experiment was performed in at least two independent runs. In every run, three sets of imaging data were acquired. Data were presented as an average of the three imaging data sets in one representative run.

2.5.10 Single Cell RNA-Seq Analysis

2.5.10.1 Age-Related Mitochondrial Change Heatmap

We used Tabula Muris Senis (TMS) processed data from https://figshare.com/projects/Tabula_Muris_Senis/64982. Fluorescence Activated Cell Sorting (FACS) instead of droplet was used to compare it against our FACS-based injury dataset, hence, eliminating the variation caused by different sequencing technologies (**Appendix Figure 3A**). From FACS-TMS data, skeletal muscle satellite cells (MuSCs) from young (3 months) and aged (24 months) male mice after making sure that there were no sex differences within MuSCs (**Appendix Figure 3B, C**).

Library preparation and sequencing were performed in McGill University Genome Quebec. Tibialis anterior muscle was obtained from young (3-6 months) and aged (21- 24 months) mice one-day post-injury. For MuSC annotation in injury scRNA-seq dataset, we selected cells which followed the criteria: *Pecam1*-ve, *Ptprc*-ve, *Ly6a*-ve, *Vcam*+ve. The heatmap was constructed with mitochondria-associated genes obtained from Jackson Laboratory's Mouse Genome Informatics, Genes and Markers Query Form. Protein coding genes that satisfied "mitochondria" gene ontology classification were selected. Data cleaning was done in R 4.0, and a *heatmap* package was used for heatmap visualization.

2.5.10.2 Single-Cell Trajectory Analysis

Homogenous MuSC population was obtained from skeletal muscle from hind limb of young (3-6 months) and aged (21-24 months) mice. These cells were cultured on soft or stiff PDMS substrates for one week. These cultured cells were then sent for scRNA-seq library preparation at the Genomics Core at the University of Pittsburgh. Sequencing and pre-processing of the scRNA-seq samples were done at Genewiz. *Scanpy* package in Python was used to read and analyze the cell ranger counts. Batch correction was performed using *harmonypy* package, and the four samples were combined. These batch corrected samples were then used for downstream analysis. Unsupervised clustering was performed, and myogenic markers were visualized on the tSNE projection. The clusters that display no myogenic markers were eliminated from our analysis, and the clusters that displayed myogenic markers were annotated based on stages of differentiation. *Palantir* package in Python was used for trajectory analysis, pseudotime visualization, and heatmap trajectory for genes of interest.

2.5.11 Transcription Factor Enrichment Analysis

Transcription factor enrichment analysis was performed using ChIP-X Enrichment Analysis Version 3 (ChEA3) (Keenan et al., 2019). In this analysis, the name of the four genes (*Nme2*, *Bloc1s1*, *Gstp1*, and *Gstp2*) was used as an input variable.

2.5.12 Latrunculin A Administration

First, aged muscle progenitors were plated on soft and stiff substrates. The cells were cultured for five days, after which they were treated with 0.001, 0.01, 0.1, and 0.5 µM Lat A for

one hour. The cells were washed with media two times, after which they were cultured for additional two days and fixed with 2% PFA for SIRT3 protein expression analysis. We chose the 0.1 μM dose to be most effective as it elicited a significantly increased response in Sirt3 expression. Based on the dose-testing experiment, we next administered 0.1 μM Lat A to young and aged MuSCs that were cultured on stiff substrates for five days and compared the treatment profile to untreated age-matched controls on soft and stiff substrates. The cells were treated with Lat A for one hour and then washed with culture media twice prior to culturing them for additional two days. Cells were fixed in 2% PFA, and SIRT3 expression was evaluated as per the immunofluorescence protocol mentioned above.

2.5.13 BAPN Administration and Cardiotoxin Injury

Saline or BAPN (290 μg/μL in normal saline; approximately 550μg per gram of animal weight) was subcutaneously injected daily into the nape of the neck of aged animals for six weeks. Four weeks after initiation of BAPN or saline injections, TA muscles were injured via intramuscular injection of cardiotoxin (10 μL of 1 mg/mL; 217503, Sigma-Aldrich) (**Figure 5A**). Two weeks after injury, TAs were harvested for hydroxyproline assay to test collagen crosslinking or histology to compare myofiber regeneration across groups.

2.5.14 Hydroxyproline Assay

The concentration of mature crosslinked collagen and non-cross-linked and immature crosslinked collagen were determined based on a method previously described (Smith, Hammers, Sweeney, & Barton, 2016). Briefly, freshly harvested TA muscles were weighted, snap-frozen,

and pulverized with a mortar and pestle over dry ice. The samples were rinsed in 1 mL of PBS on a shaker for 30 minutes at 4 °C. After centrifuging at 16,000g for 30 minutes at 4 °C, PBS was replaced with a 1:6 (weight: volume) solution of 0.5M acetic acid with 1 mg/mL pepsin for non-cross-linked collagen digestion and stirred overnight at 4 °C. The samples were then centrifuged at 16,000g for 30 minutes at 4 °C. Next, the supernatant was collected as the pepsin-soluble fraction (PSF), or non-cross-linked and immature crosslinked collagen, and the pellet was kept as the pepsin-insoluble fraction (PIF), or mature crosslinked collagen. A 1:1 volume of 4M NaCl was added to PSF and incubated on a shaker for 30 minutes at 4 °C before 30 minutes of centrifugation at 16,000g at 4 °C. The supernatant was then discarded. The collagen contents of the PSF and PIF were measured using Hydroxyproline Assay Kit (ab222941, Abcam, Cambridge, UK) by following the manufacturer's instructions. For the measurement of PSF samples, one-fifth of the reagents were used to lyse and hydrolyze the samples to increase the concentration.

2.5.15 Muscle Regeneration Analysis

Muscle tissues were frozen by completely immersing in liquid nitrogen-cooled 2-Methylbutane for 1 minute. Frozen muscles were sectioned at 10 μm thickness using CryoStar NX50 Cryostat (Thermo Fisher Scientific, Waltham, MA). Muscle sections were then fixed in 2% paraformaldehyde solution (J19943K2, Thermo Fisher Scientific) diluted in PBS followed by three 5-minute PBS washes at room temperature. Samples were permeabilized with 0.01% Triton X-100 in PBS for 15 minutes and blocked with 3% bovine serum albumin (A7906, Sigma-Aldrich) in 0.01% Triton X-100 in PBS (blocking buffer) for 1 hour at room temperature. The sample slides were incubated with Rat anti-Laminin (ab79057, Abcam, Cambridge, UK) in 5% goat serum (191356, MP Biomedicals, Solon, OH) in blocking buffer overnight at 4 °C. The slides were

washed for 5 minutes 3 times with PBS followed by incubation with goat anti-Rat IgG (H+L) Alexa Fluor 594 secondary antibody (A11012, Thermo Fisher Scientific) at 1:500 dilution for 60 minutes at room temperature. After three 5-minute PBS washes, the samples were incubated with 4',6-diamidino-2-phenylindole (DAPI) (422801, BioLegend, San Diego, CA) for 2 minutes at room temperature. The slides were washed once with PBS for 5 minutes before coverslips (12-545-100, Thermo Fisher Scientific) were mounted with Gelvatol mounting media (Source: Center of Biologic Imaging, University of Pittsburgh) and let dry. Images were taken using inverted microscopy (Observer Z1, Carl Zeiss AG, Oberkochen, Germany) with a 20x objective lens (420650-9901-000, Carl Zeiss AG). The area of centrally nucleated myofibers was measured using ImageJ software using a previously established protocol (Mula, Lee, Liu, Yang, & Peterson, 2013).

2.5.16 *In-Situ* Muscle Contractile Testing

The force-producing capacity of mice after an acute injury was tested 14 days post-injury using an *in-situ* testing apparatus (Model 809B, Aurora Scientific Inc, Canada), a stimulator (Model 701C, Aurora Scientific Inc, Canada), and a force transducer (Aurora Scientific Inc, Canada). The animals were first anesthetized using isoflurane, and then the peroneal nerve of the leg being tested was exposed through a small incision that was placed lateral to the knee. Mice were then placed supine on a warm platform, with the foot of the leg being tested placed flat on the footplate. The Achilles tendon of the leg was cut using a scalpel. The limb was stabilized with cloth tape on the knee and foot. Electrodes were placed over the peroneal nerve for stimulation. The ankle was positioned at 20° of plantarflexion (the position determined to result in the greatest force output). Muscle peak twitch, time to peak twitch, and half-relaxation time were quantified at this position. The tetanic force was determined by subsequent stimulations at 10, 30, 50, 80, 100,

120, 150 Hz with two minutes rest between each contraction, and a force-frequency curve was obtained. Final force values were normalized to cross-sectional muscle area to obtain specific force, as previously described (Brooks & Faulkner, 1988).

2.5.17 Statistics

Analyses were performed using GraphPad Prism version 9 software. Kolmogorov-Smirnov test and F-test were initially performed to assess normality and equality of variance, respectively. For all ANOVA analyses resulting in a p-value of less than 0.05, appropriate post hoc tests were performed. Methods for post hoc testing were described in figure legends. For multiple comparisons, alpha was adjusted using a multiple-comparison correction method such as Bonferroni correction to reduce the type I error (false-positive) inflation.

2.5.18 Steps to Ensure Rigor

Animals were assessed prior to the studies, and any animals with obvious signs of health problems were excluded. All animals included were randomized to one of the experimental groups. Animals were ear-tagged, and samples were number-coded with the ear tag number. Using the coded numbers, all investigators performing endpoint analyses were blinded to each experimental group whenever possible. We followed the standard criteria for inclusion and exclusion of data for each experiment and analysis.

2.5.19 Data Availability

The data supporting the results of this paper can be made available by the corresponding author upon reasonable request.

2.6 Acknowledgments

The study was supported by NIA R01 AG061005 (F.A. and P.L.), NIA R01 AG052978 (F.A.), and NIEHS R01 ES025529 (F.A. and A.B.). The authors thank Gregory Gibson from the Center of Biological Imaging, the University of Pittsburgh for their guidance with multiphoton microscopy, Samuel K. Luketich and Drake D. Pedersen for their help with biaxial mechanical testing, Philip R. LeDuc for the guidance with PDMS fabrication, and Nanoscale Fabrication & Characterization Facility (NFCF), the University of Pittsburgh for providing access to the spin-coater for PDMS fabrication.

2.7 Author Information - Affiliations

Department of Physical Medicine and Rehabilitation, University of Pittsburgh, Pittsburgh, PA, 15213, U.S.A.

H. Mamiya, A. Sahu, S. Sivakumar, H. Iijima, A. Pius, Z. Clemens, A. Miller, S. N. Shinde, and F. Ambrosio

Department of Bioengineering, University of Pittsburgh, Pittsburgh, PA, 15261, U.S.A.

H. Mamiya, S. Sivakumar, L. Richards, A. M. Robertson D. A. Vorp, A. D'Amore, and F. Ambrosio

Department of Environmental and Occupational Health, University of Pittsburgh, PA, 15261, U.S.A.

A. Sahu, Z. Clemens, A. Barchowsky, and F. Ambrosio

Multiscale in Mechanical and Biological Engineering, University of Zaragoza, Zaragoza, 50018, Spain,

G. Nasello

Department of Mechanical Engineering and Material Science, University of Pittsburgh, PA, 15261, U.S.A.

A. M. Robertson

Department of Surgery, University of Pittsburgh, Pittsburgh, PA, 15213, U.S.A.

D. A. Vorp

Department of Cardiothoracic Surgery, University of Pittsburgh, Pittsburgh, PA, 15213, U.S.A.

D. A. Vorp

Department of Chemical and Petroleum Engineering, University of Pittsburgh, Pittsburgh, PA, 15261, U.S.A.

D. A. Vorp

Department of Neurology & Neurological Sciences, Stanford University, CA, 94305, U.S.A.

T. A. Rando

The Paul F. Glenn Center for the Biology of Aging, Stanford University School of Medicine, Stanford, CA, 94305, U.S.A.

T. A. Rando

Center for Tissue Regeneration, Restoration and Repair, Veterans Affairs Hospital, Palo Alto, CA, 94036, U.S.A.

T. A. Rando

Department of Pharmacology & Chemical Biology, University of Pittsburgh, PA, 15232, U.S.A.

A. Barchowsky

Department of Orthopaedic Surgery, University of Pittsburgh, Pittsburgh, PA, 15213, U.S.A.

F. Ambrosio

McGowan Institute for Regenerative Medicine, University of Pittsburgh, Pittsburgh, PA, 15219, U.S.A.

D. A. Vorp, and F. Ambrosio

2.8 Author Contributions

F.A., H.M., and A.S. provided the concept, idea, and experimental design for the studies. F.A. and H.M. wrote the manuscript. F.A., H.M., A.S., S.S., and H.I. provided data collection, analyses, interpretation, and manuscript review. G.N. provided data analysis. L. R., A.M., and S.N.S. provided data collection. A.M.R., A.B., A.D., and T.A.R. provided consultation with research design and manuscript review.

2.9 Figures

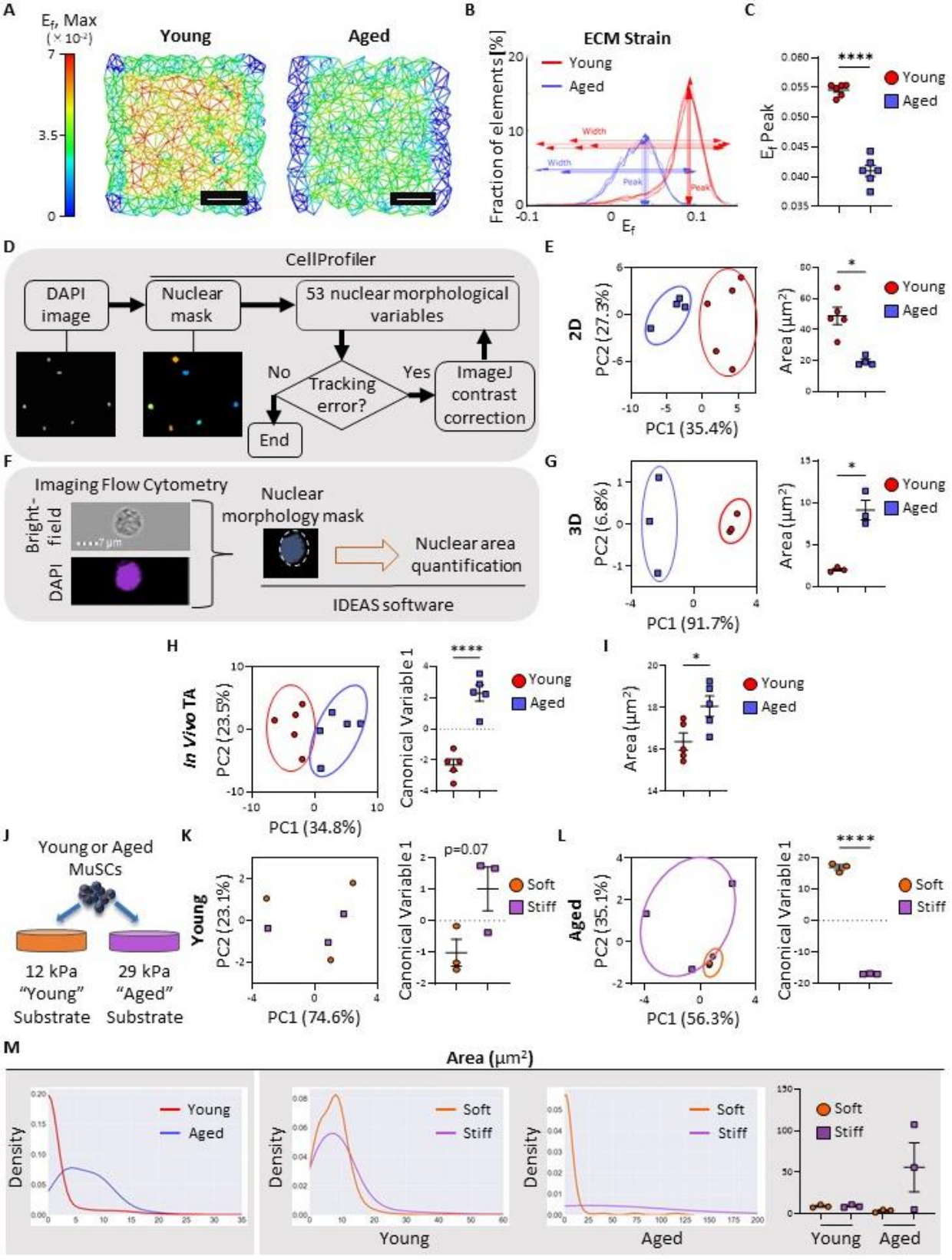
A
Ef, Max
(×10-2)
7
3.5
0
Young
Aged
B
ECM Strain
Young
Aged
Fraction of elements [%]
20
10
0
-0.1
0
0.1
Ef
Width
Peak
C
Ef Peak
****
Young
Aged
D
CellProfiler
DAPI image
Nuclear mask
53 nuclear morphological variables
No
Tracking error?
Yes
ImageJ contrast correction
End
E
2D
PC2 (27.3%)
PC1 (35.4%)
Area (µm²)
*
Young
Aged
F
Imaging Flow Cytometry
Bright-field
DAPI
Nuclear morphology mask
Nuclear area quantification
IDEAS software
G
3D
PC2 (6.8%)
PC1 (91.7%)
Area (µm²)
*
Young
Aged
H
In Vivo TA
PC2 (23.5%)
PC1 (34.8%)
Canonical Variable 1
****
Young
Aged
I
Area (µm²)
*
Young
Aged
J
Young or Aged MuSCs
12 kPa "Young" Substrate
29 kPa "Aged" Substrate
K
Young
PC2 (23.1%)
PC1 (74.6%)
Canonical Variable 1
p=0.07
Soft
Stiff
L
Aged
PC2 (35.1%)
PC1 (56.3%)
Canonical Variable 1
****
Soft
Stiff
M
Area (µm²)
Density
Young
Aged
Soft
Stiff
Young
Aged

Figure 1 Stiffness of young and aged skeletal muscle were measured *ex vivo* and impact of the various stiffness on MuSC morphologies was evaluated.

(A) In-plane maximum Green strain energy maps of young and aged muscle collagen fibrils. Higher strain energy is shown in red. Scale: 50μm. (B) Histogram of In-plane Green strain deformation, Ef (n=5/group). (C) Comparison of the peak Green strain energy in the histogram (n=5/group; **** p < 0.0001). (D) Flow chart of the nuclear morphological feature extraction using CellProfiler. (E) PCA of adherent MuSC nuclear morphologies and comparison of MuSC nuclear area (n=4-5/group; *P=0.0159). (F) Flow chart of the nuclear morphological feature extraction and analysis using imaging flow cytometry and IDEAS software, respectively. (G) PCA of 3D MuSC nuclear morphologies and comparison of MuSC nuclear are (n=3/group; *p=0.0243). (H) PCA and LDA of young and aged nuclear morphologies in TA muscle sections (n=5/group; ****p<0.0001). (I) Young and aged nuclear area of TA muscle sections (n=5/group; *p=0.0293). (J) Schematic of MuSC culture experiments on PDMS with various stiffness. (K) PCA and LDA of 3D young MuSC nuclear morphologies after PDMS culture (n=3/group; p=0.0678). (L) PCA and LDA of 3D aged MuSC nuclear morphologies after PDMS culture (n=3/group; ****p<0.0001). (M) Representative Kernel density plots of MuSC nuclear area and comparison of averages from each image flow cytometry experiment for young and aged MuSCs cultured on soft or stiff substrate (n=3/group; Interaction p=0.114).

(E) two-tailed Mann-Whitney test. (G) two-tailed t-test with Welch's correction. (H, I, K, L) two-tailed t-test. (M) Two-way ANOVA. Data are represented as mean ± SEM.

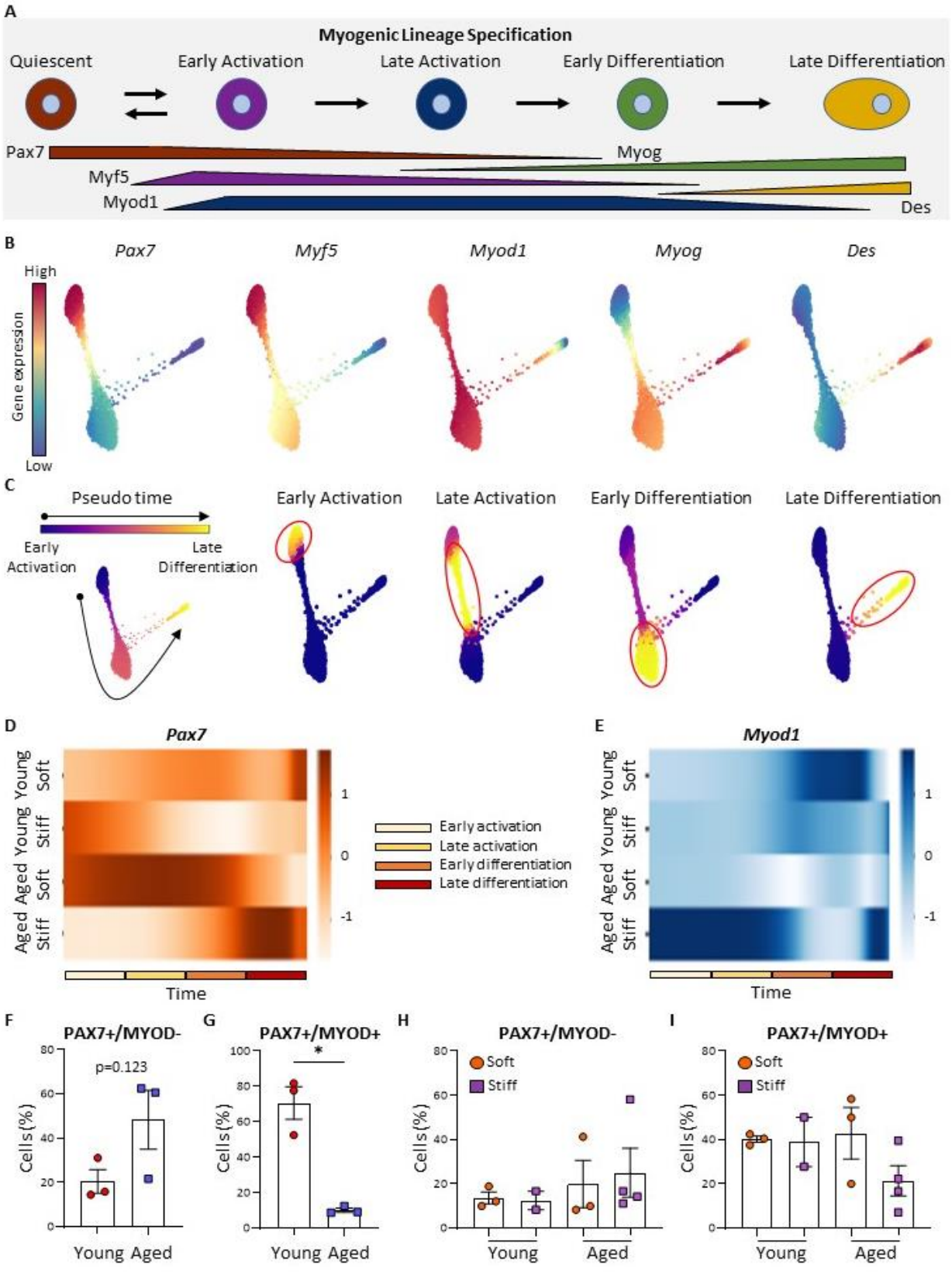
A
Myogenic Lineage Specification
Quiescent
Early Activation
Late Activation
Early Differentiation
Late Differentiation
Pax7
Myf5
Myod1
Myog
Des
B
Pax7
Myf5
Myod1
Myog
Des
High
Low
Gene expression
C
Pseudo time
Early Activation
Late Differentiation
Early Activation
Late Activation
Early Differentiation
Late Differentiation
D
Pax7
Young Soft
Young Stiff
Aged Soft
Aged Stiff
Time
Early activation
Late activation
Early differentiation
Late differentiation
E
Myod1
Time
F
PAX7+/MYOD-
p=0.123
Cells (%)
Young Aged
G
PAX7+/MYOD+
*
Cells (%)
Young Aged
H
PAX7+/MYOD-
Soft
Stiff
Cells (%)
Young
Aged
I
PAX7+/MYOD+
Soft
Stiff
Cells (%)
Young
Aged

Figure 2 Young muscle like compliant microenvironment shifts aged MuSC fate toward young like MuSC. (A) Schematic of MuSC myogenic lineage specification. (B) Myogenic markers expression on tSNE projection. Young and aged MuSCs cultured on soft and stiff were combined after batch correction. In the color bar, red indicates high expression while blue indicates low expression. (C) Pseudotime analysis of MuSCs indicating four stages of differentiation based on myogenic marker expression. Black arrow indicates the direction of pseudotime. (D) ***Pax7*** **expression along pseudotime indicates increase of** ***Pax7*** **expression into later stages of differentiation in aged MuSCs. (E)** ***Myod1*** **expression along pseudotime indicates blunted** ***Myod1*** **into the later stages of differentiation in aged MuSCs. (F) Quiescent MuSC population in freshly isolated young and aged MuSCs (n=3/group; p=0.125). (G) Activated MuSC population in freshly isolated young and aged MuSCs (n=3/group; *p=0.021). (H) Quiescent MuSC population in young and aged MuSCs cultured on soft or stiff substrate (n=2-3/group; Interaction p=0.759). (I) Activated MuSC population in young and aged MuSCs cultured on soft or stiff substrate (n=2-3/group; Interaction p=0.269). (F) two-tailed t-test. (G) two-tailed t-test with Welch's correction. (H, I) Two-way ANOVA. Data are represented as mean ± SEM.**

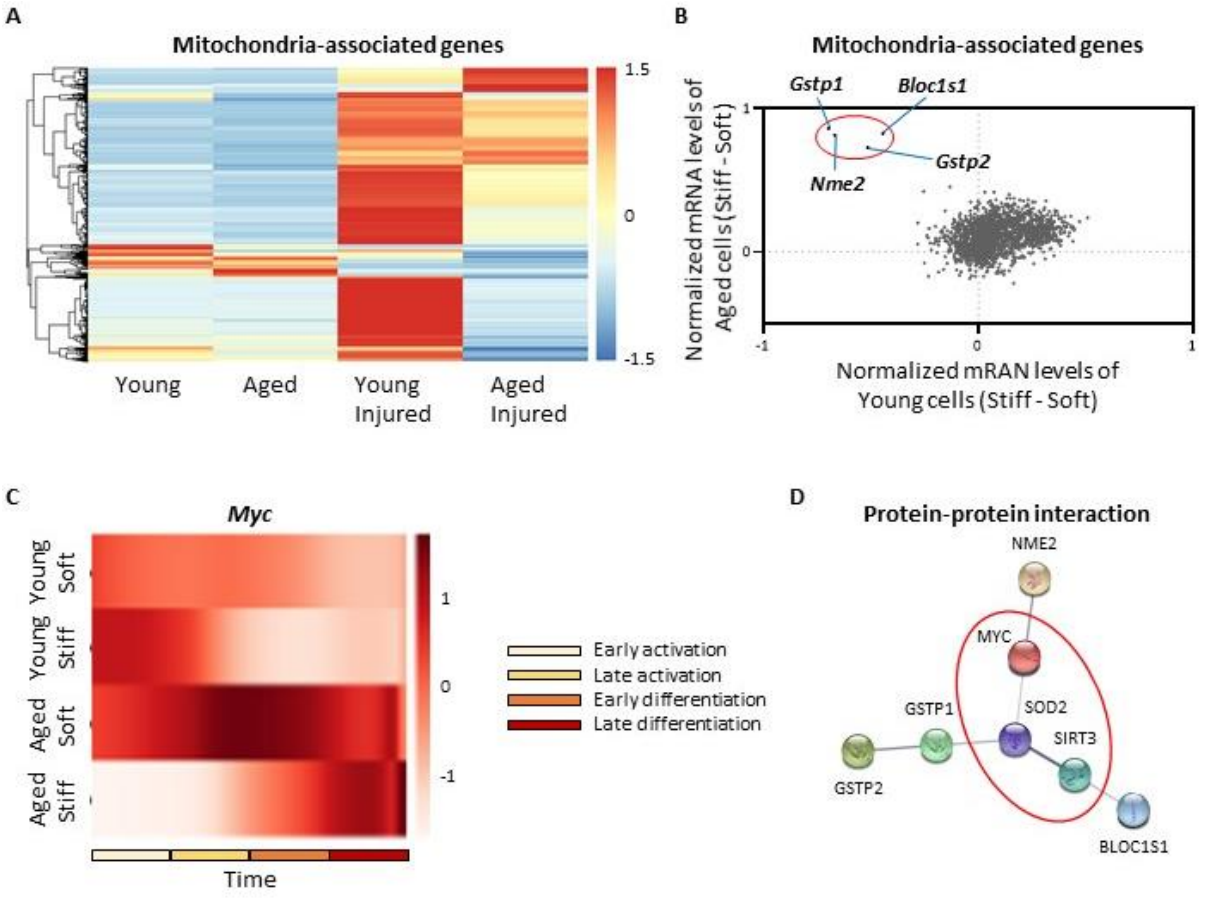
A
Mitochondria-associated genes
1.5
0
-1.5
Young
Aged
Young Injured
Aged Injured
B
Mitochondria-associated genes
Gstp1
Bloc1s1
Gstp2
Nme2
Normalized mRNA levels of Aged cells (Stiff - Soft)
Normalized mRAN levels of Young cells (Stiff - Soft)
C
Myc
Young Soft
Young Stiff
Aged Soft
Aged Stiff
Time
Early activation
Late activation
Early differentiation
Late differentiation
D
Protein-protein interaction
NME2
MYC
GSTP1
SOD2
SIRT3
GSTP2
BLOC1S1
E
Aged MuSCs on Stiff Microenvironment
BLOC-1
Inactivation
NME2
MYC
SIRT3
Activation
SOD2
GSTP1
GSTP2
mtROS and Mitochondrial dysfunction
Antioxidants
SIRT3 Degradation

Figure 3 MYC-SIRT3 axis is an upstream of age-dependent mechanosensitive mitochondrial genes. (A) Heatmap of mitochondria-associated gene expression among naïve young and aged MuSCs, and young and aged MuSCs isolated 1 dpi. (B) Scatter plot of Mitochondria-associated gene expression alterations with respect to stiffness. (C) *Myc* expression increases with aging and stiffness along the pseudotime. (D) Protein-protein network of the four mitochondria-associated genes and their upstream regulators — MYC, SIRT3, and SOD2. (E) Schematic showing MYC mediated degradation of SIRT3, which, in turn, affects antioxidant activity.

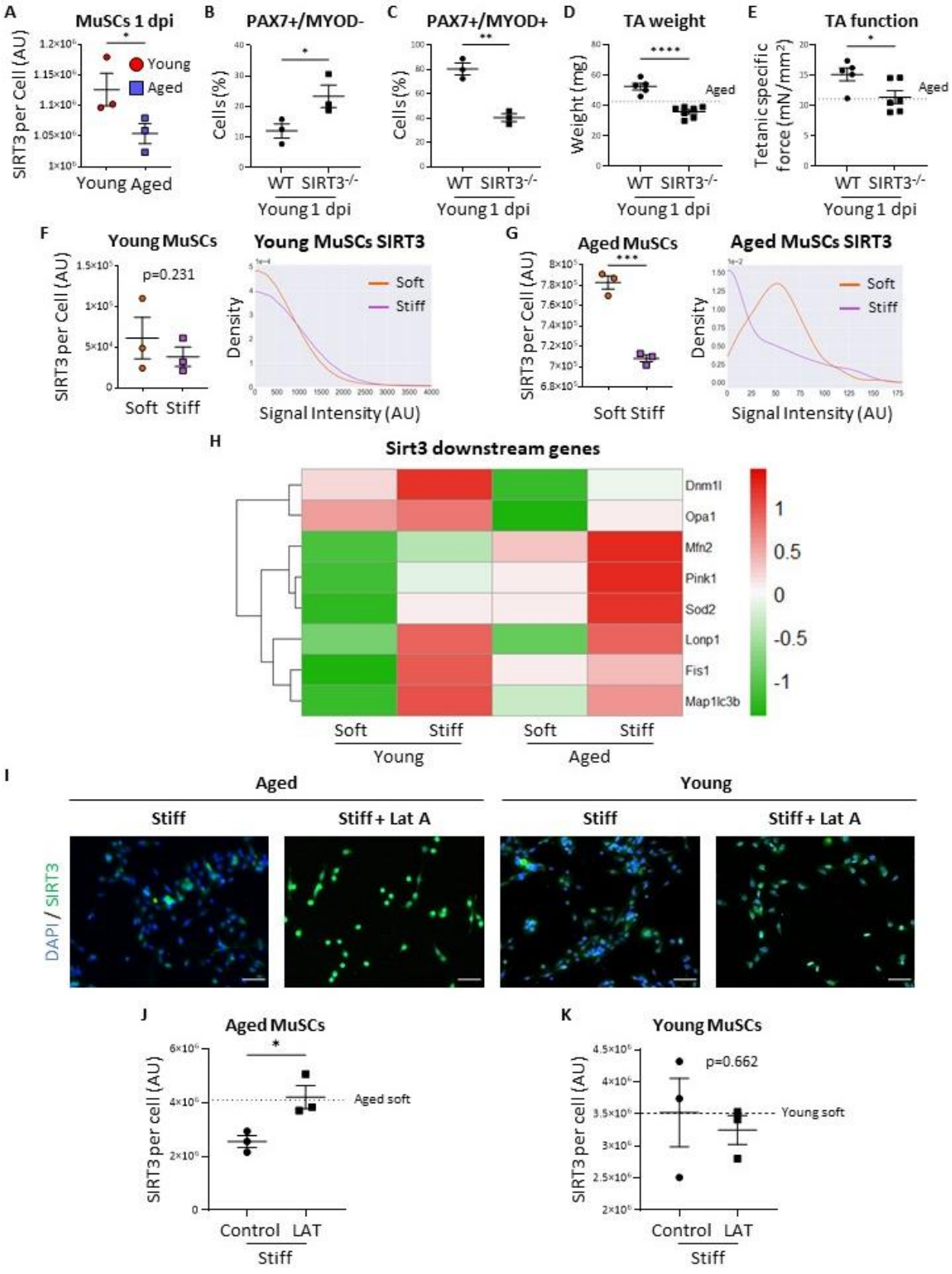
A
MuSCs 1 dpi
SIRT3 per Cell (AU)
Young
Aged
Young Aged
B
PAX7+/MYOD-
Cells (%)
WT SIRT3-/-
Young 1 dpi
C
PAX7+/MYOD+
Cells (%)
WT SIRT3-/-
Young 1 dpi
D
TA weight
Weight (mg)
Aged
WT SIRT3-/-
Young 1 dpi
E
TA function
Tetanic specific force (mN/mm2)
Aged
WT SIRT3-/-
Young 1 dpi
F
Young MuSCs
SIRT3 per Cell (AU)
p=0.231
Soft Stiff
Young MuSCs SIRT3
Density
Soft
Stiff
Signal Intensity (AU)
G
Aged MuSCs
SIRT3 per Cell (AU)
Soft Stiff
Aged MuSCs SIRT3
Density
Soft
Stiff
Signal Intensity (AU)
H
Sirt3 downstream genes
Dnm1l
Opa1
Mfn2
Pink1
Sod2
Lonp1
Fis1
Map1lc3b
1
0.5
0
-0.5
-1
Soft Stiff Soft Stiff
Young
Aged
I
Aged
Young
Stiff
Stiff + Lat A
Stiff
Stiff + Lat A
DAPI / SIRT3
J
Aged MuSCs
SIRT3 per cell (AU)
Aged soft
Control LAT
Stiff
K
Young MuSCs
SIRT3 per cell (AU)
p=0.662
Young soft
Control LAT
Stiff

Figure 4 SIRT3 is an age-dependent, mechanosensitive mitochondrial protein that is critical for MuSC activation and muscle regeneration.

(A) SIRT3 expression of MuSCs harvested from young and aged TAs 1 dpi (n=3/group; *p=0.0413). (B) Quiescent MuSC population in freshly isolated young WT and SIRT3$^{-/-}$ MuSCs at 1 dpi (n=3/group; *p=0.0301). (C) Activated MuSC population in freshly isolated young WT and SIRT3$^{-/-}$ MuSCs at 1 dpi (n=3/group; **p=0.0011). (D) TA weights of WT and SIRT3$^{-/-}$ mice at 14 dpi (n=5-7/group; ****p<0.0001) (E) Force producing capacity of TA from young WT and SIRT3$^{-/-}$ mice at 14 dpi (n=5-6/group; *p=0.0344). (F) SIRT3 expression of young MuSCs cultured on soft or stiff substrate (n=3/group; p=0.231). (G) SIRT3 expression of aged MuSCs cultured on soft or stiff substrate (n=3/group; *p=0.0003). (H) Heatmap of *Sirt3* downstream genes showing potential mitochondrial stress. (I) Representative images of SIRT3 expression of control or Lat A treated MuSCs cultured on a stiff substrate. (J) SIRT3 expression of aged MuSCs on stiff substrate with or without Lat A treatment (n=3/group; *p=0.0273). (K) SIRT3 expression of young MuSCs on stiff substrate with or without Lat A treatment (n=3/group; p=0.662).

(A-C, F, G) one-tailed t-test. (D, E, J, K) two-tailed t-test. Data are represented as mean ± SEM.

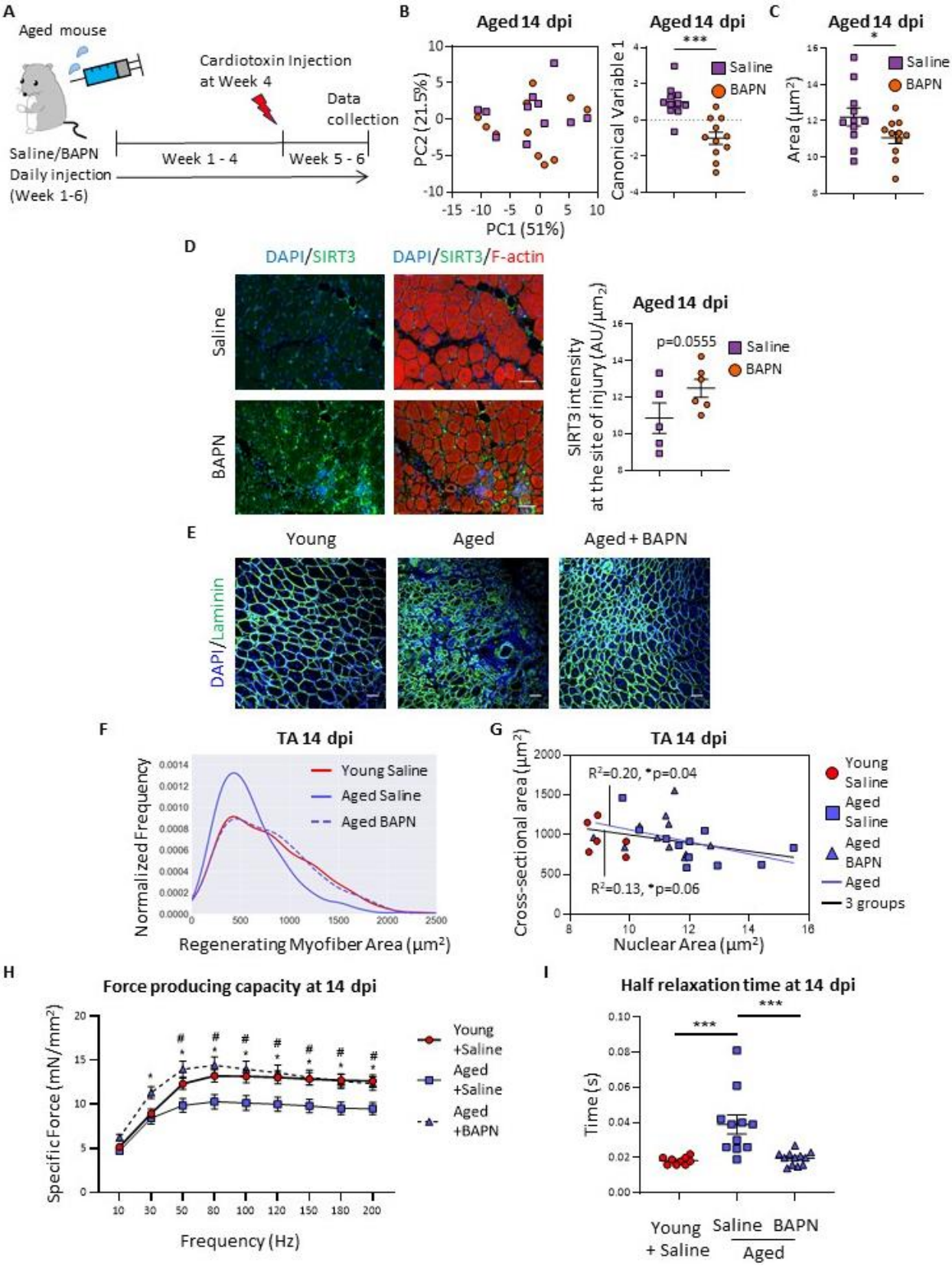
A
Aged mouse
Cardiotoxin Injection at Week 4
Data collection
Saline/BAPN Daily injection (Week 1-6)
Week 1 - 4
Week 5 - 6
B
Aged 14 dpi
PC2 (21.5%)
PC1 (51%)
Aged 14 dpi
Canonical Variable 1
***
Saline
BAPN
C
Aged 14 dpi
*
Area (µm²)
Saline
BAPN
D
DAPI/SIRT3
DAPI/SIRT3/F-actin
Saline
BAPN
Aged 14 dpi
SIRT3 intensity at the site of injury (AU/µm²)
p=0.0555
Saline
BAPN
E
Young
Aged
Aged + BAPN
DAPI/Laminin
F
TA 14 dpi
Normalized Frequency
Young Saline
Aged Saline
Aged BAPN
Regenerating Myofiber Area (µm²)
G
TA 14 dpi
Cross-sectional area (µm²)
R²=0.20, *p=0.04
R²=0.13, *p=0.06
Nuclear Area (µm²)
Young Saline
Aged Saline
Aged BAPN
Aged
3 groups
H
Force producing capacity at 14 dpi
Specific Force (mN/mm²)
Frequency (Hz)
Young +Saline
Aged +Saline
Aged +BAPN
I
Half relaxation time at 14 dpi
***
***
Time (s)
Young + Saline
Saline
BAPN
Aged

Figure 5 The effect of BAPN treatment on muscle regenerative capacity and quality.

(A) Schematic of the BAPN injection and cardiotoxin injury. (B) PCA and LDA of aged nuclear morphologies of TA sections at 14 dpi (n=11/group; ****p<0.0001). (C) aged nuclear area of TA section at 14 dpi (n=11/group; ****p=0.0345). (D) SIRT3 expression of TAs from saline or BAPN injected aged animals 14 dpi and their representative images (n=5-6/group; p=0.0555). (E) Representative immunohistological images of the sites of maximum cardiotoxin injury for each experimental group at 14 dpi stained with DAPI and laminin. Scale bar: 50 μm. (F) Histogram showing centrally nucleated regenerating myofiber area of TA muscles at 14 dpi. (G) Scatter plot showing a correlation between cross-sectional area of regenerating myofibers and nuclear area at 14 dpi, and regression lines for young and aged data (aged, R^2=0.196, p=0.0389; all groups, R^2=0.131, p=0.0586). (H) Force-frequency curves obtained from *in situ* contractile testing analysis of specific force of TA muscle at 14 dpi (n = 7 – 11/group, * p < 0.05 when comparing aged control with aged BAPN, # p < 0.05 when comparing young control with aged control). (I) Half relaxation time obtained from *in situ* contractile testing analysis of TA muscle at 14 dpi (n = 9 – 12/group, ***p=0.0007). (C, D) one-tailed t-test (G) simple linear regression. (H) mixed two-way ANOVA with Tukey post-hoc test. (I) two-way ANOVA with Sidak post-hoc test. Data are represented as mean ± SEM.

Table 1 Muscle stiffness measured with various techniques by various groups.

Testing modality	Elastic Modulus	Stress-Strain Range	Clamping method	E definition	n	Sample	Sample Cond.	Author	Year
AFM; passive elasticity (Hertz cone model)	C=12, C2C12=12-15, mdx=18kPa	Indentation of 1-2um on 100um thick smpls	N/A	peak moduli of hist.	multiple locations x 3 animals(387)	mouse EDL (Ctrl(3,13,21mo), mdx(3,9,15mo))	Fresh in DMEM within 8h	Engler et. al.	2004
small-amplitude oscillatory shear rheometry	12kPa	at 5% strain	N/A	E=2(1+v)G', assuming v=0.5	n=5mice, 10 TAs	mouse TA		Gilbert et.al.	2010
Uniaxial	Linear modulus; Longitudinal=447kPa, Transverse=22.4kPa	until failure or the stroke length limit of 50mm	sinusoidally-grooved clamps	linear region of the curve	n=6 for each test	rabbit EDL	Frozen once	Morrow DA. et. al.	2010
Uniaxial	single fiber~6kPa, bundle~40kPa	~10% strain	suture	quadratic fits to fully stress-relaxed data	fibers;n=17, bundles;n=10	mouse EDL	glycerinated relaxation solution O/N	Meyer GA. et.al.	2011
Ultrasound	7kPa(30Hz), 25kPa(60Hz),79kPa(average of 18 conditions(2direction x 3 Hz x 3 knee flexion angles))	N/A	N/A	Calculated based on sound wave propagation speed	n=10	human quadriceps (21-30yr old)	in vivo	Levinson SF. et.al.	1995
Magnetic resonance elastography (MRE)	Shear modulus; young(18-27)=35.8kPa, old(38-55)=14.85kPa, bovine=23.8kPa	N/A	N/A	shear modulus (mu) = (mass density)*(shear wave speed)^2	n=5(human), 10(bovine)	human biceps brachii (18-55yr old), peroneus tertius and extensor digitorum longus	in vivo (human), fresh <36hr (bovine)	Dresner MA. et.al.	2001
MRE	Shear modulus; biceps brachii=17.9, flexor digitorum profundus=8.7, soleus=12.5, gastrocnemius=9.9kPa	N/A	N/A	shear modulus (mu) = (mass density)*(shear wave speed)^2	n=12	human biceps brachii, flexor digitorum profundus, soleus, gastrocnemius (27-38yr old)	in vivo	Uffmann K. et.al.	2004
MRE	12.8kPa	N/A	N/A	shear modulus (mu) = (mass density)*(shear wave speed)^2 at 100Hz, density assumed to be 1000kg/m^3	n=19	human tibialis anterior (50-70yr old female)	in vivo	Domire ZJ. et.al.	2009
Supersonic shear imaging (SSI)	Shear elastic modulus = 3.54kPa	N/A	N/A	shear modulus (mu) = (mass density)*(shear wave speed)^2 at 1Hz, density assumed to be 1000kg/m^3	n=30 (25 male, 5 female)	human (18-32yr old); GM, TA, VL, RF, TB, BB, BR, APO, and ADM	in vivo	Lacourpaille L. et.al.	2012
Shear wave ultrasound elastography (SWUE)	12.78kPa(l ight pressure), 18.51kPa(medium), 32.39kPa(hard)	N/A	N/A	SWUE sonogram data	n=40 (both legs of 20 subjects; 14 males, 6 females)	human rectus femoris (21-33yr old)	in vivo	Kot BCW. et.al.	2012

3.0 Conclusions, Discussion, and Future Directions

3.1 Stiffness of the Micro-Scale MuSC Niche and Its Impact on MuSC Fate

Aged MuSCs typically display a myogenic-to-fibrogenic conversion, leading to scar tissue formation and ECM accumulation (Brack et al., 2007). As a result, muscle stiffness increases, driving a cascade of muscle weakness, increased susceptibility to recurrent injury, and further fibrotic tissue accumulation — a devastating cycle. To break out of this vicious circle and maintain healthier muscle, investigations into the mechanisms of age-associated MuSC functional decline are warranted. The work provided here demonstrated the proof-of-concept *in vitro* and *in vivo* that aged muscle regenerative capacity can be enhanced through modulation of biophysical ECM properties in skeletal muscle. These data shed light on the tissue biophysical properties as a potential therapeutic avenue and a diagnostic measure for muscle quality in the elderly population.

It has been widely accepted that skeletal muscle composition and its mechanical properties change with advancing age. Given the mechanosensitivity of stem cells, including MuSCs, it is not surprising that the age-associated alterations of muscle biophysical properties impede MuSC function, a vital component for maintaining healthy muscle. Nonetheless, there are bountiful questions regarding how cells react to various biophysical properties of their microenvironment and the mechanisms by which the cells relay these biomechanical cues to change their behavior. Among several biomechanical properties of a tissue, numerous previous studies examined the impact of rigidity on stem cell behavior (Engler et al., 2006; Gilbert et al., 2010). Whereas these studies provided valuable contributions to our understanding of the critical role of stiffness on stem cell fate (Cosgrove et al., 2014; Engler et al., 2006; Gilbert et al., 2010; Quarta et al., 2016), our

knowledge has been largely limited to cellular responses to supraphysiological plastic tissue culture dish (over 3×10^6 kPa) in the most extreme case or model systems that engineer stiffness ranges to mimic that of various tissues (10^{-1} ~ 10^6 kPa) in the best case. (Budday, Ovaert, Holzapfel, Steinmann, & Kuhl, 2020; Cox & Erler, 2011; Engler et al., 2006; Gilbert et al., 2010). However, the impact of stiffness alterations on stem cells in the context of aging or pathology is far less understood. The results presented in this dissertation have provided evidence for the importance of physiological levels of age-related alterations in muscle stiffness on MuSC fate and, ultimately, on skeletal muscle regenerative capacity.

Despite the previous studies suggesting an increase in muscle rigidity over time, large ranges of aged muscle stiffness values have been reported (Alfuraih et al., 2019; Eby et al., 2015; Gajdosik et al., 1999). The discrepancy in the findings is likely due, at least in part, to inconsistencies in the experimental parameters and methods used across different laboratories. For example, atomic force microscopy (AFM) is a widely used technique to measure cell and tissue stiffnesses. In an AFM study comparing stiffness of breast cancer cells using varying probe geometries, vertical indenting speeds, and ambient temperatures, authors demonstrated up to 10-fold differences in the elastic modulus readings (Wu et al., 2018). Strikingly, this group also demonstrated that various techniques, such as AFM and Particle-tracking microrheology, resulted in as large as 1,000-fold difference among different techniques in the stiffness measurement of the same cell line (Wu et al., 2018). These findings highlight the critical importance of testing conditions on biophysical measures of biological systems. Moreover, due to the highly heterogeneous nature of muscle tissue at the microscopic level, AFM measurements can vary significantly depending on where the probe lands. As a result, AFM measurements are likely to be overly reductionist as compared to what cells actually sense *in vivo*. Muscle tissue stiffness

measurements can similarly vary considerably among various groups depending on the method used (**Table 1**). Given the age-associated ECM accumulation and change in biomechanical properties of collagen fibril network surrounding myofibers — as opposed to biophysical alterations in the myofibers themselves (Gao et al., 2008; Lacraz et al., 2015; Mann et al., 2011; Stearns-Reider et al., 2017) — we utilized an experimentally-derived computational simulation of microscale collagen fibril network mechanical behavior to unveil the stiffness of aged muscle (elastic modulus E: 25 – 40 kPa). This computational simulation of microscale mechanical behavior, which is experimentally derived from macroscale measurement of muscle tissue, is technically innovative.

In evaluating the downstream phenotypic responses to increased stiffness properties of the aged skeletal muscle microenvironment, we proposed a novel mechanism by which niche stiffness dictates stem cell behavior. We found that stiffnesses engineered to mimic "young" or "aged" skeletal muscle induced distinct responses in nuclear size. Specifically, we found that nuclear area became similar to that of young MuSC nuclei when aged MuSCs were cultured on a compliant substrate. Interestingly, young MuSCs displayed a certain resistance to nuclear size changes in response to substrates of varying stiffness, and there was no difference in the nuclear area of young MuSCs when cultured on soft or stiff substrates. This finding suggests an age-dependent mechanosensitivity of MuSCs within physiological stiffness ranges. Based on these data, we posited that the increased sensitivity to extrinsic factors of aged MuSCs contributes to the tendency for aberrant lineage specification over time.

Cell nuclear morphology influences gene expression via heterochromatin reorganization, thus potentially regulating cell fate (Dahl et al., 2010). Consistent with a link between nuclear morphology and cell fate, the observed nuclear area changes of aged MuSC on a soft substrate

caused alterations in gene expression that were consistent with differentiation kinetics that more closely resembled that of young MuSCs. Young MuSC differentiation kinetics, however, were not significantly altered in the presence of a soft or stiff substrate. While the positive impact of young muscle elasticity on MuSCs was previously demonstrated by enhanced MuSC engraftment following transplantation (Cosgrove et al., 2014; Gilbert et al., 2010), the mechanisms underlying the beneficial effect of soft substrate compliance on aged MuSC behavior is poorly understood.

In this work, we identified four mechanosensitive mitochondrial genes — Nme2, Bloc1s1, Gstp1, and Gstp2 — whose expression changes differentially according to age. Furthermore, transcription factor enrichment analysis and protein-protein network analysis revealed that through the interaction with the four factors, MYC, SIRT3, and SOD2 may play a central role at the protein level, relaying age-dependent mechanosensitivity to age-associated MuSC differentiation kinetic alteration via modification of mitochondrial function. In this study, MuSCs isolated from $SIRT3^{-/-}$ mice one-day post-injury exhibited increased PAX7+/MYOD- and decreased PAX7+/MYOD+ cells showing hindered differentiation kinetics. Also, our data suggest that aged MuSCs exposed to stiff microenvironment upregulate MYC, which promotes ubiquitination-mediated SIRT3 degradation, resulting in decreased oxidative phosphorylation (S.-T. Li et al., 2020; Mendelsohn & Larrick, 2014; Yao et al., 2014). Indeed, we found that aged MuSCs cultured on a stiff substrate displayed reduced SIRT3 levels as compared to aged MuSCs cultured on a soft substrate. Decreased SIRT3 levels and potentially its deacetylase activity results in inactivation of SOD2, which leads to mitochondrial ROS accumulation, ultimately causing mitochondrial damage and MuSC fate alterations (Meng et al., 2019; Yin et al., 2018). In addition to the role of SIRT3 in the regulation of oxidative phosphorylation and mitochondrial ROS, SIRT3 has multiple roles in maintaining mitochondrial functions, such as mitochondrial dynamics, metabolic pathways, and

mitophagy, which dictate MuSC fate (Ansari et al., 2017; Lombard et al., 2011; Meng et al., 2019; Samant et al., 2014). Nonetheless, whether and how SIRT3 may influence age-associated MuSC functional decline and muscle regeneration is not clear. We demonstrated that post-injury increase in SIRT3 levels associated with stiffness modulation correlates with enhanced muscle regeneration and function, thereby highlighting the importance of biophysical properties on SIRT3 expression in aged animals. Specifically, we showed increased SIRT3 levels, regenerating myofiber area, and force producing capacity at 14 days post-injury when aged mice were treated with BAPN.

Stem cells are the primary cell population that dictates tissue regenerative capacity. However, over the past decades, despite the considerable effort, there have been limited numbers of FDA-approved clinical applications of stem cell-based therapy (FDA, 2019). This limited clinical translation is likely due, at least in part, to the negative impact of host niche factors on stem cell fate (Becerra, Santos-Ruiz, Andrades, & Marí-Beffa, 2011; Boldrin, Neal, Zammit, Muntoni, & Morgan, 2012). Among the host niche factors contributing to donor cell responses, a combination of both biochemical and biophysical stimuli dictate the fate of transplanted cells (Cosgrove et al., 2014). While widely used polystyrene cell culture dishes are advantageous for *in vitro* studies owing to their durability, cost-effectiveness, and accessibility, cells cultured on these dishes clearly behave significantly differently from the cells *in vivo*. Supraphysiological cell culture conditions may, at least in part, explain the translational barrier between *in vitro* and *in vivo* findings. Although it is nearly impossible and not practical to completely mimic the *in vivo* condition *in vitro* with current technology, biomimetic approaches are likely critical for further advancement of the field. As cell response seems to be more similar to *in vivo* cell response, biomimetic approaches are a more useful model to better predict cell response in situations such as drug toxicity and efficacy in a preclinical model. Therefore, there have been increasing efforts

to engineer biomaterials with tunable biomechanical properties to harness the regenerative capacity of stem cells. Such approaches have the potential to considerably expand our understanding of stem cell behavior in response to various biomechanical properties in the biomimetic microenvironment *in vitro* and will pave the way for cell-based therapeutic interventions (Madl, Heilshorn, & Blau, 2018).

Throughout these current studies, we focused on the significance of microenvironment stiffness on stem cell fate. However, numerous other biophysical properties have also been demonstrated to influence cell behavior. Such biophysical properties include viscoelasticity, surface topology, ECM composition, and dynamic mechanical stress.

3.1.1 Viscoelasticity

Typically, PDMS and polyacrylamide hydrogel are used as substrates with soft tissue stiffness to investigate mechanobiological questions. These materials are purely elastic, meaning that the materials display spring-like mechanical behavior. However, native tissues and ECM are typically not purely elastic materials and behave as viscoelastic solids, whose stiffness is dependent on time and magnitude of deformation (Janmey, Fletcher, & Reinhart-King, 2020). When the stress is applied, viscoelastic solids deform slowly and eventually reach a constant deformation. When the stress is released, the material slowly recovers its original state. Notably, viscoelastic substrates can be distinguished from pure elastic substrates by cells, which is demonstrated in a study where primary rat hepatic stellate cells exhibited less differentiation into myofibroblasts on substrates with higher viscoelasticity (Charrier, Pogoda, Wells, & Janmey, 2018). Viscoelasticity and the ability of cells to sense viscoelastic properties of the substrate add another layer and complexity to fully understanding mechanisms by which age-related ECM

changes may affect stem cell functioning. To the best of our knowledge, there have been no studies to date that have investigated the sensitivity of MuSCs to varying viscoelastic characteristics of skeletal muscle and whether such sensitivity changes over time.

3.1.2 Surface Topology and ECM Composition

Another biophysical microenvironmental factor that clearly dictates stem cell fate is surface topology. For instance, mesenchymal stem cells were directed toward either proliferation or differentiation into an osteogenic lineage depending on the offset in pit placement of nano-scale patterned surface lattice geometry (Dalby et al., 2007; McMurray et al., 2011). Another study exhibited that a smoother surface (Ra: 22.8 nm) drove myogenic differentiation, whereas a rougher surface (Ra: 90.9 nm) promoted osteogenic differentiation (Hu et al., 2011). In addition, it has been recognized that ECM geometric micropatterning influences myotube formation *in vitro*. A study demonstrated that wider ECM line (200 µm) and smaller spacing (10 µm) was preferred for myotube formation as opposed to narrower ECM line (50 µm) and larger spacing (20 µm) (Duffy, Sun, & Feinberg, 2016). While these studies with various surface topologies provide some insights into how cells respond to simple geometric features, *in vivo* ECM architecture is far more complex as compared to the fabricated substrates for the *in vitro* studies. Thus, implications of *in vitro* studies need to be carefully evaluated for the acquired knowledge to be applied *in vivo* and in clinical settings. At the moment, surface topologies would be best used to direct stem cells into a specific cell lineage and to make a tissue construct.

3.1.3 Dynamic Mechanical Stimuli

Given that most, if not all, organs in our body experience regular dynamic mechanical stimuli, it is not surprising that cells are so highly responsive to dynamic mechanical stimuli. Indeed, cyclic mechanical stimuli enhance the proliferation of muscle-derived stem cells *in vitro* (Ambrosio et al., 2010). In other *in vitro* studies, it was reported that myofiber diameter, myotube ratio, striated fibers, and cell alignment increased with uniaxial mechanical stimulation (Pennisi, Olesen, de Zee, Rasmussen, & Zachar, 2011; Powell, Smiley, Mills, & Vandenburgh, 2002). The impact of dynamic mechanical stimuli on cell behavior changed with varying parameters such as frequencies (Qu et al., 2007) and amplitudes (Ghazanfari, Tafazzoli-Shadpour, & Shokrgozar, 2009).

3.1.4 Mechanical Memory

Further adding to the mechanobiological complexity is the fact that cells can store mechano-sensed information, a phenomenon known as “mechanical memory” (Balestrini, Chaudhry, Sarrazy, Koehler, & Hinz, 2012). Typically, under physiological stiffness, the mechanical memory of stem cells is reversible. However, under supraphysiological stiffnesses, stem cell fate can be influenced irreversibly by the historical stiffness properties of the microenvironment (C. Yang, Tibbitt, Basta, & Anseth, 2014). The longer the culture time on polystyrene dishes, the more likely that concomitant changes in the cell behavior will become irreversible. For example, YAP and RUNX2 translocate into the nucleus of hMSCs on tissue culture polystyrene (TCPS), which has supraphysiological stiffness, and relocate back to the cytoplasm when the cells are transferred to a soft hydrogel with ~2kPa stiffness if the duration of

the cell culture on the TCPS is one day (C. Yang et al., 2014). However, when hMSCs are cultured on TCPS for 7 days, YAP persists in nuclei even after transfer to the soft hydrogel (C. Yang et al., 2014). In our study, aged MuSCs remember the stiffness of aged muscle during cell culture on substrates with various stiffness. This is likely why aged MuSCs cultured on substrates with various stiffness did not show the same MuSC differentiation marker profile as young MuSCs. By uncovering the mechanisms by which cells store mechanical memory, we may be able to obtain some insights into how seemingly irreversible cell function alterations due to chronic tissue stiffening, such as age-related tissue stiffening and fibrosis, could be treated. Mechanical memory may play a significant role in the age-associated alterations in mechanosensitivity observed in our work. Understanding the mechanisms of how cells store mechanical memory would provide better insight in MuSC aging.

Currently, mechanical memory is widely considered to be stored as epigenetic memory, but there could be additional mechanisms, such as mitochondria (Cheikhi et al., 2019; Killaars et al., 2019; Lele, Brock, & Peyton, 2020). Of note, it is also likely that cells have mechanisms to store mechano-sensed information other than stiffness. Indeed, substrate surface topology has been shown to regulate the epigenetic state of cells (Downing et al., 2013). A deeper understanding of mechanical memory is essential to find better treatments to reverse the biomechanically transformed cell fate of diseases in which tissue mechanical properties are altered, such as with fibrosis, which is often found in age-associated conditions.

3.2 Future Directions and Concluding Thoughts

Given the mechano-sensitivity of cells, it is evident that biomechanical stimuli are vital factors to maintain muscle quality and regenerative capacity (Joanisse et al., 2016). This mechano-responsive property of muscle to increase its size in response to an exercise is a target of rehabilitative medicine (Aagaard et al., 2001; Rando & Ambrosio, 2018; Seynnes, de Boer, & Narici, 2007), and exercise enhances muscle regeneration after injury (Hwang, Ra, Lee, Lee, & Ghil, 2006). The beneficial effect of exercise has also been applied to regenerative medicine. This combination of regenerative medicine and rehabilitative principles is at the heart of the emerging field of regenerative rehabilitation (Rando & Ambrosio, 2018). In a successful example of this approach, cyclic mechanical stimuli enhanced the migration of muscle-derived stem cells *in vivo* (Ambrosio et al., 2010). Moreover, implantation of biomaterials seeded with MuSCs resulted in better muscle functional recovery when combined with an exercise regimen (Quarta et al., 2017). While these studies demonstrated promising outcomes of a regenerative rehabilitation approach, parameters of mechanical stimuli such as frequency, duration, intensity, and the timing after an injury, need to be rigorously investigated (Rando & Ambrosio, 2018). Without optimal parameters, it is possible that mechanical stimuli could lead to insufficient or, in the worst-case, adverse effects on tissue regeneration.

3.2.1 The Influence of Biophysical Niche Characteristics on Stem Cell Fate

The various biomechanical properties and the response of the heterogenous cells to the microenvironment *in vivo*, which are discussed here, add challenges in studying the influence of biophysical niche characteristics on stem cell fate. First, the beneficial effect of biomechanical

dosing is induced not only via the direct impact on the host or transplanted stem cells but also via the indirect influence on stem cell fate by modulation of the stem cell niche (Kjaer, 2004; Miller et al., 2005). *In vivo*, such direct and indirect mechanical properties are inextricably intertwined and difficult to disentangle. Moreover, while rigorous studies with careful experimental design and a detailed report of methods are vital to propel the field of rehabilitative medicine and regenerative rehabilitation, the advancement of new biomaterials is critical to study the impacts of biomechanical signals on cells and their mechanisms *in vitro*. Increased accessibility to better biomaterials and to biomimicry cell culture systems, such as organ-on-chip models, is a promising new frontier to enhance the predictability of *in vivo* pre-clinical studies and, ultimately, clinical trials.

Appendix A Supplementary Information to Section 2

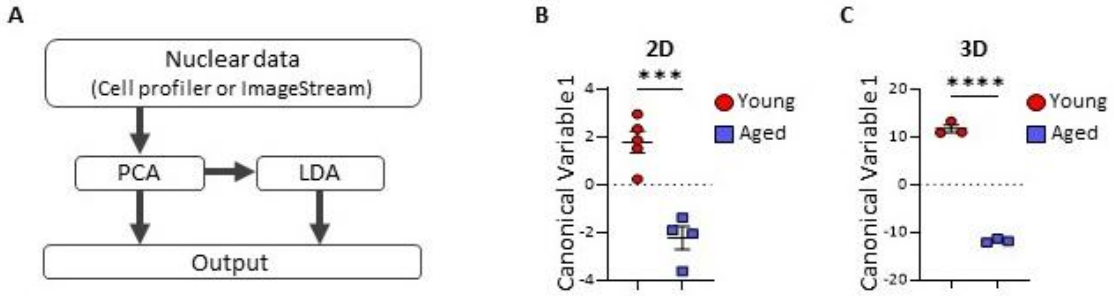

Appendix Figure 1 Stiffness of young and aged skeletal muscle were measured ex vivo and impact of the various stiffness on MuSC morphologies was evaluated.

(A) Flow chart of unsupervised PCA and supervised LDA of the nuclear morphological features. (B) LDA of adherent MuSC nuclear morphologies (n=4-5/group; ***P<0.0005). (C) LDA of 3D MuSC nuclear morphologies (n=3/group; ****p<0.0001).

(B, C) two-tailed t-test. Data are represented as mean ± SEM.

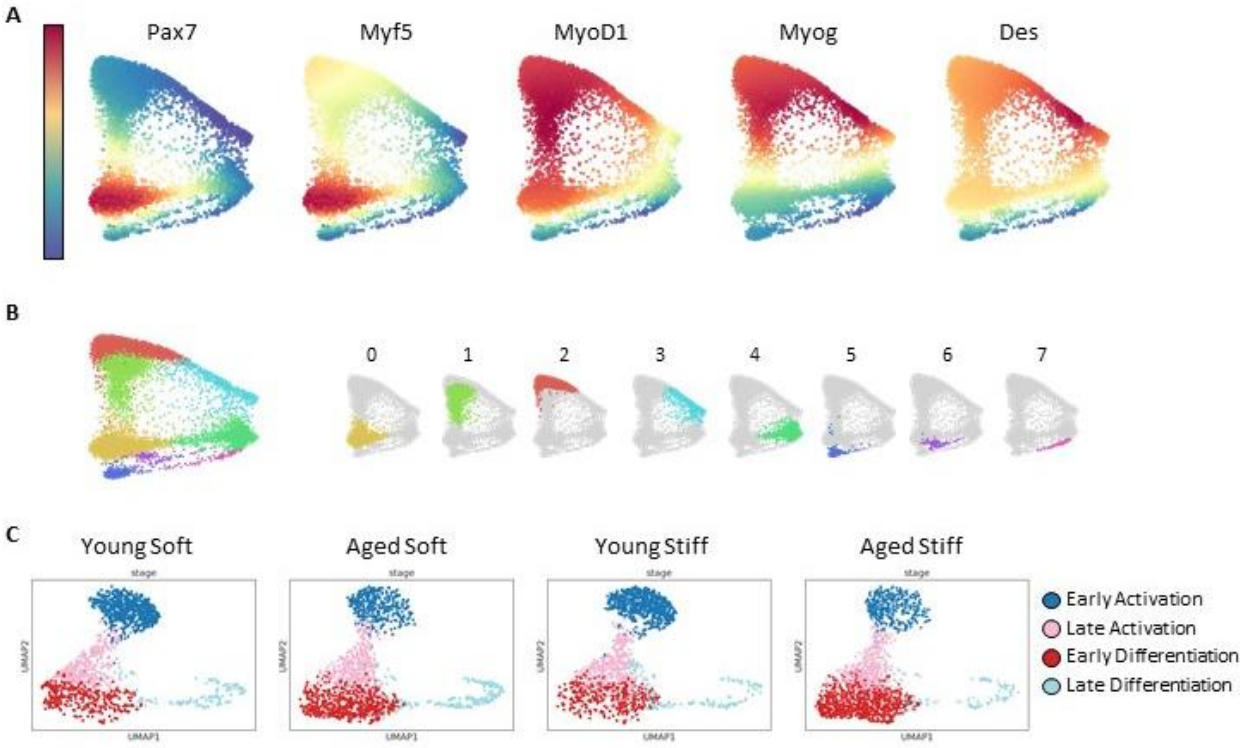

Appendix Figure 2 Annotating stages of differentiation in combined PDMS cultured MuSC scRNA-seq data. (A) Myogenic markers represented on tSNE projection of combined batch corrected samples. In the color bar, red indicates high expression while blue indicates low expression. (B) Unsupervised clustering indicates that clusters 5, 6, and 7 do not display any myogenic markers, and hence were excluded from downstream analysis. (C) UMAP projection displaying four stages of differentiation in the four experimental groups individually.

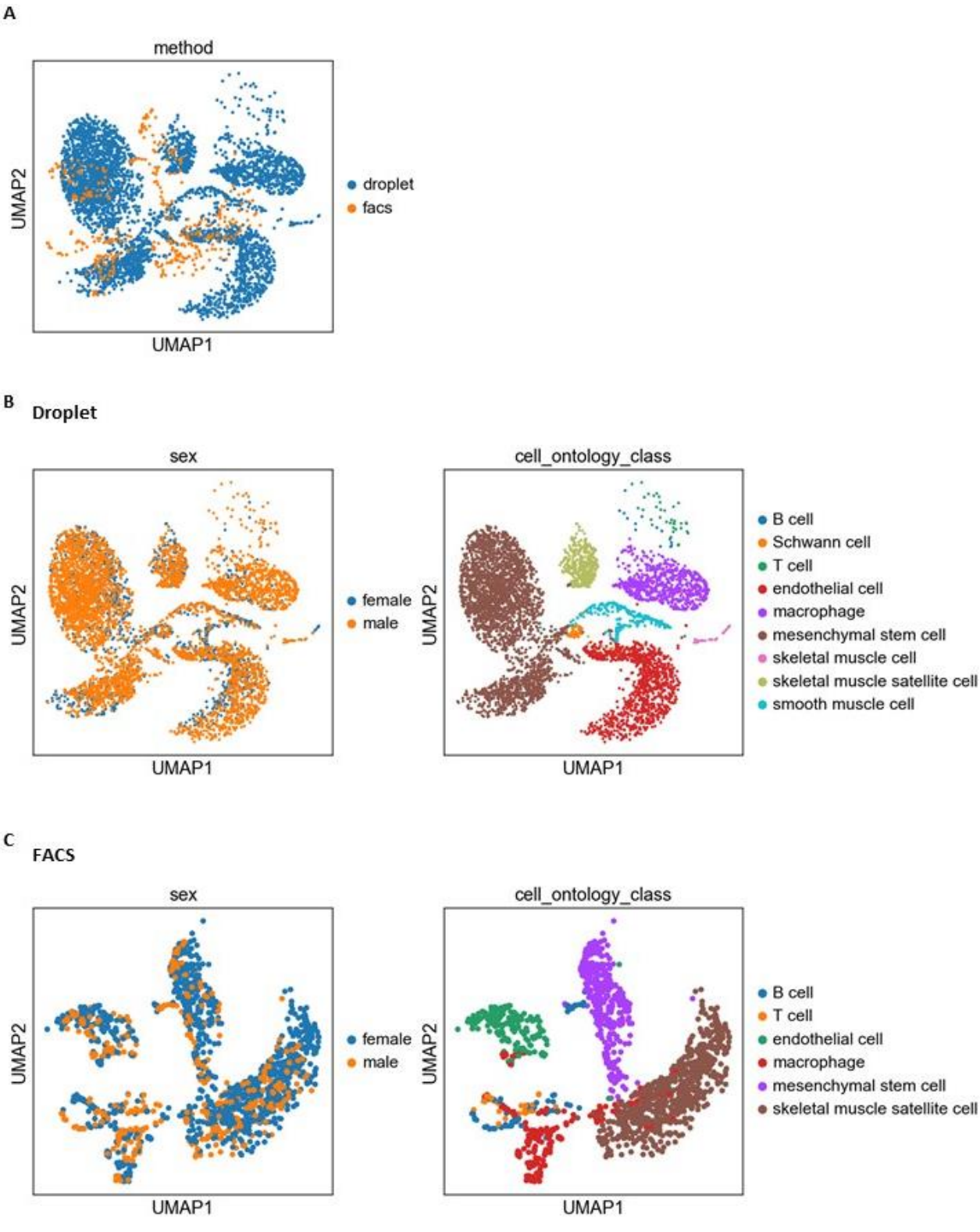
A
method
UMAP2
UMAP1
droplet
facs
B
Droplet
sex
UMAP2
UMAP1
female
male
cell_ontology_class
UMAP2
UMAP1
B cell
Schwann cell
T cell
endothelial cell
macrophage
mesenchymal stem cell
skeletal muscle cell
skeletal muscle satellite cell
smooth muscle cell
C
FACS
sex
UMAP2
UMAP1
female
male
cell_ontology_class
UMAP2
UMAP1
B cell
T cell
endothelial cell
macrophage
mesenchymal stem cell
skeletal muscle satellite cell

Appendix Figure 3 Selecting MuSCs from Tabula Muris Senis dataset to visualize age-related mitochondrial changes.

(A) UMAP projection displaying FACS and droplet methodologies. Droplet data was chosen for our analysis to eliminate variation introduced by sequencing methodology. (B) Cell annotation in droplet indicates that there are no sex differences in stem cell population. (C) Cell annotation in FACS also indicates that there are no sex differences in stem cell population.

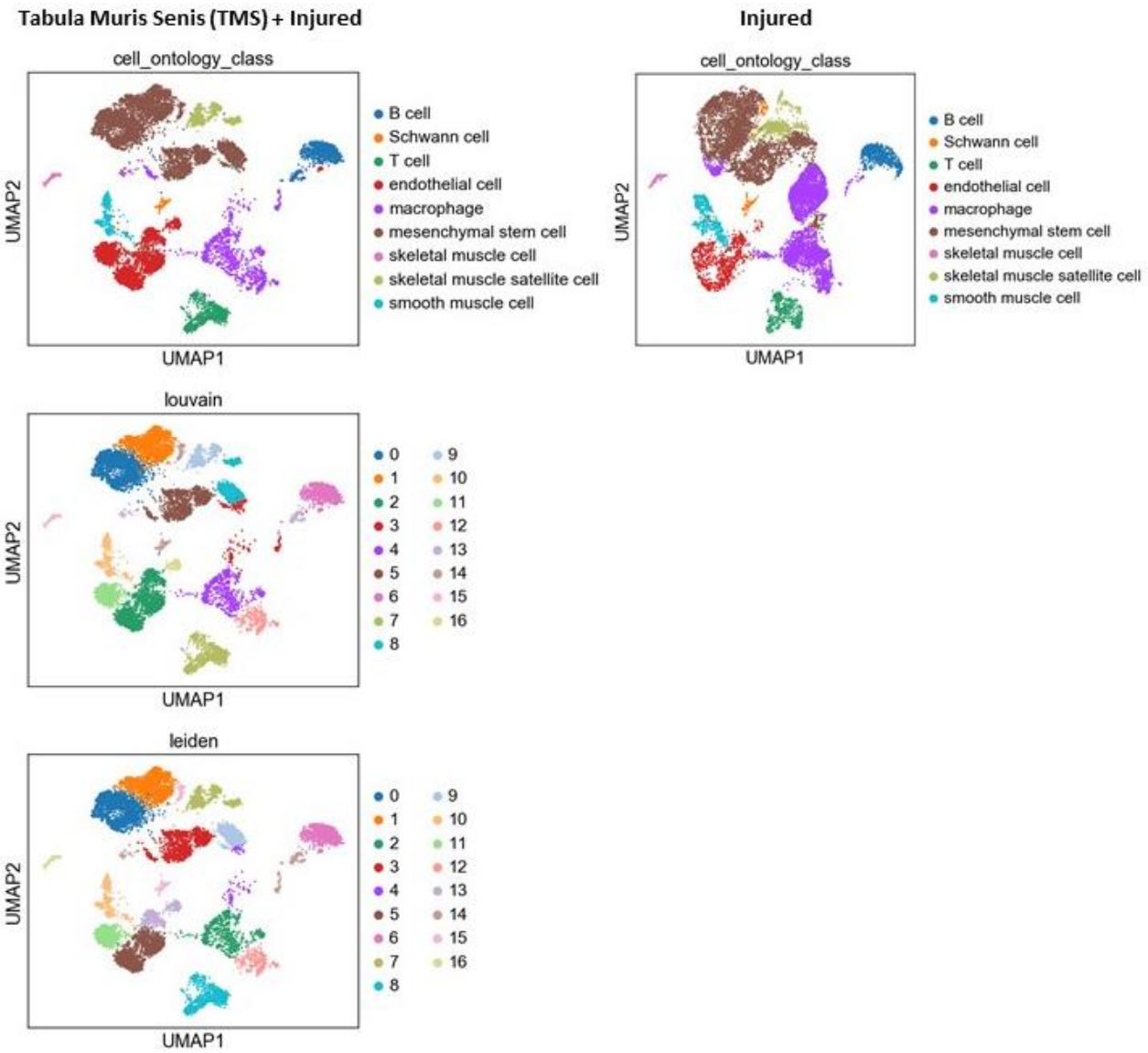

Appendix Figure 4 The cells from TMS droplet data and injury scRNA-seq were combined and batch corrected for preprocessing, louvain and leiden clustering.

Cell annotation for injury scRNA-seq was done based on gene markers from TMS annotations, and clustering. The UMAP projections show similarities in cell types.

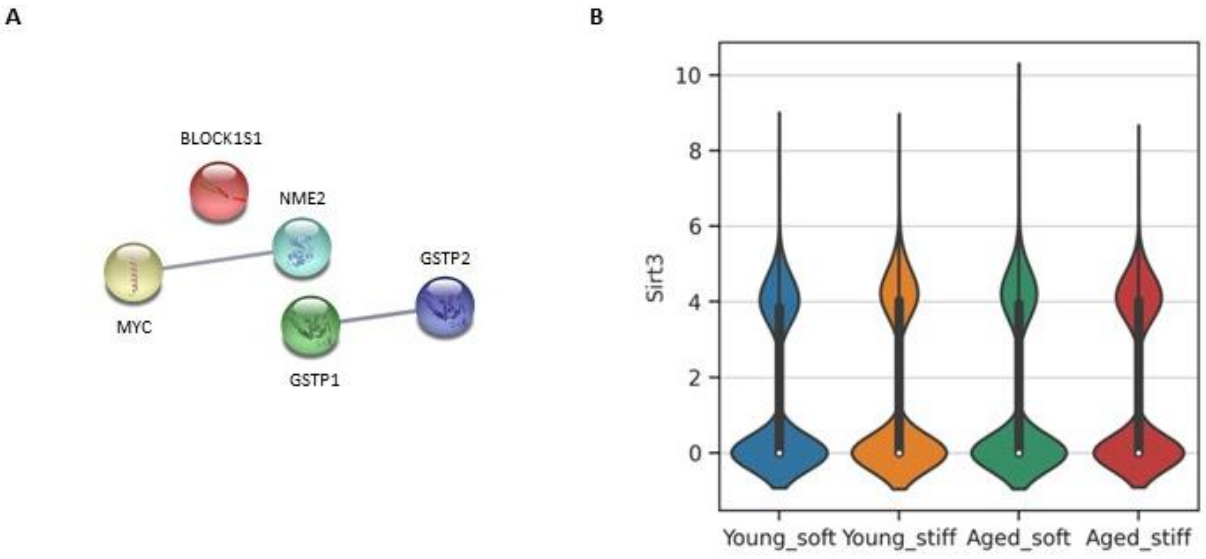

Appendix Figure 5 Understanding how substrate stiffness modulates mitochondrial genes.

(A) Disconnected protein-protein interaction network with four genes that show differences in aging as well as stiffness. (B) Violin plot showing that Sirt3 gene expression does not change with aging or substrate stiffness.

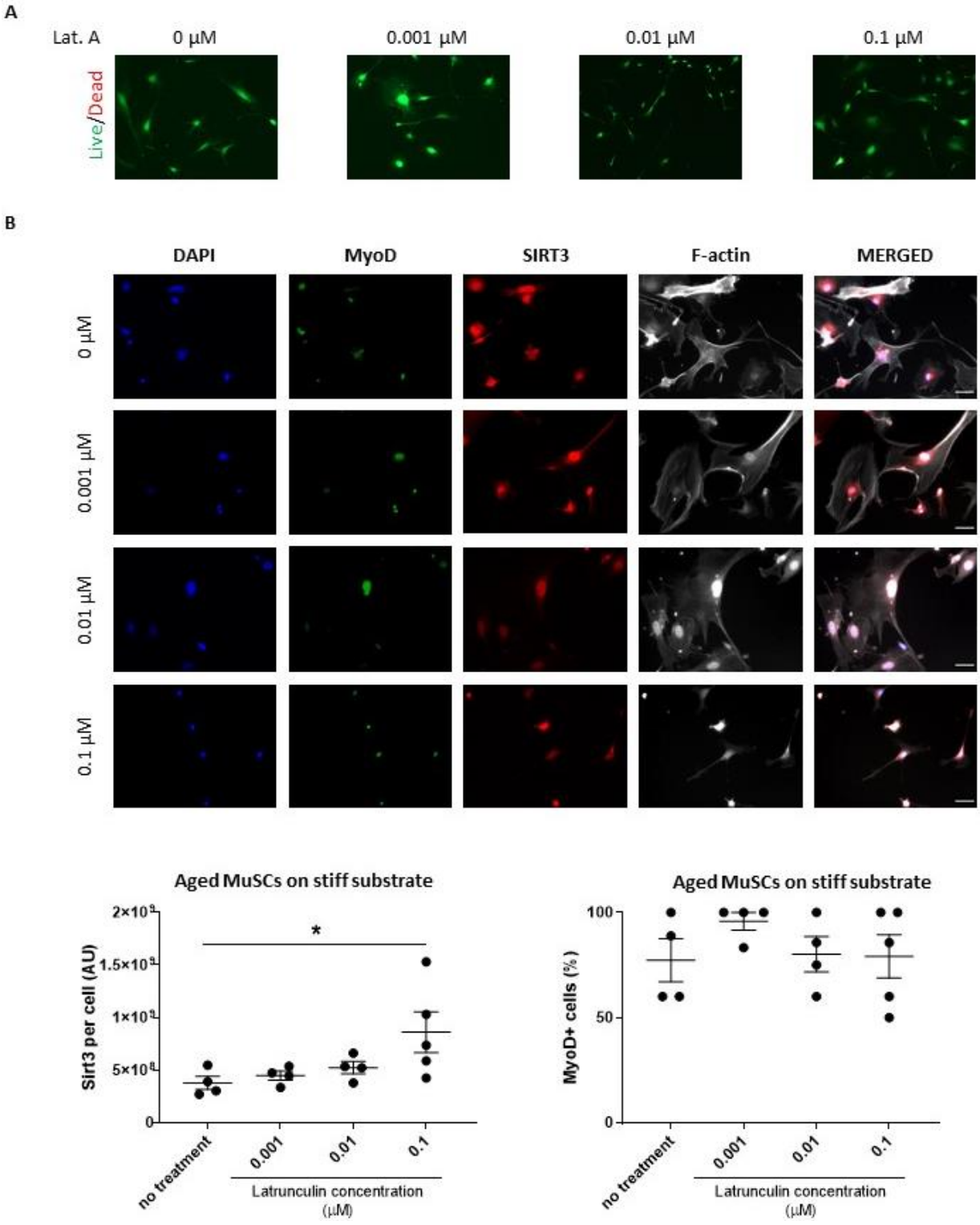
A
Lat. A
0 µM
0.001 µM
0.01 µM
0.1 µM
Live/Dead
B
DAPI
MyoD
SIRT3
F-actin
MERGED
0 µM
0.001 µM
0.01 µM
0.1 µM
Aged MuSCs on stiff substrate
Sirt3 per cell (AU)
2×10⁸
1.5×10⁸
1×10⁸
5×10⁷
0
*
no treatment
0.001
0.01
0.1
Latrunculin concentration (µM)
Aged MuSCs on stiff substrate
MyoD+ cells (%)
100
50
0
no treatment
0.001
0.01
0.1
Latrunculin concentration (µM)

Appendix Figure 6 Latrunculin A dose-response on aged muscle progenitors.

(A) Quantification of live cells in aged muscle progenitors in response to different doses of Lat A. (B) Sirt3 and MyoD quantification of aged muscle progenitors in response to different doses of Lat A. (n=4-5/group; *p=0.0378, one-way ANOVA with Dunnett post-hoc test).

A

	Heart	Aorta	Skeletal Muscle	Degeneration/regeneration, myofiber, subacute	Liver	Kidney	Infiltration, monocuclear cell	Cortex only
Saline 1	NVL	NVL	NVL	0	NVL	NVL	0	X
Saline 2	NVL	NVL	NVL	0	NVL	NVL	NVL	0
Saline 3	NVL	NVL	NVL	0	NVL	F	1 (pelvis)	0
Saline 4	NVL	NVL	NVL	0	NVL	F	2 (pelvis)	X
BAPN Low 1	NVL	NP	NVL	0	NVL	NVL	0	0
BAPN Low 2	NVL	NVL	NVL	0	NVL	F	1	X
BAPN Low 3	NVL	NVL	NVL	1	NVL	NVL	0	X
BAPN High 1	NVL	NVL	NVL	0	NVL	NVL	0	X
BAPN High 2	NVL	NVL	NVL	0	NVL	NVL	0	0
BAPN High 3	NVL	NVL	NVL	0	NVL	NVL	0	0
BAPN High 4	NVL	NVL	F	1 (focal)	NVL	NVL	0	X

NP = not present on slide
X = Cortex only
0 = Cortex and medulla
NVL = no visible lesions
F = Focal
Grading Scale: 0 = None, 1 = Minimal, 2 = Mild

B

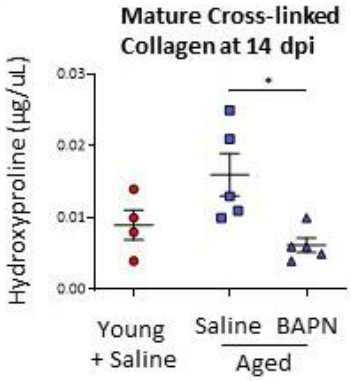

C

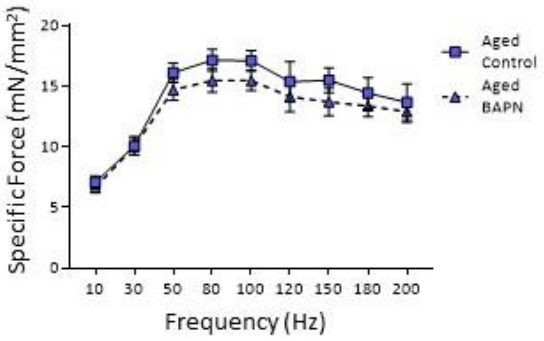

Appendix Figure 7 Effect of daily BAPN injections.

(A) Histopathological examination results. (B) The content of mature crosslinked collagen in TA muscle samples for each experimental group 14 dpi (n=4-5/group; *p=0.0330). (C) Representative SHG images of collagen fibrils and a violin plot of collagen fibril tortuosity. (D) Force-frequency curves obtained from *in situ* contractile testing analysis of specific force of uninjured TA muscle after 4 weeks of daily BAPN injections. (n=11-13/group; p=0.380 when comparing aged control with aged BAPN).

(B) two-way ANOVA with Tukey post-hoc test. (D) mixed two-way ANOVA. Data are represented as mean ± SEM.

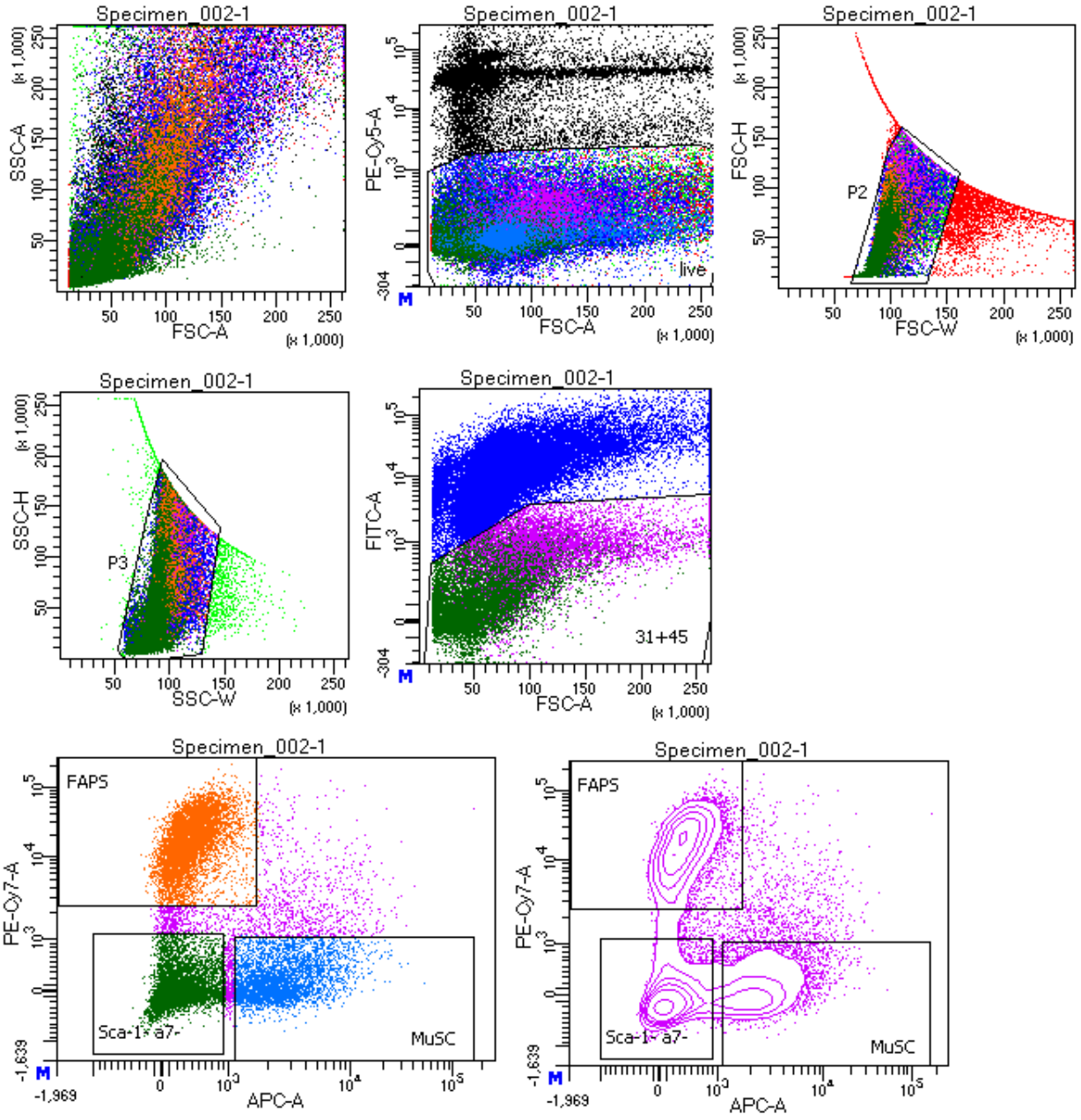

Tube: 1

Population	#Events	%Parent	%Total
All Events	94,890	####	100.0
live	75,636	79.7	79.7
P2	68,623	90.7	72.3
P3	61,963	90.3	65.3
31+45	20,000	32.3	21.1
FAPS	6,359	31.8	6.7
Sca-1- a7-	8,132	40.7	8.6
MuSC	3,875	19.4	4.1

Appendix Figure 8 Representative gating strategy for acquisition of MuSCs on FACS.

A gating strategy to collect live (PE-Cy5-) single cells that are negative for CD31 (FITC), CD45 (FITC), and Sca1 (PE-Cy7) surface markers and positive for Integrin α7 (APC).

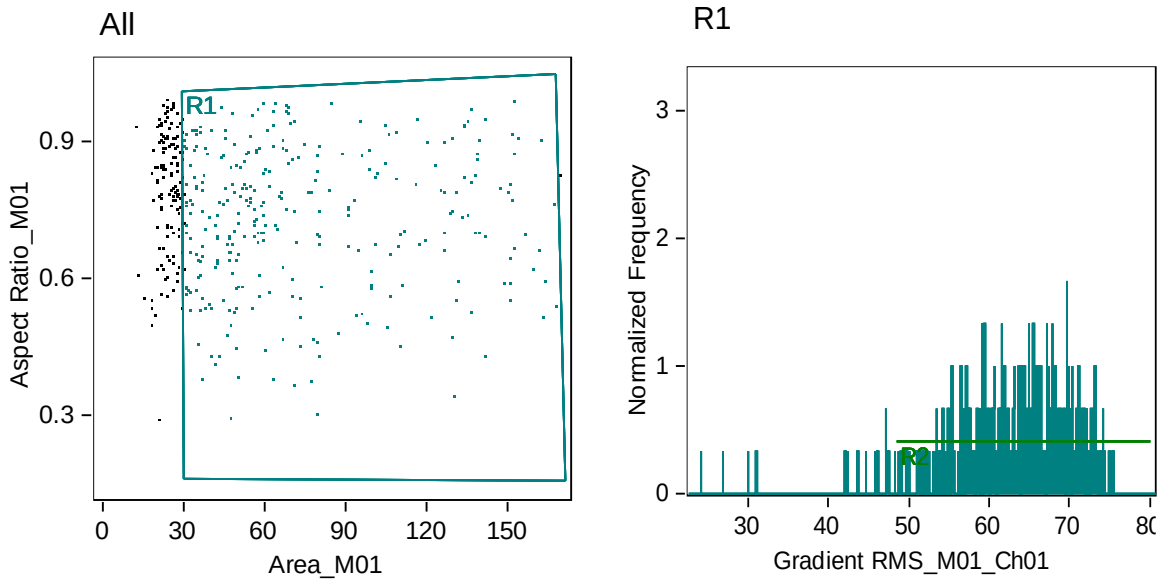

Appendix Figure 9 Representative gating strategy for acquisition of single cells on ImageStream instrument.

A gating strategy to include single cells (R1) that were focused (R2) in the imaging plane.

Appendix Table 1 Physiological data of WT and Sirt3$^{-/-}$ mouse TAs.

Group	Single Twitch Response	Muscle Weight (mg)	Muscle Length (mm at -20°)	CSA (mm²)	Norm. Torque (mNm/mm²)	Time to Max. Contraction (msec.)	1/2 Relaxation Time (msec.)
WT	0.558 ± 0.100	52.4 ± 4.8	13.6 ± 0.4	3.63 ± 0.32	6.53 ± 1.17	24.8 ± 2.8	24.0 ± 7.5
SIRT3$^{-/-}$	0.309 ± 0.084	35.9 ± 3.63	13.3 ± 0.5	2.55 ± 0.27	3.63 ± 0.98	24.7 ± 1.9	29.0 ± 6.1

Bibliography

Aagaard, P., Andersen, J. L., Dyhre-Poulsen, P., Leffers, A.-M., Wagner, A., Magnusson, S. P., … Simonsen, E. B. (2001). A mechanism for increased contractile strength of human pennate muscle in response to strength training: changes in muscle architecture. *The Journal of Physiology*, *534*(2), 613–623. https://doi.org/10.1111/j.1469-7793.2001.t01-1-00613.x

Abdel Khalek, W., Cortade, F., Ollendorff, V., Lapasset, L., Tintignac, L., Chabi, B., & Wrutniak-Cabello, C. (2014). SIRT3, a mitochondrial NAD^+-dependent deacetylase, is involved in the regulation of myoblast differentiation. *PloS One*, *9*(12), e114388. https://doi.org/10.1371/journal.pone.0114388

Ahn, B.-H., Kim, H.-S., Song, S., Lee, I. H., Liu, J., Vassilopoulos, A., … Finkel, T. (2008). A role for the mitochondrial deacetylase Sirt3 in regulating energy homeostasis. *Proceedings of the National Academy of Sciences of the United States of America*, *105*(38), 14447–14452. https://doi.org/10.1073/pnas.0803790105

Alfuraih, A. M., Tan, A. L., O'Connor, P., Emery, P., & Wakefield, R. J. (2019). The effect of ageing on shear wave elastography muscle stiffness in adults. *Aging Clinical and Experimental Research*, *31*(12), 1755–1763. https://doi.org/10.1007/s40520-019-01139-0

Ambrosio, F., Ferrari, R. J., Distefano, G., Plassmeyer, J. M., Carvell, G. E., Deasy, B. M., … Huard, J. (2010). The synergistic effect of treadmill running on stem-cell transplantation to heal injured skeletal muscle. *Tissue Engineering. Part A*, *16*(3), 839–849. https://doi.org/10.1089/ten.TEA.2009.0113

Ansari, A., Rahman, M. S., Saha, S. K., Saikot, F. K., Deep, A., & Kim, K.-H. (2017). Function of the SIRT3 mitochondrial deacetylase in cellular physiology, cancer, and neurodegenerative disease. *Aging Cell*, *16*(1), 4–16. https://doi.org/10.1111/acel.12538

Ansó, E., Weinberg, S. E., Diebold, L. P., Thompson, B. J., Malinge, S., Schumacker, P. T., … Chandel, N. S. (2017). The mitochondrial respiratory chain is essential for haematopoietic stem cell function. *Nature Cell Biology*, *19*(6), 614–625. https://doi.org/10.1038/ncb3529

Archer, S. L. (2013). Mitochondrial dynamics--mitochondrial fission and fusion in human diseases. *The New England Journal of Medicine*, *369*(23), 2236–2251. https://doi.org/10.1056/NEJMra1215233

Balestrini, J. L., Chaudhry, S., Sarrazy, V., Koehler, A., & Hinz, B. (2012). The mechanical memory of lung myofibroblasts. *Integrative Biology : Quantitative Biosciences from Nano to Macro*, *4*(4), 410–421. https://doi.org/10.1039/c2ib00149g

Bartolák-Suki, E., Imsirovic, J., Nishibori, Y., Krishnan, R., & Suki, B. (2017). Regulation of Mitochondrial Structure and Dynamics by the Cytoskeleton and Mechanical Factors. *International Journal of Molecular Sciences*, *18*(8), 7–11. https://doi.org/10.3390/ijms18081812

Becerra, J., Santos-Ruiz, L., Andrades, J. A., & Marí-Beffa, M. (2011). The stem cell niche should be a key issue for cell therapy in regenerative medicine. *Stem Cell Reviews and Reports*, *7*(2), 248–255. https://doi.org/10.1007/s12015-010-9195-5

Benard, G., Bellance, N., James, D., Parrone, P., Fernandez, H., Letellier, T., & Rossignol, R. (2007). Mitochondrial bioenergetics and structural network organization. *Journal of Cell Science*, *120*(Pt 5), 838–848. https://doi.org/10.1242/jcs.03381

Bhattacharya, D., & Scimè, A. (2020). Mitochondrial Function in Muscle Stem Cell Fates. *Frontiers in Cell and Developmental Biology*, *8*(June), 480. https://doi.org/10.3389/fcell.2020.00480

Boldogh, I. R., & Pon, L. A. (2006). Interactions of mitochondria with the actin cytoskeleton. *Biochimica et Biophysica Acta*, *1763*(5–6), 450–462. https://doi.org/10.1016/j.bbamcr.2006.02.014

Boldrin, L., Neal, A., Zammit, P. S., Muntoni, F., & Morgan, J. E. (2012). Donor satellite cell engraftment is significantly augmented when the host niche is preserved and endogenous satellite cells are incapacitated. *Stem Cells (Dayton, Ohio)*, *30*(9), 1971–1984. https://doi.org/10.1002/stem.1158

Bonnans, C., Chou, J., & Werb, Z. (2014). Remodelling the extracellular matrix in development and disease. *Nature Reviews Molecular Cell Biology*, *15*(12), 786–801. https://doi.org/10.1038/nrm3904

Brack, A. S., Conboy, M. J., Roy, S., Lee, M., Kuo, C. J., Keller, C., & Rando, T. A. (2007). Increased Wnt signaling during aging alters muscle stem cell fate and increases fibrosis. *Science (New York, N.Y.)*, *317*(5839), 807–810. https://doi.org/10.1126/science.1144090

Brack, A. S., & Muñoz-Cánoves, P. (2016). The ins and outs of muscle stem cell aging. *Skeletal Muscle*, *6*(1), 1–9. https://doi.org/10.1186/s13395-016-0072-z

Brooks, S. V, & Faulkner, J. a. (1988). Contractile properties of skeletal muscles from young, adult and aged mice. *The Journal of Physiology*, *404*, 71–82. https://doi.org/10.1113/jphysiol.1988.sp017279

Brown, K., Xie, S., Qiu, X., Mohrin, M., Shin, J., Liu, Y., … Chen, D. (2013). SIRT3 reverses aging-associated degeneration. *Cell Reports*, *3*(2), 319–327. https://doi.org/10.1016/j.celrep.2013.01.005

Brüel, A., Ortoft, G., & Oxlund, H. (1998). Inhibition of cross-links in collagen is associated with reduced stiffness of the aorta in young rats. *Atherosclerosis*, *140*(1), 135–145. https://doi.org/10.1016/S0021-9150(98)00130-0

Budday, S., Ovaert, T. C., Holzapfel, G. A., Steinmann, P., & Kuhl, E. (2020). Fifty Shades of Brain: A Review on the Mechanical Testing and Modeling of Brain Tissue. *Archives of Computational Methods in Engineering*, *27*(4), 1187–1230. https://doi.org/10.1007/s11831-019-09352-w

Burdon, R. H. (1995). Superoxide and hydrogen peroxide in relation to mammalian cell proliferation. *Free Radical Biology and Medicine*, *18*(4), 775–794. https://doi.org/10.1016/0891-5849(94)00198-S

Carleton, J. B., D'Amore, A., Feaver, K. R., Rodin, G. J., & Sacks, M. S. (2015). Geometric characterization and simulation of planar layered elastomeric fibrous biomaterials. *Acta Biomaterialia*, *12*(1), 93–101. https://doi.org/10.1016/j.actbio.2014.09.049

Carpenter, A. E., Jones, T. R., Lamprecht, M. R., Clarke, C., Kang, I. H., Friman, O., … Sabatini, D. M. (2006). CellProfiler: image analysis software for identifying and quantifying cell phenotypes. *Genome Biology*, *7*(10), R100. https://doi.org/10.1186/gb-2006-7-10-r100

Castilho, R. M., Squarize, C. H., Chodosh, L. A., Williams, B. O., & Gutkind, J. S. (2009). mTOR mediates Wnt-induced epidermal stem cell exhaustion and aging. *Cell Stem Cell*, *5*(3), 279–289. https://doi.org/10.1016/j.stem.2009.06.017

Chakkalakal, J. V., Jones, K. M., Basson, M. A., & Brack, A. S. (2012). The aged niche disrupts muscle stem cell quiescence. *Nature*, *490*(7420), 355–360. https://doi.org/10.1038/nature11438

Charrier, E. E., Pogoda, K., Wells, R. G., & Janmey, P. A. (2018). Control of cell morphology and differentiation by substrates with independently tunable elasticity and viscous dissipation. *Nature Communications*, *9*(1), 449. https://doi.org/10.1038/s41467-018-02906-9

Cheikhi, A., Wallace, C., St Croix, C., Cohen, C., Tang, W.-Y., Wipf, P., … Barchowsky, A. (2019). Mitochondria are a substrate of cellular memory. *Free Radical Biology & Medicine*, *130*(September 2018), 528–541. https://doi.org/10.1016/j.freeradbiomed.2018.11.028

Chen, L.-F., Liao, H.-Y. M., Ko, M.-T., Lin, J.-C., & Yu, G.-J. (2000). A new LDA-based face recognition system which can solve the small sample size problem. *Pattern Recognition*, *33*(10), 1713–1726. https://doi.org/10.1016/S0031-3203(99)00139-9

Chen, W., Wang, L., You, W., & Shan, T. (2020). Myokines mediate the cross talk between skeletal muscle and other organs. *Journal of Cellular Physiology*, (August), jcp.30033. https://doi.org/10.1002/jcp.30033

Clarfield, A. M. (1990). Dr. Ignatz Nascher and the birth of geriatrics. *CMAJ : Canadian Medical Association Journal = Journal de l'Association Medicale Canadienne*, *143*(9), 944–945, 948. Retrieved from http://www.ncbi.nlm.nih.gov/pubmed/2224727

Cogliati, S., Frezza, C., Soriano, M. E., Varanita, T., Quintana-Cabrera, R., Corrado, M., … Scorrano, L. (2013). Mitochondrial cristae shape determines respiratory chain supercomplexes assembly and respiratory efficiency. *Cell*, *155*(1), 160–171. https://doi.org/10.1016/j.cell.2013.08.032

Conboy, I. M., Conboy, M. J., Smythe, G. M., & Rando, T. A. (2003). Notch-mediated restoration of regenerative potential to aged muscle. *Science (New York, N.Y.)*, *302*(5650), 1575–1577. https://doi.org/10.1126/science.1087573

Conboy, I. M., Conboy, M. J., Wagers, A. J., Girma, E. R., Weissman, I. L., & Rando, T. A. (2005). Rejuvenation of aged progenitor cells by exposure to a young systemic environment. *Nature*, *433*(7027), 760–764. https://doi.org/10.1038/nature03260

Cosgrove, B. D., Gilbert, P. M., Porpiglia, E., Mourkioti, F., Lee, S. P., Corbel, S. Y., … Blau, H. M. (2014). Rejuvenation of the muscle stem cell population restores strength to injured aged muscles. *Nature Medicine*, *20*(3), 255–264. https://doi.org/10.1038/nm.3464

Cox, T. R., & Erler, J. T. (2011). Remodeling and homeostasis of the extracellular matrix: implications for fibrotic diseases and cancer. *Disease Models & Mechanisms*, *4*(2), 165–178. https://doi.org/10.1242/dmm.004077

Crane, J. D., Devries, M. C., Safdar, A., Hamadeh, M. J., & Tarnopolsky, M. A. (2010). The effect of aging on human skeletal muscle mitochondrial and intramyocellular lipid ultrastructure. *Journals of Gerontology - Series A Biological Sciences and Medical Sciences*, *65*(2), 119–128. https://doi.org/10.1093/gerona/glp179

Cuevas-Trisan, R. (2017). Balance Problems and Fall Risks in the Elderly. *Physical Medicine and Rehabilitation Clinics of North America*, *28*(4), 727–737. https://doi.org/10.1016/j.pmr.2017.06.006

D'Amore, A., Amoroso, N., Gottardi, R., Hobson, C., Carruthers, C., Watkins, S., … Sacks, M. S. (2014). From single fiber to macro-level mechanics: A structural finite-element model for elastomeric fibrous biomaterials. *Journal of the Mechanical Behavior of Biomedical Materials*, *39*, 146–161. https://doi.org/10.1016/j.jmbbm.2014.07.016

D'Amore, A., Nasello, G., Luketich, S. K., Denisenko, D., Jacobs, D. L., Hoff, R., … Wagner, W. R. (2018). Meso-scale topological cues influence extracellular matrix production in a large deformation, elastomeric scaffold model. *Soft Matter*, *14*(42), 8483–8495. https://doi.org/10.1039/c8sm01352g

D'Amore, A., Soares, J. S., Stella, J. A., Zhang, W., Amoroso, N. J., Mayer, J. E., … Sacks, M. S. (2016). Large strain stimulation promotes extracellular matrix production and stiffness in an elastomeric scaffold model. *Journal of the Mechanical Behavior of Biomedical Materials*, *62*, 619–635. https://doi.org/10.1016/j.jmbbm.2016.05.005

D'Amore, A., Stella, J. A., Wagner, W. R., & Sacks, M. S. (2010). Characterization of the complete fiber network topology of planar fibrous tissues and scaffolds. *Biomaterials*, *31*(20), 5345–5354. https://doi.org/10.1016/j.biomaterials.2010.03.052

Dahl, K. N., Booth-Gauthier, E. A., & Ladoux, B. (2010). In the middle of it all: mutual mechanical regulation between the nucleus and the cytoskeleton. *Journal of Biomechanics*, *43*(1), 2–8. https://doi.org/10.1016/j.jbiomech.2009.09.002

Dalby, M. J., Gadegaard, N., Tare, R., Andar, A., Riehle, M. O., Herzyk, P., … Oreffo, R. O. C. (2007). The control of human mesenchymal cell differentiation using nanoscale symmetry and disorder. *Nature Materials*, *6*(12), 997–1003. https://doi.org/10.1038/nmat2013

Delezie, J., & Handschin, C. (2018). Endocrine Crosstalk Between Skeletal Muscle and the Brain. *Frontiers in Neurology*, *9*(AUG). https://doi.org/10.3389/fneur.2018.00698

Dell'Orso, S., Juan, A. H., Ko, K., Naz, F., Perovanovic, J., Gutierrez-Cruz, G., … Sartorelli, V. (2019). Correction: Single cell analysis of adult mouse skeletal muscle stem cells in homeostatic and regenerative conditions (doi: 10.1242/dev.174177). *Development (Cambridge, England)*, *146*(13). https://doi.org/10.1242/dev.181743

Downing, T. L., Soto, J., Morez, C., Houssin, T., Fritz, A., Yuan, F., … Li, S. (2013). Biophysical regulation of epigenetic state and cell reprogramming. *Nature Materials*, *12*(12), 1154–1162. https://doi.org/10.1038/nmat3777

Dresner, M. A., Rose, G. H., Rossman, P. J., Muthupillai, R., Manduca, A., & Ehman, R. L. (2001). Magnetic resonance elastography of skeletal muscle. *Journal of Magnetic Resonance Imaging*, *13*(2), 269–276. https://doi.org/10.1002/1522-2586(200102)13:2<269::AID-JMRI1039>3.0.CO;2-1

Duarte, A., Poderoso, C., Cooke, M., Soria, G., Cornejo Maciel, F., Gottifredi, V., & Podestá, E. J. (2012). Mitochondrial Fusion Is Essential for Steroid Biosynthesis. *PLoS ONE*, *7*(9), 1–12. https://doi.org/10.1371/journal.pone.0045829

Duffy, R. M., Sun, Y., & Feinberg, A. W. (2016). Understanding the Role of ECM Protein Composition and Geometric Micropatterning for Engineering Human Skeletal Muscle. *Annals of Biomedical Engineering*, *44*(6), 2076–2089. https://doi.org/10.1007/s10439-016-1592-8

Dupont, S., Morsut, L., Aragona, M., Enzo, E., Giulitti, S., Cordenonsi, M., … Piccolo, S. (2011). Role of YAP/TAZ in mechanotransduction. *Nature*, *474*(7350), 179–183. https://doi.org/10.1038/nature10137

Eby, S. F., Cloud, B. A., Brandenburg, J. E., Giambini, H., Song, P., Chen, S., … An, K.-N. (2015). Shear wave elastography of passive skeletal muscle stiffness: Influences of sex and age throughout adulthood. *Clinical Biomechanics*, *30*(1), 22–27. https://doi.org/10.1016/j.clinbiomech.2014.11.011

El'darov, C. M., Vays, V. B., Vangeli, I. M., Kolosova, N. G., & Bakeeva, L. E. (2015). Morphometric examination of mitochondrial ultrastructure in aging cardiomyocytes. *Biochemistry (Moscow)*, *80*(5), 604–609. https://doi.org/10.1134/S0006297915050132

Engler, A. J., Griffin, M. A., Sen, S., Bönnemann, C. G., Sweeney, H. L., & Discher, D. E. (2004). Myotubes differentiate optimally on substrates with tissue-like stiffness: pathological implications for soft or stiff microenvironments. *The Journal of Cell Biology*, *166*(6), 877–887. https://doi.org/10.1083/jcb.200405004

Engler, A. J., Sen, S., Sweeney, H. L., & Discher, D. E. (2006). Matrix elasticity directs stem cell lineage specification. *Cell*, *126*(4), 677–689. https://doi.org/10.1016/j.cell.2006.06.044

FDA. (2019). FDA Warns About Stem Cell Therapies. Retrieved March 4, 2021, from https://www.fda.gov/consumers/consumer-updates/fda-warns-about-stem-cell-therapies

Finegold, J. A., Asaria, P., & Francis, D. P. (2013). Mortality from ischaemic heart disease by country, region, and age: Statistics from World Health Organisation and United Nations. *International Journal of Cardiology*, *168*(2), 934–945. https://doi.org/10.1016/j.ijcard.2012.10.046

Franceschi, C., Garagnani, P., Morsiani, C., Conte, M., Santoro, A., Grignolio, A., … Salvioli, S. (2018). The continuum of aging and age-related diseases: Common mechanisms but different rates. *Frontiers in Medicine*, *5*(MAR). https://doi.org/10.3389/fmed.2018.00061

Freitas-Rodríguez, S., Folgueras, A. R., & López-Otín, C. (2017). The role of matrix metalloproteinases in aging: Tissue remodeling and beyond. *Biochimica et Biophysica Acta. Molecular Cell Research*, *1864*(11 Pt A), 2015–2025. https://doi.org/10.1016/j.bbamcr.2017.05.007

Gajdosik, R. L., Vander Linden, D. W., & Williams, A. K. (1999). Influence of Age on Length and Passive Elastic Stiffness Characteristics of the Calf Muscle-Tendon Unit of Women. *Physical Therapy*, *79*(9), 827–838. https://doi.org/10.1093/ptj/79.9.827

Gandarillas, A., & Watt, F. M. (1997). c-Myc promotes differentiation of human epidermal stem cells. *Genes and Development*, *11*(21), 2869–2882. https://doi.org/10.1101/gad.11.21.2869

Gao, Y., Kostrominova, T. Y., Faulkner, J. A., & Wineman, A. S. (2008). Age-related changes in the mechanical properties of the epimysium in skeletal muscles of rats. *Journal of Biomechanics*, *41*(2), 465–469. https://doi.org/10.1016/j.jbiomech.2007.09.021

García-Prat, L., Martínez-Vicente, M., Perdiguero, E., Ortet, L., Rodríguez-Ubreva, J., Rebollo, E., … Muñoz-Cánoves, P. (2016). Autophagy maintains stemness by preventing senescence. *Nature*, *529*(7584), 37–42. https://doi.org/10.1038/nature16187

García-Prat, L., & Muñoz-Cánoves, P. (2017). Aging, metabolism and stem cells: Spotlight on muscle stem cells. *Molecular and Cellular Endocrinology*, *445*, 109–117. https://doi.org/10.1016/j.mce.2016.08.021

Ghazanfari, S., Tafazzoli-Shadpour, M., & Shokrgozar, M. A. (2009). Effects of cyclic stretch on proliferation of mesenchymal stem cells and their differentiation to smooth muscle cells. *Biochemical and Biophysical Research Communications*, *388*(3), 601–605. https://doi.org/10.1016/j.bbrc.2009.08.072

Ghosh, S., & Zhou, Z. (2014). Genetics of aging, progeria and lamin disorders. *Current Opinion in Genetics & Development*, *26*, 41–46. https://doi.org/10.1016/j.gde.2014.05.003

Gilbert, P. M., Havenstrite, K. L., Magnusson, K. E. G., Sacco, A., Leonardi, N. A., Kraft, P., … Blau, H. M. (2010). Substrate elasticity regulates skeletal muscle stem cell self-renewal in culture. *Science (New York, N.Y.)*, *329*(5995), 1078–1081. https://doi.org/10.1126/science.1191035

Gillies, A. R., & Lieber, R. L. (2011). Structure and function of the skeletal muscle extracellular matrix. *Muscle & Nerve*, *44*(3), 318–331. https://doi.org/10.1002/mus.22094

Gopinath, S. D., & Rando, T. A. (2008). Stem Cell Review Series: Aging of the skeletal muscle stem cell niche. *Aging Cell*, *7*(4), 590–598. https://doi.org/10.1111/j.1474-9726.2008.00399.x

Gosselin, L. E., Adams, C., Cotter, T. A., McCormick, R. J., & Thomas, D. P. (1998). Effect of exercise training on passive stiffness in locomotor skeletal muscle: role of extracellular matrix. *Journal of Applied Physiology (Bethesda, Md. : 1985)*, *85*(3), 1011–1016. https://doi.org/10.1152/jappl.1998.85.3.1011

Green and John C. Reed, D. R. (1998). Mitochondria and Apoptosis. *Science*, *281*(5381), 1309–1312. https://doi.org/10.1126/science.281.5381.1309

Hackenbrock, C. R. (1966). Ultrastructural bases for metabolically linked mechanical activity in mitochondria. I. Reversible ultrastructural changes with change in metabolic steady state in isolated liver mitochondria. *The Journal of Cell Biology*, *30*(2), 269–297. https://doi.org/10.1083/jcb.30.2.269

Hansen, M., & Kennedy, B. K. (2016). Does Longer Lifespan Mean Longer Healthspan? *Trends in Cell Biology*, *26*(8), 565–568. https://doi.org/10.1016/j.tcb.2016.05.002

Herbert, J. M., Bono, F., & Savi, P. (1996). The mitogenic effect of H2O2 for vascular smooth muscle cells is mediated by an increase of the affinity of basic fibroblast growth factor for its receptor. *FEBS Letters*, *395*(1), 43–47. https://doi.org/10.1016/0014-5793(96)00998-2

Heron, M. (2019). Deaths: Leading Causes for 2017. *National Vital Statistics Reports : From the Centers for Disease Control and Prevention, National Center for Health Statistics, National Vital Statistics System*, *68*(6), 1–77. Retrieved from http://www.ncbi.nlm.nih.gov/pubmed/32501203

Heys, K. R., Cram, S. L., & Truscott, R. J. W. (2004). Massive increase in the stiffness of the human lens nucleus with age: the basis for presbyopia? *Molecular Vision*, *10*, 956–963. Retrieved from http://www.ncbi.nlm.nih.gov/pubmed/15616482

Hinds, J. W., & McNelly, N. A. (1977). Aging of the rat olfactory bulb: growth and atrophy of constituent layers and changes in size and number of mitral cells. *The Journal of Comparative Neurology*, *72*(3), 345–367. https://doi.org/10.1002/cne.901710304

Hinits, Y., Williams, V. C., Sweetman, D., Donn, T. M., Ma, T. P., Moens, C. B., & Hughes, S. M. (2011). Defective cranial skeletal development, larval lethality and haploinsufficiency in Myod mutant zebrafish. *Developmental Biology*, *358*(1), 102–112. https://doi.org/10.1016/j.ydbio.2011.07.015

History | National Institute on Aging. (n.d.). Retrieved July 31, 2020, from https://www.nia.nih.gov/about/history

Hori, S., Hiramuki, Y., Nishimura, D., Sato, F., & Sehara-Fujisawa, A. (2019). PDH-mediated metabolic flow is critical for skeletal muscle stem cell differentiation and myotube formation during regeneration in mice. *FASEB Journal : Official Publication of the Federation of American Societies for Experimental Biology*, *33*(7), 8094–8109. https://doi.org/10.1096/fj.201802479R

Hu, X., Park, S.-H., Gil, E. S., Xia, X.-X., Weiss, A. S., & Kaplan, D. L. (2011). The influence of elasticity and surface roughness on myogenic and osteogenic-differentiation of cells on silk-elastin biomaterials. *Biomaterials*, *32*(34), 8979–8989. https://doi.org/10.1016/j.biomaterials.2011.08.037

Hwang, J. H., Ra, Y.-J., Lee, K. M., Lee, J. Y., & Ghil, S. H. (2006). Therapeutic effect of passive mobilization exercise on improvement of muscle regeneration and prevention of fibrosis after laceration injury of rat. *Archives of Physical Medicine and Rehabilitation*, *87*(1), 20–26. https://doi.org/10.1016/j.apmr.2005.08.002

Iberite, F., Salerno, M., Canale, C., Rosa, A., & Ricotti, L. (2019). Influence of substrate stiffness on human induced pluripotent stem cells: preliminary results. *Conference Proceedings : ... Annual International Conference of the IEEE Engineering in Medicine and Biology Society. IEEE Engineering in Medicine and Biology Society. Annual Conference*, *2019*, 1039–1043. https://doi.org/10.1109/EMBC.2019.8857397

Janmey, P. A., Fletcher, D. A., & Reinhart-King, C. A. (2020). Stiffness Sensing by Cells. *Physiological Reviews*, *100*(2), 695–724. https://doi.org/10.1152/physrev.00013.2019

Jazwinski, S. M., & Kim, S. (2019). Examination of the dimensions of biological age. *Frontiers in Genetics*, *10*(MAR), 1–7. https://doi.org/10.3389/fgene.2019.00263

Jin, G., Xu, C., Zhang, X., Long, J., Rezaeian, A. H., Liu, C., … Lin, H.-K. (2018). Atad3a suppresses Pink1-dependent mitophagy to maintain homeostasis of hematopoietic progenitor cells. *Nature Immunology*, *19*(1), 29–40. https://doi.org/10.1038/s41590-017-0002-1

Joanisse, S., Nederveen, J. P., Baker, J. M., Snijders, T., Iacono, C., & Parise, G. (2016). Exercise conditioning in old mice improves skeletal muscle regeneration. *FASEB Journal : Official Publication of the Federation of American Societies for Experimental Biology*, *30*(9), 3256–3268. https://doi.org/10.1096/fj.201600143RR

Joseph, A.-M., Adhihetty, P. J., Buford, T. W., Wohlgemuth, S. E., Lees, H. A., Nguyen, L. M. D., … Leeuwenburgh, C. (2012). The impact of aging on mitochondrial function and biogenesis pathways in skeletal muscle of sedentary high- and low-functioning elderly individuals. *Aging Cell*, *11*(5), 801–809. https://doi.org/10.1111/j.1474-9726.2012.00844.x

Kasper, G., Mao, L., Geissler, S., Draycheva, A., Trippens, J., Kühnisch, J., … Klose, J. (2009). Insights into mesenchymal stem cell aging: involvement of antioxidant defense and actin cytoskeleton. *Stem Cells (Dayton, Ohio)*, *27*(6), 1288–1297. https://doi.org/10.1002/stem.49

Keenan, A. B., Torre, D., Lachmann, A., Leong, A. K., Wojciechowicz, M. L., Utti, V., … Ma'ayan, A. (2019). ChEA3: transcription factor enrichment analysis by orthogonal omics integration. *Nucleic Acids Research*, *47*(W1), W212–W224. https://doi.org/10.1093/nar/gkz446

Khacho, M., Clark, A., Svoboda, D. S., Azzi, J., MacLaurin, J. G., Meghaizel, C., … Slack, R. S. (2016). Mitochondrial Dynamics Impacts Stem Cell Identity and Fate Decisions by Regulating a Nuclear Transcriptional Program. *Cell Stem Cell*, *19*(2), 232–247. https://doi.org/10.1016/j.stem.2016.04.015

Killaars, A. R., Grim, J. C., Walker, C. J., Hushka, E. A., Brown, T. E., & Anseth, K. S. (2019). Extended Exposure to Stiff Microenvironments Leads to Persistent Chromatin Remodeling in Human Mesenchymal Stem Cells. *Advanced Science (Weinheim, Baden-Wurttemberg, Germany)*, *6*(3), 1801483. https://doi.org/10.1002/advs.201801483

Kim, T.-J., Sun, J., Lu, S., Zhang, J., & Wang, Y. (2014). The regulation of β-adrenergic receptor-mediated PKA activation by substrate stiffness via microtubule dynamics in human MSCs. *Biomaterials*, *35*(29), 8348–8356. https://doi.org/10.1016/j.biomaterials.2014.06.018

Kimmel, J. C., Hwang, A. B., Scaramozza, A., Marshall, W. F., & Brack, A. S. (2020). Aging induces aberrant state transition kinetics in murine muscle stem cells. *Development (Cambridge, England)*, (March). https://doi.org/10.1242/dev.183855

Kincaid, B., & Bossy-Wetzel, E. (2013). Forever young: SIRT3 a shield against mitochondrial meltdown, aging, and neurodegeneration. *Frontiers in Aging Neuroscience*, *5*(SEP), 48. https://doi.org/10.3389/fnagi.2013.00048

Kjaer, M. (2004). Role of extracellular matrix in adaptation of tendon and skeletal muscle to mechanical loading. *Physiological Reviews*, *84*(2), 649–698. https://doi.org/10.1152/physrev.00031.2003

Kozakowska, M., Pietraszek-Gremplewicz, K., Jozkowicz, A., & Dulak, J. (2015). The role of oxidative stress in skeletal muscle injury and regeneration: focus on antioxidant enzymes. *Journal of Muscle Research and Cell Motility*, *36*(6), 377–393. https://doi.org/10.1007/s10974-015-9438-9

Krishnan, R. (2020). Introduction to the Monograph. *BMH Medical Journal*, *7*, 2–7.

Lacraz, G., Rouleau, A.-J., Couture, V., Söllrald, T., Drouin, G., Veillette, N., … Grenier, G. (2015). Increased Stiffness in Aged Skeletal Muscle Impairs Muscle Progenitor Cell Proliferative Activity. *PloS One*, *10*(8), e0136217. https://doi.org/10.1371/journal.pone.0136217

Lammerding, J., Hsiao, J., Schulze, P. C., Kozlov, S., Stewart, C. L., & Lee, R. T. (2005). Abnormal nuclear shape and impaired mechanotransduction in emerin-deficient cells. *The Journal of Cell Biology*, *170*(5), 781–791. https://doi.org/10.1083/jcb.200502148

Latil, M., Rocheteau, P., Châtre, L., Sanulli, S., Mémet, S., Ricchetti, M., … Chrétien, F. (2012). Skeletal muscle stem cells adopt a dormant cell state post mortem and retain regenerative capacity. *Nature Communications*, *3*(May), 903. https://doi.org/10.1038/ncomms1890

Lavasani, M., Robinson, A. R., Lu, A., Song, M., Feduska, J. M., Ahani, B., … Huard, J. (2012). Muscle-derived stem/progenitor cell dysfunction limits healthspan and lifespan in a murine progeria model. *Nature Communications*, *3*(1), 608. https://doi.org/10.1038/ncomms1611

Le Grand, F., & Rudnicki, M. A. (2007). Skeletal muscle satellite cells and adult myogenesis. *Current Opinion in Cell Biology*, *19*(6), 628–633. https://doi.org/10.1016/j.ceb.2007.09.012

Lee, R., & Mason, A. (2017). Cost of Aging. *Finance & Development*, *54*(1), 7–9. https://doi.org/10.1016/j.physbeh.2017.03.040

Lee, W. J., Liu, L. K., Hwang, A. C., Peng, L. N., Lin, M. H., & Chen, L. K. (2017). Dysmobility Syndrome and Risk of Mortality for Community-Dwelling Middle-Aged and Older Adults: The Nexus of Aging and Body Composition. *Scientific Reports*, *7*(1), 1–9. https://doi.org/10.1038/s41598-017-09366-z

Lele, T. P., Brock, A., & Peyton, S. R. (2020). Emerging Concepts and Tools in Cell Mechanomemory. *Annals of Biomedical Engineering*, *48*(7), 2103–2112. https://doi.org/10.1007/s10439-019-02412-z

Li, J., Stouffs, M., Serrander, L., Banfi, B., Bettiol, E., Charnay, Y., … Jaconi, M. E. (2006). The NADPH oxidase NOX4 drives cardiac differentiation: Role in regulating cardiac transcription factors and MAP kinase activation. *Molecular Biology of the Cell*, *17*(9), 3978–3988. https://doi.org/10.1091/mbc.e05-06-0532

Li, S.-T., Huang, D., Shen, S., Cai, Y., Xing, S., Wu, G., … Gao, P. (2020). Myc-mediated SDHA acetylation triggers epigenetic regulation of gene expression and tumorigenesis. *Nature Metabolism*, *2*(3), 256–269. https://doi.org/10.1038/s42255-020-0179-8

Liao, Y.-H., Chen, S.-Y., Chou, S.-Y., Wang, P.-H., Tsai, M.-R., & Sun, C.-K. (2013). Determination of chronological aging parameters in epidermal keratinocytes by in vivo harmonic generation microscopy. *Biomedical Optics Express*, *4*(1), 77–88. https://doi.org/10.1364/BOE.4.000077

Ligon, L. A., & Steward, O. (2000). Role of microtubules and actin filaments in the movement of mitochondria in the axons and dendrites of cultured hippocampal neurons. *The Journal of Comparative Neurology*, *427*(3), 351–361. https://doi.org/10.1002/1096-9861(20001120)427:3<351::aid-cne3>3.0.co;2-r

Liu, H., Fergusson, M. M., Castilho, R. M., Liu, J., Cao, L., Chen, J., … Finkel, T. (2007). Augmented Wnt signaling in a mammalian model of accelerated aging. *Science (New York, N.Y.)*, *317*(5839), 803–806. https://doi.org/10.1126/science.1143578

Liu, L., Charville, G. W., Cheung, T. H., Yoo, B., Santos, P. J., Schroeder, M., & Rando, T. A. (2018). Impaired Notch Signaling Leads to a Decrease in p53 Activity and Mitotic Catastrophe in Aged Muscle Stem Cells. *Cell Stem Cell*, *23*(4), 544-556.e4. https://doi.org/10.1016/j.stem.2018.08.019

Liu, L., Cheung, T. H., Charville, G. W., & Rando, T. A. (2015). Isolation of skeletal muscle stem cells by fluorescence-activated cell sorting. *Nature Protocols*, *10*(10), 1612–1624. https://doi.org/10.1038/nprot.2015.110

Liu, Y. J., McIntyre, R. L., Janssens, G. E., & Houtkooper, R. H. (2020). Mitochondrial fission and fusion: A dynamic role in aging and potential target for age-related disease. *Mechanisms of Ageing and Development*, *186*(February), 111212. https://doi.org/10.1016/j.mad.2020.111212

Liu, Z., He, Q., Ding, X., Zhao, T., Zhao, L., & Wang, A. (2015). SOD2 is a C-myc target gene that promotes the migration and invasion of tongue squamous cell carcinoma involving cancer stem-like cells. *The International Journal of Biochemistry & Cell Biology*, *60*, 139–146. https://doi.org/10.1016/j.biocel.2014.12.022

Lombard, D. B., Tishkoff, D. X., & Bao, J. (2011). Mitochondrial sirtuins in the regulation of mitochondrial activity and metabolic adaptation. *Handbook of Experimental Pharmacology*, *206*(1), 163–188. https://doi.org/10.1007/978-3-642-21631-2_8

López-Otín, C., Blasco, M. A., Partridge, L., Serrano, M., & Kroemer, G. (2013). The hallmarks of aging. *Cell*, *153*(6), 1194. https://doi.org/10.1016/j.cell.2013.05.039

Luo, W., Chen, J., Li, L., Ren, X., Cheng, T., Lu, S., … Hanotte, O. (2019). c-Myc inhibits myoblast differentiation and promotes myoblast proliferation and muscle fibre hypertrophy by regulating the expression of its target genes, miRNAs and lincRNAs. *Cell Death and Differentiation*, *26*(3), 426–442. https://doi.org/10.1038/s41418-018-0129-0

Madl, C. M., Heilshorn, S. C., & Blau, H. M. (2018). Bioengineering strategies to accelerate stem cell therapeutics. *Nature*, *557*(7705), 335–342. https://doi.org/10.1038/s41586-018-0089-z

Majmundar, A. J., Lee, D. S. M., Skuli, N., Mesquita, R. C., Kim, M. N., Yodh, A. G., … Simon, M. C. (2015). HIF modulation of Wnt signaling regulates skeletal myogenesis in vivo. *Development (Cambridge, England)*, *142*(14), 2405–2412. https://doi.org/10.1242/dev.123026

Mammoto, T., Jiang, E., Jiang, A., & Mammoto, A. (2013). Extracellular matrix structure and tissue stiffness control postnatal lung development through the lipoprotein receptor-related protein 5/Tie2 signaling system. *American Journal of Respiratory Cell and Molecular Biology*, *49*(6), 1009–1018. https://doi.org/10.1165/rcmb.2013-0147OC

Mann, C. J., Perdiguero, E., Kharraz, Y., Aguilar, S., Pessina, P., Serrano, A. L., & Muñoz-Cánoves, P. (2011). Aberrant repair and fibrosis development in skeletal muscle. *Skeletal Muscle*, *1*(1), 21. https://doi.org/10.1186/2044-5040-1-21

MAURO, A. (1961). Satellite cell of skeletal muscle fibers. *The Journal of Biophysical and Biochemical Cytology*, *9*, 493–495. https://doi.org/10.1083/jcb.9.2.493

Max Roser, Esteban Ortiz-Ospina, & Hannah Ritchie. (2013). Life Expectancy. Retrieved July 27, 2020, from Our World in Data website: https://ourworldindata.org/life-expectancy#life-expectancy-has-improved-globally

McBride, H. M., Neuspiel, M., & Wasiak, S. (2006). Mitochondria: More Than Just a Powerhouse. *Current Biology*, *16*(14), R551–R560. https://doi.org/10.1016/j.cub.2006.06.054

McDonald, R. B. (2013). *Biology of Aging*. Retrieved from https://www.google.com/books/edition/_/6TImAgAAQBAJ?hl=en&gbpv=1&pg=PR4&dq=Basic+Concepts+in+the+Biology+of+Aging+McDonald,+Roger

McLeod, M., Breen, L., Hamilton, D. L., & Philp, A. (2016). Live strong and prosper: the importance of skeletal muscle strength for healthy ageing. *Biogerontology*, *17*(3), 497–510. https://doi.org/10.1007/s10522-015-9631-7

McMurray, R. J., Gadegaard, N., Tsimbouri, P. M., Burgess, K. V., McNamara, L. E., Tare, R., … Dalby, M. J. (2011). Nanoscale surfaces for the long-term maintenance of mesenchymal stem cell phenotype and multipotency. *Nature Materials*, *10*(8), 637–644. https://doi.org/10.1038/nmat3058

McNerny, E. M. B., Gong, B., Morris, M. D., & Kohn, D. H. (2015). Bone fracture toughness and strength correlate with collagen cross-link maturity in a dose-controlled lathyrism mouse model. *Journal of Bone and Mineral Research : The Official Journal of the American Society for Bone and Mineral Research*, *30*(3), 455–464. https://doi.org/10.1002/jbmr.2356

Melkov, A., & Abdu, U. (2018). Regulation of long-distance transport of mitochondria along microtubules. *Cellular and Molecular Life Sciences : CMLS*, *75*(2), 163–176. https://doi.org/10.1007/s00018-017-2590-1

Melov, S., Coskun, P., Patel, M., Tuinstra, R., Cottrell, B., Jun, A. S., … Wallace, D. C. (1999). Mitochondrial disease in superoxide dismutase 2 mutant mice. *Proceedings of the National Academy of Sciences*, *96*(3), 846–851. https://doi.org/10.1073/pnas.96.3.846

Mendelsohn, A. R., & Larrick, J. W. (2014). Partial reversal of skeletal muscle aging by restoration of normal NAD^+ levels. *Rejuvenation Research*, *17*(1), 62–69. https://doi.org/10.1089/rej.2014.1546

Meng, H., Yan, W.-Y., Lei, Y.-H., Wan, Z., Hou, Y.-Y., Sun, L.-K., & Zhou, J.-P. (2019). SIRT3 Regulation of Mitochondrial Quality Control in Neurodegenerative Diseases. *Frontiers in Aging Neuroscience*, *11*(November), 313. https://doi.org/10.3389/fnagi.2019.00313

Metter, E. J., Talbot, L. A., Schrager, M., & Conwit, R. (2002). Skeletal muscle strength as a predictor of all-cause mortality in healthy men. *The Journals of Gerontology Series A: Biological Sciences and Medical Sciences*, *57*(10), B359–B365. https://doi.org/10.1093/gerona/57.10.B359

Meyer, J. N., Leuthner, T. C., & Luz, A. L. (2017). Mitochondrial fusion, fission, and mitochondrial toxicity. *Toxicology*, *391*(March), 42–53. https://doi.org/10.1016/j.tox.2017.07.019

Miller, B. F., Olesen, J. L., Hansen, M., Døssing, S., Crameri, R. M., Welling, R. J., … Rennie, M. J. (2005). Coordinated collagen and muscle protein synthesis in human patella tendon and quadriceps muscle after exercise. *The Journal of Physiology*, *567*(Pt 3), 1021–1033. https://doi.org/10.1113/jphysiol.2005.093690

Minamino, T., & Komuro, I. (2008). Vascular aging: insights from studies on cellular senescence, stem cell aging, and progeroid syndromes. *Nature Clinical Practice. Cardiovascular Medicine*, *5*(10), 637–648. https://doi.org/10.1038/ncpcardio1324

Mooney, D. J., Langer, R., & Ingber, D. E. (1995). Cytoskeletal filament assembly and the control of cell spreading and function by extracellular matrix. *Journal of Cell Science*, *108 (Pt 6*(6), 2311–2320. Retrieved from http://www.ncbi.nlm.nih.gov/pubmed/7673351

Morley, J. E. (2004). A brief history of geriatrics. *The Journals of Gerontology. Series A, Biological Sciences and Medical Sciences*, *59*(11), 1132–1152. https://doi.org/10.1093/gerona/59.11.1132

Morris, R. L., & Hollenbeck, P. J. (1995). Axonal transport of mitochondria along microtubules and F-actin in living vertebrate neurons. *The Journal of Cell Biology*, *131*(5), 1315–1326. https://doi.org/10.1083/jcb.131.5.1315

Mula, J., Lee, J. D., Liu, F., Yang, L., & Peterson, C. A. (2013). Automated image analysis of skeletal muscle fiber cross-sectional area. *Journal of Applied Physiology (Bethesda, Md. : 1985)*, *114*(1), 148–155. https://doi.org/10.1152/japplphysiol.01022.2012

Nasello, G., Vautrin, A., Pitocchi, J., Wesseling, M., Kuiper, J. H., Pérez, M. Á., & García-Aznar, J. M. (2021). Mechano-driven regeneration predicts response variations in large animal model based on scaffold implantation site and individual mechano-sensitivity. *Bone*, *144*, 115769. https://doi.org/10.1016/j.bone.2020.115769

Nemir, S., & West, J. L. (2010). Synthetic materials in the study of cell response to substrate rigidity. *Annals of Biomedical Engineering*, *38*(1), 2–20. https://doi.org/10.1007/s10439-009-9811-1

Norddahl, G. L., Pronk, C. J., Wahlestedt, M., Sten, G., Nygren, J. M., Ugale, A., … Bryder, D. (2011). Accumulating mitochondrial DNA mutations drive premature hematopoietic aging phenotypes distinct from physiological stem cell aging. *Cell Stem Cell*, *8*(5), 499–510. https://doi.org/10.1016/j.stem.2011.03.009

Oustanina, S., Hause, G., & Braun, T. (2004). Pax7 directs postnatal renewal and propagation of myogenic satellite cells but not their specification. *The EMBO Journal*, *23*(16), 3430–3439. https://doi.org/10.1038/sj.emboj.7600346

Pajerowski, J. D., Dahl, K. N., Zhong, F. L., Sammak, P. J., & Discher, D. E. (2007). Physical plasticity of the nucleus in stem cell differentiation. *Proceedings of the National Academy of Sciences of the United States of America*, *104*(40), 15619–15624. https://doi.org/10.1073/pnas.0702576104

Panciera, T., Azzolin, L., Cordenonsi, M., & Piccolo, S. (2017). Mechanobiology of YAP and TAZ in physiology and disease. *Nature Reviews. Molecular Cell Biology*, *18*(12), 758–770. https://doi.org/10.1038/nrm.2017.87

Pathak, R. U., Soujanya, M., & Mishra, R. K. (2021). Deterioration of nuclear morphology and architecture: A hallmark of senescence and aging. *Ageing Research Reviews*, *67*(February), 101264. https://doi.org/10.1016/j.arr.2021.101264

Pedersen, B. K., & Febbraio, M. (2005). Muscle-derived interleukin-6—A possible link between skeletal muscle, adipose tissue, liver, and brain. *Brain, Behavior, and Immunity*, *19*(5), 371–376. https://doi.org/10.1016/j.bbi.2005.04.008

Pennisi, C. P., Olesen, C. G., de Zee, M., Rasmussen, J., & Zachar, V. (2011). Uniaxial cyclic strain drives assembly and differentiation of skeletal myocytes. *Tissue Engineering. Part A*, *17*(19–20), 2543–2550. https://doi.org/10.1089/ten.TEA.2011.0089

Phillip, J. M., Aifuwa, I., Walston, J., & Wirtz, D. (2015). The Mechanobiology of Aging. *Annual Review of Biomedical Engineering*, *17*, 113–141. https://doi.org/10.1146/annurev-bioeng-071114-040829

Powell, C. A., Smiley, B. L., Mills, J., & Vandenburgh, H. H. (2002). Mechanical stimulation improves tissue-engineered human skeletal muscle. *American Journal of Physiology. Cell Physiology*, *283*(5), C1557-65. https://doi.org/10.1152/ajpcell.00595.2001

PubMed. (n.d.). Retrieved July 31, 2020, from https://pubmed.ncbi.nlm.nih.gov/

Qiu, X., Brown, K., Hirschey, M. D., Verdin, E., & Chen, D. (2010). Calorie restriction reduces oxidative stress by SIRT3-mediated SOD2 activation. *Cell Metabolism*, *12*(6), 662–667. https://doi.org/10.1016/j.cmet.2010.11.015

Qu, M.-J., Liu, B., Wang, H.-Q., Yan, Z.-Q., Shen, B.-R., & Jiang, Z.-L. (2007). Frequency-dependent phenotype modulation of vascular smooth muscle cells under cyclic mechanical strain. *Journal of Vascular Research*, *44*(5), 345–353. https://doi.org/10.1159/000102278

Quarta, M., Brett, J. O., DiMarco, R., De Morree, A., Boutet, S. C., Chacon, R., … Rando, T. A. (2016). An artificial niche preserves the quiescence of muscle stem cells and enhances their therapeutic efficacy. *Nature Biotechnology*, *34*(7), 752–759. https://doi.org/10.1038/nbt.3576

Quarta, M., Cromie, M., Chacon, R., Blonigan, J., Garcia, V., Akimenko, I., … Rando, T. A. (2017). Bioengineered constructs combined with exercise enhance stem cell-mediated treatment of volumetric muscle loss. *Nature Communications*, *8*, 15613. https://doi.org/10.1038/ncomms15613

Rando, T. A., & Ambrosio, F. (2018). Regenerative Rehabilitation: Applied Biophysics Meets Stem Cell Therapeutics. *Cell Stem Cell*, *22*(3), 306–309. https://doi.org/10.1016/j.stem.2018.02.003

Rocheteau, P., Gayraud-Morel, B., Siegl-Cachedenier, I., Blasco, M. A., & Tajbakhsh, S. (2012). A subpopulation of adult skeletal muscle stem cells retains all template DNA strands after cell division. *Cell*, *148*(1–2), 112–125. https://doi.org/10.1016/j.cell.2011.11.049

Rosant, C., Nagel, M.-D., & Pérot, C. (2007). Aging affects passive stiffness and spindle function of the rat soleus muscle. *Experimental Gerontology*, *42*(4), 301–308. https://doi.org/10.1016/j.exger.2006.10.007

Roshanravan, B., Patel, K. V., Fried, L. F., Robinson-Cohen, C., de Boer, I. H., Harris, T., … Kestenbaum, B. (2017). Association of Muscle Endurance, Fatigability, and Strength With Functional Limitation and Mortality in the Health Aging and Body Composition Study. *The Journals of Gerontology. Series A, Biological Sciences and Medical Sciences*, *72*(2), 284–291. https://doi.org/10.1093/gerona/glw210

Roth, S. M., Martel, G. F., Ivey, F. M., Lemmer, J. T., Metter, E. J., Hurley, B. F., & Rogers, M. A. (2000). Skeletal muscle satellite cell populations in healthy young and older men and women. *The Anatomical Record*, *260*(4), 351–358. https://doi.org/10.1002/1097-0185(200012)260:4<350::AID-AR30>3.0.CO;2-6

Rudnicki, M. A., Schnegelsberg, P. N. J., Stead, R. H., Braun, T., Arnold, H. H., & Jaenisch, R. (1993). MyoD or Myf-5 is required for the formation of skeletal muscle. *Cell*, *75*(7), 1351–1359. https://doi.org/10.1016/0092-8674(93)90621-v

Ruiz, J. R., Sui, X., Lobelo, F., Morrow, J. R., Jackson, A. W., Sjöström, M., & Blair, S. N. (2008). Association between muscular strength and mortality in men: prospective cohort study. *BMJ (Clinical Research Ed.)*, *337*(7661), a439. https://doi.org/10.1136/bmj.a439

Ruzankina, Y., Pinzon-Guzman, C., Asare, A., Ong, T., Pontano, L., Cotsarelis, G., … Brown, E. J. (2007). Deletion of the developmentally essential gene ATR in adult mice leads to age-related phenotypes and stem cell loss. *Cell Stem Cell*, *1*(1), 113–126. https://doi.org/10.1016/j.stem.2007.03.002

Ryall, J. G., Dell'Orso, S., Derfoul, A., Juan, A., Zare, H., Feng, X., … Sartorelli, V. (2015). The NAD(+)-dependent SIRT1 deacetylase translates a metabolic switch into regulatory epigenetics in skeletal muscle stem cells. *Cell Stem Cell*, *16*(2), 171–183. https://doi.org/10.1016/j.stem.2014.12.004

Sahu, A., Mamiya, H., Shinde, S. N., Cheikhi, A., Winter, L. L., Vo, N. V, … Ambrosio, F. (2018). Age-related declines in α-Klotho drive progenitor cell mitochondrial dysfunction and impaired muscle regeneration. *Nature Communications*, *9*(1), 4859. https://doi.org/10.1038/s41467-018-07253-3

Samant, S. A., Zhang, H. J., Hong, Z., Pillai, V. B., Sundaresan, N. R., Wolfgeher, D., … Gupta, M. P. (2014). SIRT3 deacetylates and activates OPA1 to regulate mitochondrial dynamics during stress. *Molecular and Cellular Biology*, *34*(5), 807–819. https://doi.org/10.1128/MCB.01483-13

Schäfer, R., Knauf, U., Zweyer, M., Högemeier, O., De Guarrini, F., Liu, X., … Wernig, A. (2006). Age dependence of the human skeletal muscle stem cell in forming muscle tissue. *Artificial Organs*, *30*(3), 130–140. https://doi.org/10.1111/j.1525-1594.2006.00199.x

Schultz, E. (1974). A quantitative study of the satellite cell population in postnatal mouse lumbrical muscle. *The Anatomical Record*, *180*(4), 589–595. https://doi.org/10.1002/ar.1091800405

Schultz, E., & Lipton, B. H. (1982). Skeletal muscle satellite cells: changes in proliferation potential as a function of age. *Mechanisms of Ageing and Development*, *20*(4), 377–383. https://doi.org/10.1016/0047-6374(82)90105-1

Schultz, M. B., & Sinclair, D. A. (2016). When stem cells grow old: Phenotypes and mechanisms of stem cell aging. *Development (Cambridge)*, *143*(1), 3–14. https://doi.org/10.1242/dev.130633

Scorrano, L., Ashiya, M., Buttle, K., Weiler, S., Oakes, S. A., Mannella, C. A., & Korsmeyer, S. J. (2002). A distinct pathway remodels mitochondrial cristae and mobilizes cytochrome c during apoptosis. *Developmental Cell*, *2*(1), 55–67. https://doi.org/10.1016/s1534-5807(01)00116-2

Scott, I., Webster, B. R., Li, J. H., & Sack, M. N. (2012). Identification of a molecular component of the mitochondrial acetyltransferase programme: a novel role for GCN5L1. *The Biochemical Journal*, *443*(3), 655–661. https://doi.org/10.1042/BJ20120118

Seale, P., Sabourin, L. A., Girgis-Gabardo, A., Mansouri, A., Gruss, P., & Rudnicki, M. A. (2000). Pax7 is required for the specification of myogenic satellite cells. *Cell*, *102*(6), 777–786. https://doi.org/10.1016/s0092-8674(00)00066-0

Seynnes, O. R., de Boer, M., & Narici, M. V. (2007). Early skeletal muscle hypertrophy and architectural changes in response to high-intensity resistance training. *Journal of Applied Physiology*, *102*(1), 368–373. https://doi.org/10.1152/japplphysiol.00789.2006

Shefer, G., Van de Mark, D. P., Richardson, J. B., & Yablonka-Reuveni, Z. (2006). Satellite-cell pool size does matter: Defining the myogenic potency of aging skeletal muscle. *Developmental Biology*, *294*(1), 50–66. https://doi.org/10.1016/j.ydbio.2006.02.022

Shi, X., & Garry, D. J. (2006). Muscle stem cells in development, regeneration, and disease. *Genes and Development*, *20*(13), 1692–1708. https://doi.org/10.1101/gad.1419406

Siekevitz, P. (1957). Powerhouse of the Cell. *Scientific American*, *197*(1), 131–144. https://doi.org/10.1038/scientificamerican0757-131

Sinha, M., Jang, Y. C., Oh, J., Khong, D., Wu, E. Y., Manohar, R., … Wagers, A. J. (2014). Restoring systemic GDF11 levels reverses age-related dysfunction in mouse skeletal muscle. *Science (New York, N.Y.)*, *344*(6184), 649–652. https://doi.org/10.1126/science.1251152

Smith, L. R., Hammers, D. W., Sweeney, H. L., & Barton, E. R. (2016). Increased collagen cross-linking is a signature of dystrophin-deficient muscle. *Muscle and Nerve*, *54*(1), 71–78. https://doi.org/10.1002/mus.24998

Sousa-Victor, P., Gutarra, S., García-Prat, L., Rodriguez-Ubreva, J., Ortet, L., Ruiz-Bonilla, V., … Muñoz-Cánoves, P. (2014). Geriatric muscle stem cells switch reversible quiescence into senescence. *Nature*, *506*(7488), 316–321. https://doi.org/10.1038/nature13013

Spagnol, S. T., & Dahl, K. N. (2014). Active cytoskeletal force and chromatin condensation independently modulate intranuclear network fluctuations. *Integrative Biology : Quantitative Biosciences from Nano to Macro*, *6*(5), 523–531. https://doi.org/10.1039/c3ib40226f

Spengler, D. M., Baylink, D. J., & Rosenquist, J. B. (1977). Effect of beta-aminopropionitrile on bone mechanical properties. *The Journal of Bone and Joint Surgery. American Volume*, *59*(5), 670–672. Retrieved from http://www.ncbi.nlm.nih.gov/pubmed/873962

Stadtman, E. R. (2002). Importance of individuality in oxidative stress and aging. *Free Radical Biology and Medicine*, *33*(5), 597–604. https://doi.org/10.1016/S0891-5849(02)00904-8

Stearns-Reider, K. M., D'Amore, A., Beezhold, K., Rothrauff, B., Cavalli, L., Wagner, W. R., … Ambrosio, F. (2017). Aging of the skeletal muscle extracellular matrix drives a stem cell fibrogenic conversion. *Aging Cell*, *16*(3), 518–528. https://doi.org/10.1111/acel.12578

Tang, A. H., & Rando, T. A. (2014). Induction of autophagy supports the bioenergetic demands of quiescent muscle stem cell activation. *The EMBO Journal*, *33*(23), 2782–2797. https://doi.org/10.15252/embj.201488278

Tao, R., Coleman, M. C., Pennington, J. D., Ozden, O., Park, S. H., Jiang, H., … Gius, D. (2010). Sirt3-Mediated Deacetylation of Evolutionarily Conserved Lysine 122 Regulates MnSOD Activity in Response to Stress. *Molecular Cell*, *40*(6), 893–904. https://doi.org/10.1016/j.molcel.2010.12.013

Thomas, D. P., McCormick, R. J., Zimmerman, S. D., Vadlamudi, R. K., & Gosselin, L. E. (1992). Aging- and training-induced alterations in collagen characteristics of rat left ventricle and papillary muscle. *The American Journal of Physiology*, *263*(3 Pt 2), H778-83. https://doi.org/10.1152/ajpheart.1992.263.3.H778

Tojkander, S., Gateva, G., & Lappalainen, P. (2012). Actin stress fibers--assembly, dynamics and biological roles. *Journal of Cell Science*, *125*(Pt 8), 1855–1864. https://doi.org/10.1242/jcs.098087

United Nations. (2017). Department of Economic and Social Affairs, Population Division (2017). In *World population ageing 2017 - Highlights*.

Urciuolo, A., Quarta, M., Morbidoni, V., Gattazzo, F., Molon, S., Grumati, P., … Bonaldo, P. (2013). Collagen VI regulates satellite cell self-renewal and muscle regeneration. *Nature Communications*, *4*(May), 1964. https://doi.org/10.1038/ncomms2964

Vale, R. D. (2003). The molecular motor toolbox for intracellular transport. *Cell*, *112*(4), 467–480. https://doi.org/10.1016/s0092-8674(03)00111-9

Veal, E. A., Day, A. M., & Morgan, B. A. (2007). Hydrogen peroxide sensing and signaling. *Molecular Cell*, *26*(1), 1–14. https://doi.org/10.1016/j.molcel.2007.03.016

Weber, T. A., & Reichert, A. S. (2010). Impaired quality control of mitochondria: Aging from a new perspective. *Experimental Gerontology*, *45*(7–8), 503–511. https://doi.org/10.1016/j.exger.2010.03.018

Webster, M., Witkin, K. L., & Cohen-Fix, O. (2009). Sizing up the nucleus: nuclear shape, size and nuclear-envelope assembly. *Journal of Cell Science*, *122*(Pt 10), 1477–1486. https://doi.org/10.1242/jcs.037333

Weir, H. J., Yao, P., Huynh, F. K., Escoubas, C. C., Goncalves, R. L., Burkewitz, K., … Mair, W. B. (2017). Dietary Restriction and AMPK Increase Lifespan via Mitochondrial Network and Peroxisome Remodeling. *Cell Metabolism*, *26*(6), 884-896.e5. https://doi.org/10.1016/j.cmet.2017.09.024

WHO. (2018). Ageing and health. Retrieved from https://www.who.int/news-room/fact-sheets/detail/ageing-and-health

Willems, M. E. T., Miller, G. R., & Stauber, W. T. (2001). Force deficits after stretches of activated rat muscle-tendon complex with reduced collagen cross-linking. *European Journal of Applied Physiology*, *85*(5), 405–411. https://doi.org/10.1007/s004210100480

Wilson, A., Murphy, M. J., Oskarsson, T., Kaloulis, K., Bettess, M. D., Oser, G. M., … Trumpp, A. (2004). c-Myc controls the balance between hematopoietic stem cell self-renewal and differentiation. *Genes & Development*, *18*(22), 2747–2763. https://doi.org/10.1101/gad.313104

Wu, P.-H., Aroush, D. R.-B., Asnacios, A., Chen, W.-C., Dokukin, M. E., Doss, B. L., … Wirtz, D. (2018). A comparison of methods to assess cell mechanical properties. *Nature Methods*, *15*(7), 491–498. https://doi.org/10.1038/s41592-018-0015-1

Yamauchi, M, Woodley, D. T., & Mechanic, G. L. (1988). Aging and cross-linking of skin collagen. *Biochemical and Biophysical Research Communications*, *152*(2), 898–903. Retrieved from http://www.ncbi.nlm.nih.gov/pubmed/3130057

Yamauchi, Mitsuo, & Sricholpech, M. (2012). Lysine post-translational modifications of collagen. *Essays in Biochemistry*, *52*, 113–133. https://doi.org/10.1042/bse0520113

Yamauchi, Mitsuo, Terajima, M., & Shiiba, M. (2019). Lysine Hydroxylation and Cross-Linking of Collagen. In *Methods in Molecular Biology* (Vol. 1934, pp. 309–324). https://doi.org/10.1007/978-1-4939-9055-9_19

Yang, C., Tibbitt, M. W., Basta, L., & Anseth, K. S. (2014). Mechanical memory and dosing influence stem cell fate. *Nature Materials*, *13*(6), 645–652. https://doi.org/10.1038/nmat3889

Yang, X., Yang, S., Wang, C., & Kuang, S. (2017). The hypoxia-inducible factors HIF1α and HIF2α are dispensable for embryonic muscle development but essential for postnatal muscle regeneration. *The Journal of Biological Chemistry*, *292*(14), 5981–5991. https://doi.org/10.1074/jbc.M116.756312

Yao, Y., Li, C., Zhou, X., Zhang, Y., Lu, Y., Chen, J., … Ma, Y. (2014). PIWIL2 induces c-Myc expression by interacting with NME2 and regulates c-Myc-mediated tumor cell proliferation. *Oncotarget*, *5*(18), 8466–8477. https://doi.org/10.18632/oncotarget.2327

Yeoh, O. H. (1993). Some Forms of the Strain Energy Function for Rubber. *Rubber Chemistry and Technology*, *66*(5), 754–771. https://doi.org/10.5254/1.3538343

Yi, L., & Rossi, F. (2011). Purification of progenitors from skeletal muscle. *Journal of Visualized Experiments : JoVE*, *2*(49), 2–7. https://doi.org/10.3791/2476

Yin, Y., Zong, R., Bao, X., Zheng, X., Cui, H., Liu, Z., & Zhou, Y. (2018). Oxidative stress suppresses cellular autophagy in corneal epithelium. *Investigative Ophthalmology and Visual Science*, *59*(8), 3286–3293. https://doi.org/10.1167/iovs.18-24057

Yousef, H., Conboy, M. J., Mamiya, H., Zeiderman, M., Schlesinger, C., Schaffer, D. V, & Conboy, I. M. (2014). Mechanisms of action of hESC-secreted proteins that enhance human and mouse myogenesis. *Aging*, *6*(5), 1–19. Retrieved from http://www.ncbi.nlm.nih.gov/pubmed/25109702

Zammit, P. S., Heslop, L., Hudon, V., Rosenblatt, J. D., Tajbakhsh, S., Buckingham, M. E., … Partridge, T. A. (2002). Kinetics of myoblast proliferation show that resident satellite cells are competent to fully regenerate skeletal muscle fibers. *Experimental Cell Research*, *281*(1), 39–49. https://doi.org/10.1006/excr.2002.5653

Zeng, L., Yang, Y., Hu, Y., Sun, Y., Du, Z., Xie, Z., … Kong, W. (2014). Age-related decrease in the mitochondrial sirtuin deacetylase Sirt3 expression associated with ROS accumulation in the auditory cortex of the mimetic aging rat model. *PloS One*, *9*(2), e88019. https://doi.org/10.1371/journal.pone.0088019

Zhang, C., Ferrari, R., Beezhold, K., Stearns-Reider, K., D'Amore, A., Haschak, M., … Ambrosio, F. (2015). Arsenic Promotes NF-κB-Mediated Fibroblast Dysfunction and Matrix Remodeling to Impair Muscle Stem Cell Function. *Stem Cells (Dayton, Ohio)*, (Iii), n/a-n/a. https://doi.org/10.1002/stem.2232

Zhang, H, Zhang, H., Ryu, D., Wu, Y., Gariani, K., Wang, X., … Menzies, K. J. (2016). *NAD + repletion improves mitochondrial and stem cell function and enhances life span in mice*. *2693*(April). https://doi.org/10.1126/science.aaf2693

Zhang, Hongbo, Menzies, K. J., & Auwerx, J. (2018). The role of mitochondria in stem cell fate and aging. *Development (Cambridge)*, *145*(8). https://doi.org/10.1242/dev.143420

Zhang, Y., Lanjuin, A., Chowdhury, S. R., Mistry, M., Silva-García, C. G., Weir, H. J., … Mair, W. B. (2019). Neuronal TORC1 modulates longevity via AMPK and cell nonautonomous regulation of mitochondrial dynamics in C. elegans. *ELife*, *8*, 1–24. https://doi.org/10.7554/eLife.49158

ZIMMERMAN, S. D., MCCORMICK, R. J., VADLAMUDI, R. K., & THOMAS, D. P. (1993). Age and Training Alter Collagen Characteristics in Fast-Twitch and Slow-Twitch Rat Limb Muscle. *Journal of Applied Physiology*, *75*(4), 1670–1674.